Gap genes are involved in inviability in hybrids between *Drosophila melanogaster and D. santomea*

Wenhan Chang[1], Martin Kreitman[1], and Daniel R. Matute[2]

[1]Department of Ecology and Evolution, University of Chicago

[2]Biology Department, University of North Carolina, Chapel Hill, North Carolina

Correspondence:

Biology Department, University of North Carolina, 250 Bell Tower Road, Chapel Hill, 27599.

Tel: 919-962-2077

Fax: 919-962-1625

E-mail: dmatute@email.unc.edu

Running title: Gap genes cause hybrid inviability

ABSTRACT

Evolved changes within species lead to the inevitable loss of viability in hybrids. Inviability is also a convenient phenotype to genetically map and validate functionally divergent genes and pathways differentiating closely related species. Here we identify the *Drosophila melanogaster* form of the highly conserved essential gap gene *giant* (*gt*) as a key genetic determinant of hybrid inviability in crosses with *D. santomea*. We show that the coding region of this allele in *D. melanogaster/D. santomea* hybrids is sufficient to cause embryonic inviability not seen in either pure species. Further genetic analysis indicates that *tailless* (*tll*), another gap gene, is also involved in the hybrid defects. *giant* and *tll* are both members of the gap gene network of transcription factors that participate in establishing anterior-posterior specification of the dipteran embryo, a highly conserved developmental process. Genes whose outputs in this process are functionally conserved nevertheless evolve over short timescales to cause inviability in hybrids.

INTRODUCTION

The formation and persistence of species involves the buildup of barriers to gene flow as genome divergence accrues over time. These genetic barriers arise as species differentiate and involve breakdowns in a variety of cellular, developmental, and behavioral processes; eventually these barriers lead to reduced fitness of hybrids relative to pure species (Coyne and Orr 2004; Coughlan and Matute 2020). Hybrid inviability (HI), the condition in which interspecific hybrids do not achieve adulthood because of developmental defects, is one of these barriers. The question of how natural selection could allow such maladaptive and extreme phenotypes has been a subject of intense interest to evolutionary biologists and developmental geneticists alike (Darwin 1859; Weir 1885; Shull 1923).

Dobzhansky (Dobzhansky 1937) and Muller (Muller 1942) formulated a widely regarded genetic model in which hybrid defects, including HI, arise as a collateral effect of evolutionary divergence between populations that acquire incompatible changes in interacting loci, or Dobzhansky-Muller incompatibilities (DMIs; (Dobzhansky 1937; Muller 1942)). Because the divergent alleles at the DMIs loci only have fitness costs when they are forced together in hybrids, natural selection does not oppose the changes in each species. There is substantial evidence in support of the DM model (Maheshwari and Barbash 2011), including nearly a dozen instances in which HI alleles have been identified to the gene level (Wellbrock *et al.* 1998; Presgraves 2003; Brideau *et al.* 2006; Bomblies *et al.* 2007; Lee *et al.* 2008; Tang and Presgraves 2009; Ferree and Barbash 2009; Phadnis *et al.* 2015; Zuellig and Sweigart 2018; Powell *et al.* 2020; Moran *et al.* 2021). Some of these alleles have been shown to evolve through positive selection (Presgraves et al. 2003; Brideau et al. 2006; Bomblies et al. 2007; Tang and Presgraves 2009; Satyaki et al. 2014) while others show no clear signature of selection (Phadnis and Orr 2009). The variety of both the gene type in HI and the processes that drive allelic divergence indicates that HI can occur in a multitude of ways (Johnson 2010).

Developmental processes are generally guided by interacting regulatory genes and elements, making them a rich source of potential candidates for HI. The question arises, however, as to whether they evolve functionally at a sufficient pace to fuel the rapid

formation of DMIs in the speciation process. Developmental processes and their outputs are often deeply conserved phylogenetically, often displaying conserved functional attributes (reviewed in (Gordon and Ruvinsky 2012)). Large-effect mutations to developmental regulators are often incompatible with life, and these genes tend to be evolutionarily conserved both in sequence and phenotypic output (Manzanares *et al.* 2000; Gaunt 2002; Santini *et al.* 2003; Lee *et al.* 2006). While the developmental phenotypes in which these genes are involved generally remain similar across species, the genetic underpinnings of these crucial phenotypes may evolve (Weiss and Fullerton 2000; True and Haag 2001; Palmer and Feldman 2009; Rebeiz *et al.* 2009; Pavlicev and Wagner 2012), and if their pace of functional evolution is sufficiently fast, could contribute to HI.

Several lines of evidence elevate this possibility and thus challenge the notion that the conservation and selective constraints on regulatory genes, and the processes they direct, immunize them from possibly contributing to HI. First, recent work by us on a canonical example of a conserved regulatory gene and pathway — the gap gene *giant* in *Drosophila* and the process of pattern formation— shows contrary to expectations that this gene diverges functionally at a rapid and continuous pace in the genus, as evidenced by loss of viability in carefully controlled transgenic complementation experiments (Chang *et al.* 2021).

Second, several cases of embryonic hybrid lethality have been identified in *Drosophila*: female hybrid inviability in hybrids between *D. montana* females and *D. texana* males (Kinsey 1967), female lethality in hybrids of *D. melanogaster* females and *D. simulans* males (Sawamura and Yamamoto 1993; Sawamura *et al.* 1993b; a); and male embryonic lethality in hybrids of *D. melanogaster* females and *D. santomea* males ((Gavin-Smyth and Matute 2013), see below).

Third, even for developmental phenotypes that remain similar across phylogeny, their genetic underpinnings change occasionally in substantial ways (Weiss and Fullerton 2000; True and Haag 2001; Palmer and Feldman 2009; Rebeiz *et al.* 2009; Pavlicev and Wagner 2012). Referred to as developmental systems drift —functional divergence of genes in developmental regulatory pathways with conserved outputs — has also been documented for nematode vulva induction (Wang and Sommer 2011; Sommer 2012), and

sex determination in frogs (Cauret *et al.* 2020). Developmental systems drift has also been proposed to lead to hybrid defects (Lynch 2009). If genetic changes occur in different directions in two species, their hybrids might not have a functional pathway to produce the required developmental phenotype. This is a simple—but to date unsubstantiated— way to explain HI.

RESULTS

We first explored whether *Drosophila* hybrids other than *mel/san* also showed embryonic hybrid inviability and abdominal ablations. We examined the embryonic lethality rates and associated cuticular phenotypes from hybrid crosses between various species within the *melanogaster* supercomplex and species of the *yakuba* subgroup (Figure 1, Figure S1). Hybrid embryos between *D. santomea* and the other species in the *yakuba* subgroup — *D. teissieri* and *D. yakuba* — are mostly viable and showed no abdominal ablations in any of the six possible reciprocal crosses (Table S1; (Gavin-Smyth and Matute 2013; Turissini *et al.* 2015, 2018; Cooper *et al.* 2017)). Embryonic inviability is rare among crosses between collections of these species (but see (Cooper *et al.* 2017)). Hybrid inviability is also non-existent in hybrids between collections of species of the *simulans* species group — *D. simulans* (*sim*), *D. mauritiana* (*mau*) and *D. sechellia* (*sec*) (Figure 1, (Turissini *et al.* 2018)). The embryonic viability of male *mel/sim* and *mel/mau* hybrids is high in all cases (Table S2, (Sturtevant 1920; Sawamura *et al.* 1993a; Presgraves 2003; Matute *et al.* 2014)). The few rare embryos that failed to develop and hatch showed no abdominal ablations (Table S2).

Crosses between females of two species of the *sim* clade (*sim* and *mau*) and *san* males showed high levels of hybrid inviability, especially of males (Figure S1). These dead hybrids show the characteristic abdominal ablation. This shared phenotype with *mel* in hybrids with *san* indicated that genetic changes that ultimately lead to abdominal ablations must have occurred before the split of the three species, approximately five million years ago (Tamura *et al.* 2004; Matute *et al.* 2010; Suvorov *et al.* 2021). Genetic analysis with these crosses also confirm that the locus involved in HI resides in the *X*-

chromosome. We next identified the genetic locus that causes hybrid inviability by abdominal ablation using genetic tools available in *D. melanogaster*.

Genetic mapping shows *giant* is involved in *mel/san* HI

To identify the *X*-linked allele involved in HI, we did a genome-wide association study using a panel of inbred *D. melanogaster* lines (i.e., DGRP, (MacKay *et al.* 2012; Huang *et al.* 2014)) and studied whether any genetic variant segregating in *D. melanogaster* was associated with total inviability in hybrids with *D. santomea*. In all crosses, the hybrid males die, but the females show differential rates of survival. We found a strong association between a 16.5 kb haplotype in the *X*-chromosome and high levels of HI (Figure 2A). This haplotype harbors two genes: *CG32797 and gt*, and overlaps with a segment of the *D. melanogaster X*-chromosome (X_{mel}) previously associated with male HI (Matute and Gavin-Smyth 2014).

A similar GWAS for the incidence of abdominal ablations (Figure 2B) showed the frequency of abdominal ablations in *mel/san* hybrids (both sexes pooled) is associated with an X_{mel} haplotype that contains six genes (*CG32797, gt, tko, boi, z,* and *trol*; Figure 2B). This interval also overlaps with the region associated with HI. Gene(s) on the tip of X_{mel} cause both HI and abdominal ablations.

Next, we generated *mel/san* hybrid males with the *X*-chromosome from *D. santomea* (X_{san}) and studied whether introducing small segments of X_{mel} would cause HI. *mel/san* hybrid males with the abdominal ablation typically inherit a X_{mel} chromosome and a *Y* chromosome from *san* (Y_{san}). By using *mel* attached-*X* chromosomes (Figure S1), we manipulated chromosomal inheritance and generated hybrid F_1 males that inherit a X_{san} and a *D. melanogaster Y* chromosome (Y_{mel}). These animals do not manifest the abdominal ablation and are regularly viable (Gavin-Smyth and Matute 2013; Matute and Gavin-Smyth 2014). We obtained a similar result when we crossed *sim* attached-*X* females to *san* males; the cross produces viable hybrid F_1 males with a X_{san} and a *D. simulans Y* chromosome. To refine the region of the X_{mel} chromosome carrying the determinant of the abdominal ablation phenotype, we introduced small segments of X_{mel} (containing *mel* alleles ranging from approximately 10 to 100 genes each; as in (Cook *et al.* 2010; Venken *et al.* 2010; Matute and Gavin-Smyth 2014) into the genetic makeup of

159 X_{san}/Y_{mel} hybrid F_1 males (crossing scheme shown in Figure S2; fly stocks listed in Table
160 S3). Previous results had shown that the distal tip of X_{mel} contains an allele that causes
161 inviability in hybrid males. Measuring the rates of hybrid embryonic lethality in the
162 presence of nested *Dp(1;Y)* and *Dp(1:3)* duplications of the X_{mel} chromosome allowed us
163 to refine the genomic interval to the region encompassing the cytological region 3A3
164 (dmel6: 2,410,000-2,580,000; (Dos Santos *et al.* 2015b)). Male hybrid embryos harboring
165 X_{san} and Y_{mel} with duplications containing the 3A3 portion of X_{mel} routinely fail to hatch
166 (Figure 2C). They also show the striking abdominal ablation common in *mel/san* hybrid
167 males carrying the full-length X_{mel} and Y_{san} (Figure 2C; Figure S3). Previous results had
168 shown that the distal tip of X_{mel} contains an allele that causes inviability in hybrid males.
169 Measuring the rates of hybrid embryonic lethality in the presence of nested *Dp(1;Y)* and
170 *Dp(1:3)* duplications of the X_{mel} chromosome allowed us to refine the genomic interval to
171 the region encompassing the cytological region 3A3 (dmel6: 2,410,000-2,580,000; (Dos
172 Santos *et al.* 2015b)). The comparison of *Dp(1;Y)* and *Dp(1;3)* duplications has two
173 caveats worth noting. First, pure species *mel C(1)DX, Dp(1;3)/Dp(1;3)* females are
174 generally weaker than *C(1)DX, Dp(1;Y)* and lay fewer eggs in conspecific and
175 heterospecific crosses. We thus had lower power in crosses involving the former type of
176 females (Table S4). Second, the rate of complementation of *Dp(1;3)* and *Dp(1;Y)* is not
177 identical (Table S5) suggesting the existence of position effects.
178 Male hybrid embryos harboring X_{san} and X_{mel} duplications containing the 3A3
179 portion fail to hatch (Figure 2C). They also show the striking abdominal ablation
180 common in *mel/san* hybrid males carrying the full-length X_{mel} and Y_{san} (Figure 2D, Figure
181 S2). Notably, the overlapping region of the duplications that cause this ablation contains
182 only one gene: *giant* (Figure S2). The ablation phenotype is not found in the presence of
183 other lethality-inducing fragments from elsewhere on the X_{mel} chromosome (as found in
184 this work and (Matute and Gavin-Smyth 2014)). gt_{mel} caused HI with abdominal ablation
185 in hybrids with all examined lines from *D. santomea* confirming that the interaction is not
186 a line specific effect (Figure S4; Table S6). These experiments suggest that introducing a
187 gt_{mel} allele in a X_{san}/Y_{mel} male hybrid background is sufficient to cause lethality with
188 abdominal ablation.
189 We also did similar genetic crosses using *Dp(1;Y)* and *Dp(1;3)* duplications to

assess whether the same *X*-chromosome segments (and therefore gt_{mel}) caused HI in crosses with four additional species, two from the *simulans* species complex (*mau* and *sim*), one from the *yakuba* species complex, *D. teissieri,* and *mel* itself. In no other interspecific hybrids did gt_{mel} have a deleterious effect (either reduced viability or abdominal ablations) suggesting that the hybrid lethal effects gt_{mel} are exclusive to *mel/san* hybrids (Figures S5-S6).

The gt_{mel} allele causes inviability in both male and female hybrids

The crosses described above address the effect of the presence of a gt_{mel} allele on HI in *mel/san* hybrids. Next, we studied the absence of a functional a gt_{mel} allele using a gt_{mel} null-allele, gt_{mel}^{X11} (Perrimon *et al.* 1984; Petschek *et al.* 1987). Hybrid male embryos carrying gt^{X11} were less likely to be abdominally ablated compared to other X^{mel}/Y^{san} hybrids (mean number *of* $FM7/Y^{san}$ ablated embryos: 80.33%, Figure 3A; mean proportion *of* gt_{mel}^{X11}/Y^{san} ablated embryos: 4.41%, Figure 4B; t-test comparing the frequency of ablations in $FM7/Y^{san}$ males and gt_{mel}^{X11}/Y_{san} males: t = 23.972, df = 21.614, $P < 1 \times 10^{-10}$), and instead show other developmental defects (Figure S7).

X_{mel}/Y_{san} males with a null allele of gt_{mel} (i.e., gt_{mel}^{X11}/Y_{san}) do not show increased viability. This result is not surprising because X_{mel} harbors at least eight more dominant (or semidominant) factors that also cause embryonic inviability (Matute and Gavin-Smyth 2014), which may be specifically lethal to *mel/san* hybrids. In contrast, male hybrid embryos carrying a X_{mel} chromosome and null mutations of the genes adjacent to *gt* (*boi*, *trol*, and *tko*) show abdominal ablations (Figure S8). These experiments demonstrate that gt_{mel} is necessary for the abdominal ablation in *mel/san* hybrid males, but is not the only allele that can cause inviability in this hybrid individuals.

We also tested whether gt_{mel} had a deleterious effect on hybrid females by scoring whether any allele on X_{mel} between the cytological positions 2F1 and 3A4 affected the fitness of *mel/san* hybrid females. We used deficiency mapping and scored the number of *df(i)/san* hybrid females compared to their *FM7/san* sisters ((Coyne *et al.* 1998; Presgraves 2003), see Methods). Deviations from 1:1 expected ratio indicate the presence of alleles involved in HI. If *FM7/san* hybrids survive at a higher rate than *df(i)/san,* then the uncovered *san* segment contains a recessive allele involved in HI. If *FM7/san* hybrids

survive at a lower rate than *df(i)/san* hybrids, then the absent *mel* segment contains a dominant (or semi-dominant) allele involved in HI. The initial screening using the line *san* Carv2015.16 showed that hybrid females with a deletion for the X_{mel} region between 3A2 and 3A3 (which contains gt_{mel}) are more viable than hybrid females that carry the balancer chromosome with gt_{mel} (*df/san* to *FM7/san* ratio ≈ 2:1; Figure 3A). The minimal interval that harbors the female HI determinant contains six genes, one of them being *gt*.

We further refined the genetic analysis of this region by testing null alleles of the genes in the interval. Of the four genetically characterized genes in the mapped interval, 3A3, only mutants of gt_{mel} lead to an increase of female hybrid viability (Table S7). Females that carry gt_{mel} (*FM7::GFP/san*) emerged at a lesser frequency than their null allele-carrying sisters (gt_{mel}^{x11}*/san* Figure 3B, Table S7). This difference in viability holds when other *X*-chromosome balancers are used as well (Figure S9).

The abdominal ablation defect that is characteristic of *mel/san* males is also present in some proportion of *mel/san* female embryos that die (Gavin-Smyth and Matute 2013; Matute and Gavin-Smyth 2014). We next tested whether gt_{mel} causes abdominal ablations in female as it does in male hybrids. gt_{mel}-carrying females (*FM7::GFP/san;* Figure 3B) have abdominal ablations more frequently than their gt_{mel}^{x11}*/san* sisters (Figure 5B; t-test comparing the frequency of ablations in $FM7/X^{san}$ males and gt^{x11}/X^{san} females $t = 6.853$, $df = 16.147$, $P = 3.699 \times 10^{-6}$). These results indicate that gt_{mel}, the primary genetic determinant of the abdominal ablation in male *mel/san* hybrids, is sufficient to render some hybrid females inviable by inducing abdominal ablations. This trait varies across *san* lines, however, ranging from little inviability (e.g., *san* SYN2005, *df/san* to *FM7/san* ratio ≈ 1:1; Figure 3C) to almost complete inviability (e.g., *san* Rain42; *df/san* to *FM7/san* ratio ≈ 4:1; Figure 3C, Figure S4).

Two genes adjacent to *gt*, *CG32797* and *CG12496* have no available mutant stocks. The former, *CG32797*, is not expressed in embryos (Kaminker *et al.* 2002; Brown *et al.* 2014) and is an unlikely candidate to cause embryonic inviability in *mel/san* hybrids. *CG12496* is expressed in the early embryos (2-14 hours after egg laying, (Kaminker *et al.* 2002; Brown *et al.* 2014)), so an undetectable role in HI cannot be excluded. However, the results for the gt^{mel} allele explain a large proportion of the inviability and abdominal ablation phenotypes we observe with the larger deletion

(Figure 3B, Figure S10).

These effects of gt^{mel} are specific to the *mel/san* hybrid background, as crosses between gt^{X11}*/FM7::GFP* and males from *D. simulans*, *D. mauritiana* (Figure S11), and multiple lines of *D. melanogaster* (Figure S12) all yielded the 1:1 expectation of balancer and null-allele progeny. Taken together, the mapping efforts are consistent and reveal that the gt^{mel} allele is: (1) necessary and sufficient to cause abdominal ablation defects; (2) contributes to hybrid inviability in both male and female *mel/san* hybrids; and (3) causes defects in that are specific to hybrids that have a *san* father.

Transgenic swaps confirm *D. melanogaster gt* causes hybrid inviability

To identify the specific region(s) of the *gt* locus responsible for causing *mel/san* hybrid inviability, we generated whole-locus *gt* transgenes from *mel* and *san*, as well as coding/noncoding chimeras between them, which we integrated into the *D. melanogaster* 3rd chromosome docking site attP2 (Groth *et al.* 2004; Bischof *et al.* 2007); we replaced the endogenous gt_{mel} with these *gt* transgenes in flies carrying the *gt* null allele gt_{mel}^{X11} (Figure S13). The whole-locus gt_{mel}, also designated $gt_{mel:mel}$ to identify the species source of coding and noncoding regions respectively, is a ~27kb segment of DNA that rescues lethality in the gt_{mel}^{X11}null mutant (Manu *et al.* 2013). First, we asked whether the *gt* transgenes might carry cryptic functional elements, different from *gt* itself, that might affect viability. To disrupt the function of *gt* specifically, a ~1.73kb removable piggyBac cassette was inserted into the 5'UTR of every *gt* transgene to conditionally eliminate the gene product (Figure S13B). All of them failed to restore viability in a gt_{mel}^{X11} mutant (Table S8). To restore the wildtype transgene allele, a piggyBac transposase was employed to remove the piggyBac cassette (Thibault *et al.* 2004). This precise excision, confirmed with sequencing, does not leave behind any additional DNA. Each pair of *gt* transgenes with or without the piggyBac cassette have identical genetic backgrounds. The restored *gt* transgenes rescue lethality in a gt_{mel}^{X11} mutant (Tables 1 and 2). Thus, transgene *gt* expression itself is necessary for viability in this rescue assay.

We carried out three sets of crosses with the pure-species and chimeric transgenes (Figure S13) to measure *gt* contribution in hybrids to embryonic viability (Figure S13C), and female adult viability (Figure S13D). We first measured the relative viability of

transgene alleles in gt_{mel}^{X11}/san hybrid embryos (sexes pooled). *mel/san* hybrids carrying gt_{mel}^{X11} and the $gt_{mel:mel}$ transgene show a high prevalence of the embryonic lethal phenotype (Table 1). $gt_{san::mel}$, an allele with the gt_{san} non-coding DNA and the coding sequence from gt_{mel}, caused the embryonic lethality in *mel/san* hybrids at a similar rate than that caused by $gt_{mel:mel}$ (Table 1). In contrast, $gt_{mel:san}$, an allele with the gt_{mel} non-coding and gt_{san} coding, increased viability compared to $gt_{mel:mel}$ hybrids (Table 1). Notably, the $gt_{san::san}$ allele, which has the full gt_{san} allele, shows viability comparable to that of $gt_{mel:san}$ carriers ($X^2_1 = 0.075$, P = 0.784), but higher than chimeras carrying the gt_{mel} coding sequence ($gt_{san::mel}$ and $gt_{mel::mel}$, $X^2_1 > 4.98$, P < 0.026; Table 1). These results point to the coding region of gt_{mel} alone as being necessary for embryonic hybrid inviability.

We next evaluated the effects of these gt transgenes on a different metric of hybrid fitness – female viability. We crossed *san* males to *mel* females that were homozygous for gt_{mel}^{X11} and hemizygous for each of the four *gt* transgenes; the resulting female progeny from this cross was hybrid females carries gt_{mel}^{X11}/gt_{san} *X*-chromosomes and either a *gt* transgene or a wildtype 3_{mel} chromosome lacking a transgene (Figure S13D). The effect of the transgene on hybrid female viability can then be measured the ratio of flies with the transgene to flies with the wildtype 3_{mel} chromosome. The results are largely consistent with the results from scoring embryonic lethality: one copy of the $gt_{mel:mel}$ allele reduces hybrid female adult viability compared to hybrids females without the same transgene. This finding with transgenic *gt* is also consistent with the deficiency mapping results using *X*-chromosome balancers. Hybrid females with one $gt_{san:mel}$ allele also show a reduction of viability similar to the one observed in $gt_{mel:mel}$ carriers (Table 2); the reciprocal chimeric allele —$gt_{mel:san}$—, caused no reduction in relative viability. Finally, we find that the $gt_{san:san}$ transgene increases hybrid female adult viability compared to the control (Table 2). This increase in viability can only be explained by an epistatic interaction between coding and noncoding regions of gt_{san}, as neither the coding nor the non-coding region of gt^{san} alone confers such an increase of hybrid female viability. These results collectively suggest that the inviability is mainly attributable to coding region of gt_{mel}, consistent with its predominant role in hybrid embryonic lethality.

314 *tll_{mel} exacerbates the hybrid inviability caused by gt_{mel}*

315 Hybrid defects are usually caused by at least two interacting elements (reviewed
316 in (Maheshwari and Barbash 2011; Nosil and Schluter 2011)). *Giant* is an essential factor
317 in the gap gene regulatory network, a set of interacting genes expressed in the blastoderm
318 embryo to establish anterior-posterior patterning (Petschek *et al.* 1987; Mohler *et al.*
319 1989; Eldon and Pirrotta 1991; Kraut and Levine 1991); its function in segmentation as a
320 reciprocal transcriptional repressor of other gap genes (*Kruppel* and *knirps*; (Kraut and
321 Levine 1991; Capovilla *et al.* 1992; Wu *et al.* 1998)) is conserved in arthropods. *giant* is
322 itself repressed by the gene products of *hunchback* (Eldon and Pirrotta 1991; Kraut and
323 Levine 1991; Struhl *et al.* 1992), *tailless* (Reinitz and Levine 1990), and *hucklebein*
324 (Brönner *et al.* 1994). The proteins *Caudal* (Schulz and Tautz 1995) and *Bicoid* (Eldon
325 and Pirrotta 1991; Rivera-Pomar *et al.* 1995) activate *gt*, which localizes to two broad
326 stripes, one towards the anterior and one towards the posterior pole of the embryo
327 (reviewed in (Jaeger 2011)). Given this knowledge, we hypothesized that gap genes
328 interacting with gt_{mel} could be additional candidates contributing to inviability in *mel/san*
329 hybrids.

330 Even though gt_{mel} is involved in generating abdominal ablations, hybrids with no
331 functional gt_{mel} allele also show abdominal ablations but at lower frequency (Figure 3B,
332 (Matute and Gavin-Smyth 2014)). This means that other alleles in the genome are
333 involved in producing the maladaptive trait. We introgressed a gt_{mel}^{X11} allele into the
334 background of 200 DGRP (*Drosophila* Genetic Reference Panel) lines (Figure S14) to
335 assess whether autosomal variants segregating within *mel*, other than those in gt_{mel}, would
336 affect the frequency of abdominal ablations in hybrids. Using GWAS, we found a strong
337 association between a 75.7kb haplotype in 3L which harbors nine genes: *cindr*,
338 *CG15544*, *tll*, *Cpr100A*, *CG15545*, *CG15546*, *CG15547*, *CG12071*, and *Sap-r* (Figure 4).
339 Of these nine, the only gene known to interact with *gt* is *tll*.

340 To determine whether the two genes interact genetically in causing HI, we
341 generated double mutant females carrying loss of function mutations of *gt* and *tll*
342 (gt^{X11}*/FM7::GFP,* $tll_{mel}^{\Delta GFP}$*/TM3 Ser Sb*) and crossed them to *san* males. First, we scored
343 whether the presence of tll_{mel} had any effect on hybrid female viability by itself. We
344 found no effect of tll_{mel} in hybrid female viability in an otherwise heterozygote F1

background (*FM7::GFP /X$_{san}$, tll$_{mel}^{\Delta GFP}$/3^{san}*vs. *FM7::GFP /X$_{san}$, TM3 Sb /3$_{san}$*; Table 3). Next, we scored whether the presence of *tll$_{mel}$* had an effect on hybrid female viability in a *gt$_{mel}^{x11}$* background. Hybrid *mel/san* females that have only a functional copy of *gt$_{san}$* (i.e., carry a *gt$_{mel}^{x11}$* allele) and are hemizygous for *tll* (i.e., only have *tll$_{san}$*) are more likely to survive to adulthood than *gt$_{mel}^{x11}$*-carrying females and a functional *tll$_{mel}$* (*gt$_{mel}^{X11}$/X$_{san}$, tll$_{mel}^{\Delta GFP}$/3$_{san}$* vs. *gt^{X11}/X$_{san}$,TM3, Sb /3$_{san}$* Table 3A). These results suggest that while removing *tll$_{mel}$* on its own has no major effect on HI, removing both *gt$_{mel}$* and *tll$_{mel}$* has a positive effect in viability that is larger than removing either allele individually.

tll$_{mel}$ also has a role in the frequency of abdominal ablations. Abrogating *tll$_{mel}$* in a *gt$_{mel}$/gt$_{san}$* background has no detectable effect in the frequency of abdominal ablations in hybrid males or hybrid females with a functional copy of *gt$_{mel}$* (*FM7/X$_{san}$,tll$_{mel}^{\Delta GFP}$/3$_{san}$*vs. *FM7/X$_{san}$,TM3 Sb /3$_{san}$*, Table 3B and 3C). In a *gt$_{mel}^{x11}$* background, abrogating *tll$_{mel}$* decreases the proportion of male and female embryos showing abdominal ablations (Table 3). These results suggest —just as occurs with female viability— the absence of *gt$_{mel}$* and *tll$_{mel}$* together has a larger positive effect than the absence of each allele individually. Table S9 shows similar analyses with a different *tll* loss-of-function allele. Notably, in the conspecific crosses and the three possible interspecific crosses between *D. melanogaster* females and males from other species, *gt$_{mel}^{X11}$* and *tll$_{mel}^{\Delta GFP}$* have no effects on viability (Table S10).

Finally, we tested the effect of disrupting the *tll$_{san}$* in hybrids. *tll$_{san}^{\Delta dsRed}$* did not rescue *tll$_{mel}^{\Delta GFP}$* in hybrids. In *mel/san* hybrids, the *tll$_{san}^{\Delta dsRed}$* deletion had no effect on female viability when tested in hybrids with multiple *mel* backgrounds (Table S11). This result suggests that removing *tll$_{san}$* in *mel/san* hybrids has no effect on hybrid viability in an otherwise heterozygote hybrid background. Next, we tested the effect of *tll$_{san}^{\Delta dsRed}$* in the null-*gt$_{mel}$*, *gt$_{mel}^{x11}$* background. We find that the *tll$_{san}$* deletion does not improve viability in *gt$_{mel}^{x11}$*-carrying *mel/san* females either (Table S12). These results suggests that even in the absence of a functional *gt$_{mel}$* allele, removing *tll$_{san}$* has no effect on hybrid female viability. Since the reciprocal deletion (removing *tll$_{mel}$* and exposing the *tll$_{san}$* allele) does improve female hybrid viability in *gt$_{mel}^{x11}$*-carriers, these results indicate that the presence of *tll$_{mel}$*, but not of *tll$_{san}$*, is involved in the HI of *mel/san* female hybrids.

Molecular Evolution

Gap genes *gt* and *tll* have phylogenetically conserved roles in pattern formation, as evidenced by their functionally conserved outputs in blastoderm embryos of distantly related *Drosophila* species (Hare *et al.* 2008a) and beyond (Bucher 2004; Wilson *et al.* 2010). Yet, they have diverged sufficiently between *mel* and *san* such that they malfunction in hybrids. We therefore conducted analyses to assess the patterns and mechanism of divergence of the *gt* coding sequence in the *melanogaster* species subgroup and across the *Drosophila* genus.

Both *gt* and *tll* are highly conserved in their coding regions. The bZip domain that confers Gt protein its ability to bind DNA is highly conserved across animals (Nitta *et al.* 2015) and shows no fixed differences among *Drosophila* species (Figure S15, Chang et al. 2021). Gt shows only thirteen single amino acid substitutions in the *melanogaster* species subgroup (Figures S15 and S16), six of which occur on the branches connecting *mel* and *san*. *Giant* also contains three low complexity regions (including polyQ) that show extensive variation both within and between species (Figure S17). *tll* is also conserved in the *melanogaster* species subgroup*;* only four residues differ between the *tll* alleles in the *yakuba* clade and the *melanogaster* clade: Val509Asp, Arg1118Lys, Ser1208Thr, Leu1246Met (Figure S18). Only Val509Asp represents a change in the type of amino acid (a change from a nonpolar to an acidic residue).

We also investigated whether substitutions in these two genes might have been driven by adaptive evolution. Both genes, *gt* and *tll*, fall within the slowest-evolving quantile of genes comparing *mel* with *yak* or *san* (25% and 10% respectively) and, noting the limited power to detect selection as a result, show no signature of accelerated evolution (Table S13).

<u>DMI partner(s) of gt^{mel} is (are) unique to the *D. santomea* lineage</u>

The phylogenetic occurrence of developmental defects provides an additional hypothesis to test: we next evaluated whether the unknown genetic element(s) in the *D. santomea* genome that must interact with gt_{mel} and tll_{mel} (gt_{sim}) to cause HI are also present in *D. teissieri* (a close relative of *D. santomea*, Figure 1A). The crosses ♀*mel* ×

406 ♂*tei*, ♀*sim* × ♂*tei* and ♀*mel* × ♂*tei* all produce viable adult females and males that die as
407 late larvae/early pupae. Little embryonic lethality is observed in any of these two crosses
408 and the rare embryos that die do not show abdominal ablations (Figure 1E, Figure S1).
409 All *D. teissieri* lines showed similar levels of viability in each cross (Figure S19). These
410 results suggest that at least one of the partners of this incompatibility is specific to *san*,
411 and evolved after *san* and *tei* diverged.
412
413

DISCUSSION

Hybrid inviability is a strong barrier to gene exchange between species. While it is clear that this trait is often caused by epistatic interactions between alleles from different species, few examples have been identified to the gene level. Here, we identified two genes, *gt* and *tll,* which contribute to HI in hybrids between two *Drosophila* species. The two genes belong to the gap gene network, a highly conserved pathway that is in charge of establishing embryonic polarity in insects (Bucher 2004; Goltsev *et al.* 2004; Hare *et al.* 2008a; Wilson *et al.* 2010; Crombach *et al.* 2014; Wotton *et al.* 2015; Crombach *et al.* 2016). The *mel* alleles of these two genes are necessary and sufficient to cause a male abdominal ablation phenotype that is particularly common in hybrid males of the cross. We also find support for a third (or even more) elements that are exclusive to *D. santomea* and remain unidentified. Additional members of the gap gene network must have functionally diverged between the two species and contribute to HI. These are not the only alleles that contribute to inviability in the cross but are sufficient to cause the abdominal ablation defect that is particularly common in hybrid males of the cross (Gavin-Smyth and Matute 2013; Matute and Gavin-Smyth 2014).

The involvement of gt_{mel} and tll_{mel} in HI indicates that one or more features of their function have diverged between relatively closely related species, despite their borad conservation across the Diptera ((Goltsev *et al*. 2004; Hare *et al*. 2008a; Crombach *et al*. 2014; Wotton *et al*. 2015); but see (García-Solache *et al*. 2010; Janssens *et al*. 2014; Crombach *et al*. 2016)), bees (Wilson *et al*. 2010) and beetles (Bucher 2004; Cerny *et al*. 2008). Our results confirm speculation that HI can arise in phylogenetically conserved gene networks regulating development (True and Haag 2001; Ludwig *et al*. 2005; Schiffman and Ralph 2021). The involvement of gt_{mel} and tll_{mel} in HI suggests that their function has diverged across *Drosophila* species. Consistent with this result, precise gene replacements have also shown that *gt* alleles from different species vary in the ability to complement in a *D. melanogaster* background (Chang *et al*. 2021). Natural selection has driven the evolution of regulatory elements of many developmental genes in *Drosophila* which has led to a rapid turnover (Hare *et al*. 2008a; b; He *et al*. 2011; Ni *et al*. 2012). Yet, neither *gt* nor *tll* show signatures of positive selection in their coding sequences. Our results also suggest that the evolution of the different components involved in the DMI occurred at different times and is unlikely to have had any role on speciation. The deleterious effects caused by gt_{mel} seem to be common to *D. melanogaster* and

446 the species in the *D. simulans* clade, suggesting that the allele necessary for the
447 incompatibility evolved before these species split between three and five million years
448 ago (Tamura *et al*. 2004; Suvorov *et al*. 2021). Because the presence of gt^{mel} has no
449 quantifiable viability effect in *mel/tei* hybrids, at least one of the genetic factor(s) that
450 interact with gt^{mel} to cause abdominal ablation in hybrid embryos must have arisen after
451 *D. santomea* and *D. teissieri* split between 1 and 2.5 million years ago (Bachtrog *et al*.
452 2006; Turissini and Matute 2017). An alternative divergence scenario is that at least one
453 of the genetic components of the DMI evolved in the *tei* branch to suppress HI.
454 Regardless of which of these two scenarios is correct, the components of the DMI must
455 have evolved at different times in the two lineages, and the interactions with *giant* that
456 cause abdominal ablation could not have been involved with any speciation event in the
457 *melanogaster* species subgroup (Figure S11). Instead, these loci must have evolved
458 independently in each lineage, accumulating differences as the genomes diverged after
459 speciation, a scenario in accord with the Dobzhansky Muller model (Dobzhansky 1937;
460 Muller 1942; Coyne and Orr 2004; Matute *et al*. 2010; Moyle and Nakazato 2010; Wang
461 *et al*. 2015). Mapping the allele(s) that interact with gt^{mel} and tll^{mel} in the *D. santomea*
462 genome is the next step in describing how genomic divergence creates hybrid defects.

463 Previous comparative analyses of gap gene expression in dipterans indicates gene
464 network evolution in spite of a conserved developmental phenotype (Wotton *et al.* 2015),
465 which suggests continual fine-tuning of the genetic interactions in the gap gene network
466 within species. Coevolved compensatory changes have been proposed to cause HI in
467 instances in which the phenotypic output of a gene network is under moderate stabilizing
468 selection (Kondrashov *et al*. 2002; Johnson and Porter 2007; Tulchinsky *et al*. 2014;
469 Mack and Nachman 2017). Molecular functional evolution without phenotypic change, or
470 developmental systems drift, has been hypothesized to underlie hybrid breakdown
471 involving canalized traits such as embryogenesis and gametogenesis (True and Haag
472 2001). The HI involving gt_{mel} and tll_{mel} may exemplify compensatory changes resulting in
473 a stable phenotype when comparing pure species, but in an aberrant phenotype in
474 hybrids.

The introduction of a developmental genetics perspective to speciation studies has the potential to shed new light on the study of hybrid inviability (Cutter and Bundus 2020). Hybrid inviability is a natural experiment to test genetic interactions between diverging genomes: the molecular interactions that go awry in hybrids reveal evolutionary divergence of the genes involved, or the timing, location, or amount of their expression (Mack and Nachman 2017). The interactions between gt_{mel}, tll_{mel} and the unknown factors in the genome of *D. santomea*, had nothing to do with setting the speciation process in motion in the *melanogaster* species subgroup. They are also not involved in currently keeping species apart as *D. melanogaster* and *D. santomea* do not naturally hybridize. The results shown here should be viewed in the broad context of genome divergence and how genomes keep evolving long after speciation has occurred. This represents a path forward in terms of how to think about stability vs. change of different functional units within the genome and different developmental processes. The identification of *giant* and *tll* as genes involved in HI is the first indication that genes involved in early embryonic development, a canonical example of a conserved developmental process, functionally co-evolve at a pace sufficient to cause hybrid inviability.

493 **FIGURE 1. All the *X* chromosomes from the *mel* supercomplex cause inviability in**
494 ***mel/san* hybrids but not in *mel/tei* hybrids.** Unlike pure species (**A**. *D. santomea*; **B**. *D.*
495 *melanogaster*), F1 *mel/san* hybrid males show abdominal ablations (**C**). The nature of the
496 defect in these hybrid males is identical to that seen in *sim/san* and *mau/san* hybrid males.
497 Females from the same cross also show such ablations but more rarely and the majority
498 of dead embryos show a complete abdomen (Figure S8). Hybrids between females from
499 the *melanogaster* supercomplex and *D. teissieri* males show little embryonic lethality and
500 among the few dead embryos there are no abdominal ablations (e.g., **D.** *mel/tei* hybrid
501 male). The viability of each genotype is shown in Figure S1. **E**. Phylogenetic
502 relationships between the species of the *melanogaster* species subgroup. The heatmap
503 shows the relative occurrence of abdominal ablations in hybrid males. White: common,
504 grey: absent. Black: pairs with complete behavioral isolation.

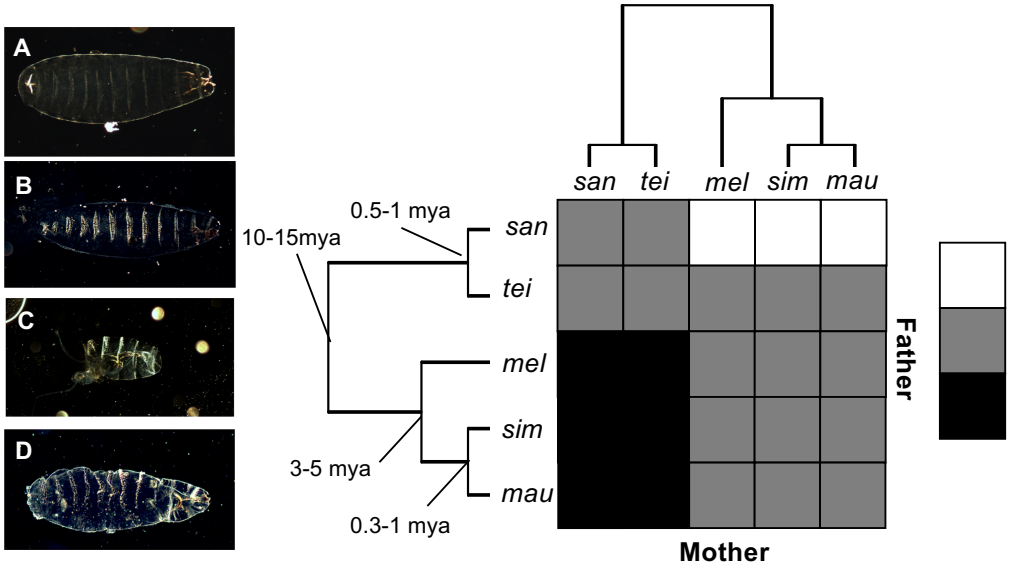

FIGURE 2. A *D. melanogaster X*-chromosome haplotype that encompasses gt^{mel} is associated with hybrid inviability and abdominal ablations in ♀ *D. melanogaster*/♂ *D. santomea* hybrid males. A. Genome-wide association study of the genetic causes of hybrid inviability in *mel/san* hybrids (both sexes pooled) using segregating variation within *D. melanogaster*. A haplotype of 54kb in the tip of the *X*-chromosome is strongly associated with the presence of abdominal ablations. The haplotype harbors six genes: *CG32797, gt, tko, boi, z,* and *trol.* **B.** Genome-wide association study of the genetic causes of abdominal ablations in *mel/san* hybrids (both sexes pooled) using segregating variation within *D. melanogaster*. A haplotype of 54kb in the tip of the *X*-chromosome is strongly associated with the presence of abdominal ablations. The haplotype harbors six genes: *CG32797, gt, tko, boi, z,* and *trol.* Green: insertions, blue: deletions, red: SNPs, purple: multinucleotide polymorphisms. Green: insertions (INS), blue: deletions (DEL), red: SNPs, purple: multinucleotide polymorphisms (MNP). **C.** We introduced small X^{mel} pieces attached to Y_{mel} to identify X_{mel}-linked alleles that cause hybrid inviability in in *mel/san* hybrids males. For all *Dp(1;Y)* duplications, we evaluated at least 50 embryos per cross were for viability. For *Dp(1;3)* duplications, we evaluate between 20-56 embryos as *C(1) DX, Dp(1;3)/ Dp(1;3)* are weak. We narrowed down the allele that causes HI to an interval of X^{mel} comprising 3A3 which only contains *giant*. White bars show duplications with no abdominal ablations. The light grey bar shows a duplication with a moderate rate of abdominal ablations; dark grey show duplications with high levels of abdominal ablations. **D.** Relative frequency of abdominal defects in five different hybrid genotypes from *D. melanogaster* and *D. santomea* crosses. Pure species embryos show no abdominal defects and show little embryonic lethality. *mel/san* hybrid males (X^{mel}/Y^{san}) frequently show a lethal characteristic abdominal ablation (red points) that is also present in some *mel/san* hybrid females (blue points). The reciprocal *mel/san* hybrid males (X^{san}/Y^{mel}) routinely survive and the few embryos who die do not show abdominal ablations (red points). X^{san}/Y^{mel} males carrying X-Y translocations [i.e., *Dp(1;Y)* in blue and *Dp(1;Y)* in red] that harbor gt^{mel} also show this lethal ablation. Dp1: *Dp(1;Y)BSC78* (stock 29802); Dps: *Dp(1;Y)BSC79* (stock 29803). A map showing the frequency of abdominal defects caused by multiple X^{mel} translocation is shown in Figure S2.

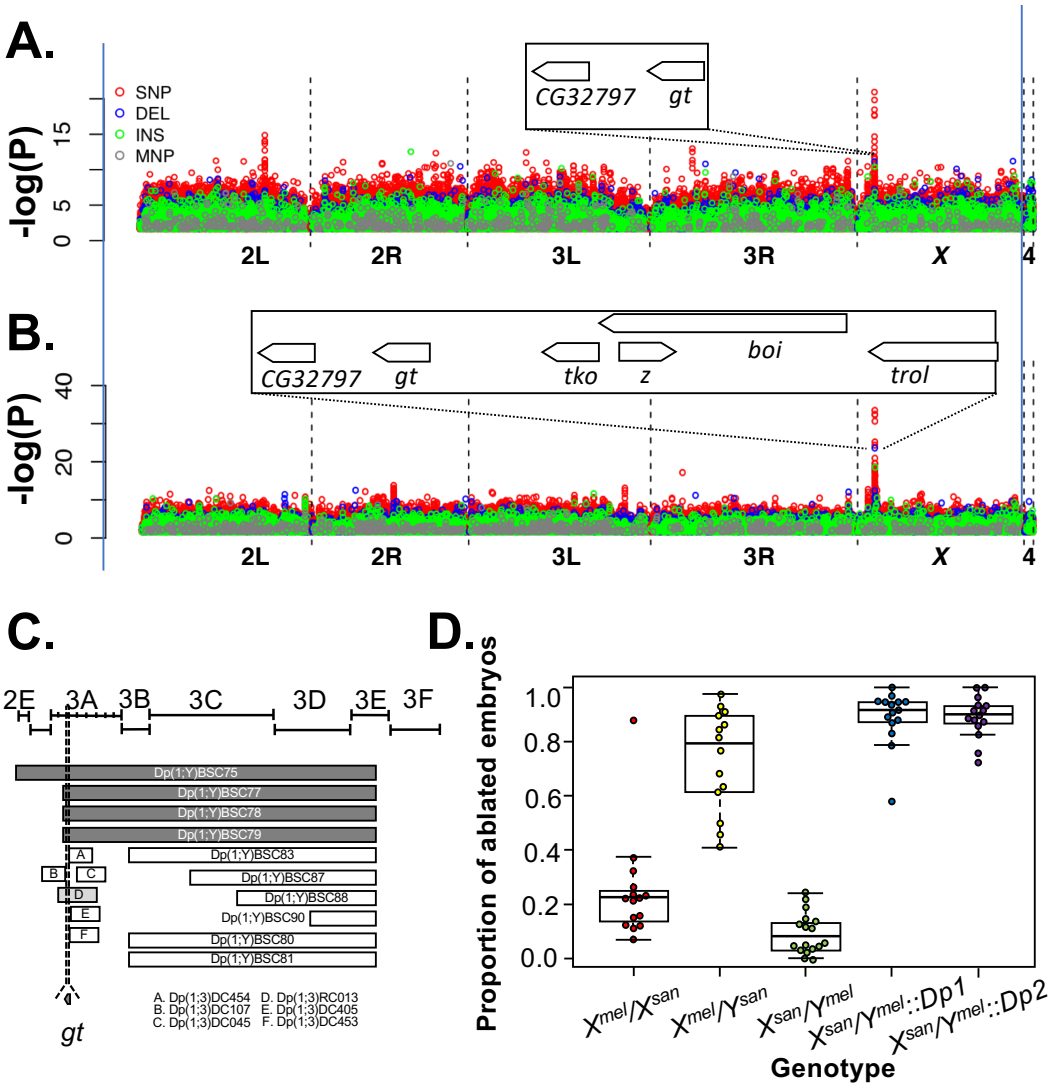
A.
SNP
DEL
INS
MNP
-log(P)
0
5
15
CG32797
gt
2L
2R
3L
3R
X
4
B.
-log(P)
0
20
40
CG32797
gt
tko
z
boi
trol
2L
2R
3L
3R
X
4
C.
2E
3A
3B
3C
3D
3E
3F
Dp(1;Y)BSC75
Dp(1;Y)BSC77
Dp(1;Y)BSC78
Dp(1;Y)BSC79
Dp(1;Y)BSC83
Dp(1;Y)BSC87
Dp(1;Y)BSC88
Dp(1;Y)BSC90
Dp(1;Y)BSC80
Dp(1;Y)BSC81
A
B
C
D
E
F
gt
A. Dp(1;3)DC454
B. Dp(1;3)DC107
C. Dp(1;3)DC045
D. Dp(1;3)RC013
E. Dp(1;3)DC405
F. Dp(1;3)DC453
D.
Proportion of ablated embryos
0.0
0.2
0.4
0.6
0.8
1.0
Xmel/Xsan
Xmel/Ysan
Xsan/Ymel
Xsan/Ymel::Dp1
Xsan/Ymel::Dp2
Genotype

537

538

FIGURE 3. *giant*^{mel} causes HI and abdominal ablations in *mel/san* females. **A**. Deficiency mapping and null-allele mapping revealed that *giant* also causes hybrid inviability in hybrid females. Grey: deficiencies that increase viability of *mel/san* F1 hybrid females (Significant linear contrasts, $P < 0.05$ after multiple comparison corrections). White: deficiencies that do not increase viability. **B.** When females fail to hatch, it is not uncommon for them to be abdominally ablated. The presence of gt_{mel} increases the frequency of abdominal ablations. **C.** Relative $gt_{mel}{}^{X11}/X_{san}$ female viability (i.e., proportion of $gt_{mel}{}^{X11}$ carriers in hybrid crosses) in twenty *D. santomea* isofemale lines. Boxes in the boxplot are ordinated from the lower median (left) to the highest (right). S1: SYN2005; S2: sanCAR1490; S3: sanCOST1250.5; S4: sanCOST1270.1; S5: sanOBAT1200; S6: sanOBAT1200.2; S7: sanRain39; S8: sanCAR1600.3; S9: Carv2015.1; S10: Carv2015.5; S11: Carv2015.11; S12: Carv2015.16; S13: Pico1680.1; S14: Pico1659.2; S15: Pico1659.3; S16: Amelia2015.1; S17: Amelia2015.6; S18: Amelia2015.12; S19: A1200.7; S20: Rain42.

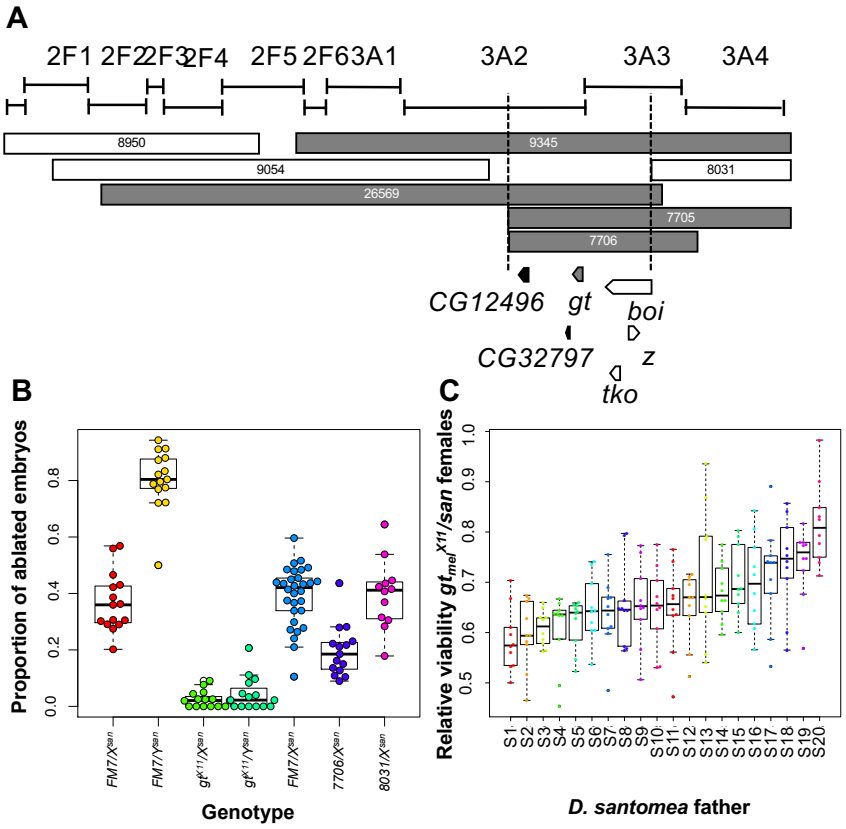
A
2F1 2F2 2F3 2F4 2F5 2F6 3A1 3A2 3A3 3A4
8950
9345
9054
8031
26569
7705
7706
CG12496
gt
boi
CG32797
z
tko
B
Proportion of ablated embryos
0.0
0.2
0.4
0.6
0.8
FM7/X^san
FM7/Y^san
gt^X11/X^san
gt^X11/Y^san
FM7/X^san
7706/X^san
8031/X^san
Genotype
C
Relative viability gt_mel^X11/san females
0.5
0.6
0.7
0.8
0.9
1.0
S1 S2 S3 S4 S5 S6 S7 S8 S9 S10 S11 S12 S13 S14 S15 S16 S17 S18 S19 S20
D. santomea father

FIGURE 4. A *D. melanogaster* third-chromosome haplotype that encompasses *tll* is associated with the prevalence of abdominal ablations in gt^{X11} mutants. Association study of autosomal genetic variants associated with the frequency of abdominal ablations in gt^{X11}/X^{san} hybrids using segregating variation within *D. melanogaster*. A haplotype of 54kb in the tip of the *X*-chromosome is strongly associated with the presence of abdominal ablations in both males (**A**) and females (**B**). Each panel shows a different chromosome arm. The haplotype 9 genes: *cindr*, *CG15544*, *tll*, *Cpr100A*, *CG15545*, *CG15546*, *CG15547*, *CG12071*, and *Sap-r.* Of these nine, *tll* is the only one known to interact with *gt*. Green: insertions, blue: deletions, red: SNPs, purple: multinucleotide polymorphisms.

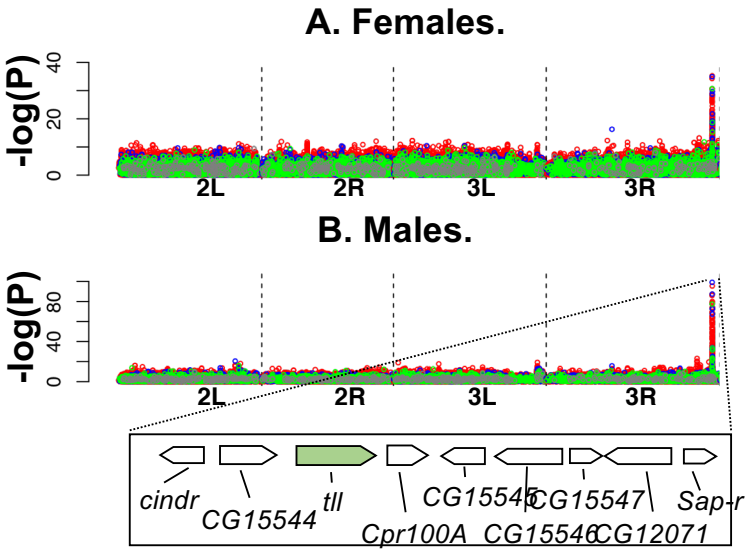
A. Females.
-log(P)
0
20
40
2L
2R
3L
3R
B. Males.
-log(P)
0
40
80
2L
2R
3L
3R
cindr
CG15544
tll
Cpr100A
CG15545
CG15546
CG15547
CG12071
Sap-r

565

566

TABLE 1. The coding region of gt_{mel} causes embryonic lethality in *mel/san* hybrids. All *gt* proteins were tagged with eGFP. We used a 2-sample test for equality of proportions to compare the proportion of dead embryos in *mel/san* gt_{mel}^{X11}, $gt_{mel:mel}$ carriers with the other three transgenes. df=1 for all tests.

Allele	Non-coding	Coding	Hatched Embryos	Dead Embryos	Relative Embryonic Lethality	χ^2	P
$gt_{mel:mel}$	*mel*	*mel*	40	17	0.298	NA	NA
$gt_{san:mel}$	*san*	*mel*	66	20	0.303	0.467	0.495
$gt_{mel:san}$	*mel*	*san*	90	10	0.100	8.676	3.22×10^{-3}
$gt_{san:san}$	*san*	*san*	51	4	0.091	7.922	4.88×10^{-3}

TABLE 2. The coding region of gt_{mel} causes female inviability in hybrid *mel/san* females. The coding region of while gt_{san} increases female hybrid viability. We used a χ^2 test to compare the number of females carrying the transgene and those without it. df=1 for all tests.

Allele	Non-coding	Coding	F_1 females with a *gt* transgene	F1 females with a 3_{mel} chromosome	Relative Hybrid Viability	χ^2	P
$gt_{mel:mel}$	*mel*	*mel*	86	116	0.741	4.455	0.035
$gt_{san:mel}$	*san*	*mel*	143	188	0.761	6.118	0.013
$gt_{mel:san}$	*mel*	*san*	173	180	0.961	0.139	0.710
$gt_{san:san}$	*san*	*san*	81	56	1.45	4.562	0.033

TABLE 3. tll_{mel} exacerbates the defects caused by gt_{mel} in *mel/san* hybrids. A. Females that carry functional gt_{mel} and tll_{mel} alleles are more likely to die than females that carry an abrogation of gt_{mel} (regardless of the genotype at *tll*) or that carry a functional gt_{mel} and a null allele of tll_{mel}. Tests with a different *tll* loss of function allele

show similar results (Table S6). **B.** *mel/san* hybrid males with functional copies of gt_{mel} and tll_{mel} are more likely to show abdominal ablations than hybrid males with an abrogated copy of tll_{mel}, an abrogated copy of gt_{mel}, or abrogated copies of both. **C.** Similar to males**,** *mel/san* hybrid females with functional copies of gt_{mel} and tll_{mel} are more likely to show abdominal ablations than hybrid males with an abrogated copy of tll_{mel}, an abrogated copy of gt_{mel}, or abrogated copies of both. In all three cases, we used a χ^2 proportion test for the two pairwise comparisons.

A. Female hybrid viability				
	FM7; sqh::mCherry/X_{san}; TM3, Act::GFP, Ser/3_{san}	*FM7; sqh::mCherry/X_{san}; $tll_{mel}^{\Delta GFP}/3_{san}$*	*gt_{mel}^{X11}; /X_{san}; TM3, Act::GFP, Ser/3_{san}*	*gt_{mel}^{X11}; /X_{san}; $tll_{mel}^{\Delta GFP}/3_{san}$*
	43	51	97	153
	χ^2_1=0.681, P=0.409		χ^2_1=12.544, P=3.975 × 10^{-4}	
B. Proportion of male embryos showing abdominal ablations (100 embryos each)				
	FM7; sqh::mCherry/Y_{san}; TM3, Act::GFP, Ser/3_{san}	*FM7; sqh::mCherry/Y_{san}; $tll_{mel}^{\Delta GFP}/3_{san}$*	*gt_{mel}^{X11}; /Y_{san}; TM3, Act::GFP, Ser/3_{san}*	*gt_{mel}^{X11}; /Y_{san}; $tll_{mel}^{\Delta GFP}/3_{san}$*
	94	88	23	9
	χ^2_1= 1.526, P= 0.217		χ^2_1= 6.287, P = 0.012	
C. **Proportion of female embryos showing abdominal ablations (100 embryos each)**				
	FM7; sqh::mCherry/X_{san}; TM3, Act::GFP, Ser/3_{san}	*FM7; sqh::mCherry/X_{san}; $tll_{mel}^{\Delta GFP}/3_{san}$*	*gt_{mel}^{X11}; /X_{san}; TM3, Act::GFP, Ser/3_{san}*	*gt_{mel}^{X11}; /X_{san}; $tll_{mel}^{\Delta GFP}/3_{san}$*
	48	35	16	6
	χ^2_1= 2.966, P= 0.085		χ^2_1= 4.137, P= 0.042	

SUPPLEMENTARY MATERIAL

TABLE OF CONTENTS

species complex.

TABLE S2. Hybrids between *D. melanogaster* females and *D. simulans* and *D. mauritiana* show no abdominal ablations or embryonic lethality.

TABLE S3. Mutant stocks used in this study

TABLE S4. *C(1)DX, Dp(1;3)/TM3* lay few eggs are thus not ideal to measure the magnitude of HI in crosses with *D. santomea*.

TABLE S5. The cross involved a gt_{mel}^{X11}/*FM7* female and a male hemizygote for the duplication.

TABLE S6. Isofemale lines from 4 species used to assess whether HI in *mel/san* hybrids was a species-specific phenomenon or a line specific phenomenon.

TABLE S7. Complementation mapping using loss-of function and hypomorphic alleles show that *gt* mutants are the only alleles in cytological region 3A3 that lead to an increase of female viability in *mel/san* hybrid.

TABLE S8. The *gt*-vector does not carry extraneous elements that rescue the viability of *D. melanogaster* gt_{mel}^{X11}-carriers.

TABLE S9. Confirmation that tll^{mel} exacerbates the defects caused by gt^{mel} in *mel/san* hybrids using a different *tll* mutant.

TABLE S10. Double mutant analysis of survival in hybrids between *D. melanogaster* females and three males from four different species (*D. melanogaster*, *D. simulans*, *D. mauritiana*, and *D. teissieri*).

TABLE S11. A $tll_{san}^{\Delta dsRed}$ has no effect on HI in crosses between *mel* females from four different backgrounds.

TABLE S12. Abrogating the tll_{san} allele has no viability effect in gt_{mel}^{X11} *mel*/san hybrids.

TABLE S13. *gt* and *tll* are slowly evolving genes as measured by the rate of aminoacid substitutions.

TABLE S14. Sequencing details and coverage for all the lines included in this study.

SUPPLEMENTARY FIGURES.

FIGURE S1. X_{mel}, X_{sim} and X_{mau} cause abdominal ablations in hybrid males with *D.*

***santomea*.**

FIGURE S2. Crossing design to assess whether small piece of the X^{mel} cause hybrid inviability and abdominal ablations.

FIGURE S3. Frequency of abdominal ablations caused by the X^{mel} translocations shown in Figure 1 in X^{san}/Y^{mel} hybrid males.

FIGURE S4. The presence of gt^{mel} causes HI in *mel/san* hybrids produced with all *D. santomea* lines but the magnitude of the inviability varies.

FIGURE S5. Crosses between *D. melanogaster* females harboring *Dp(1;Y)* duplications and males from the *simulans* species group (*D. mauritiana*, and *D. simulans*) show no evidence of male embryo lethality or abdominal ablations.

FIGURE S6. Crosses between *D. melanogaster* females harboring *Dp(1;Y)* duplications and males from different lines of *D. melanogaster* show no evidence of male embryo lethality or abdominal ablations.

FIGURE S7. Hybrid male embryos carrying a gt_{mel}^{X11} *D. melanogaster* allele show a variety of developmental defects.

FIGURE S8. *mel/san* hybrids carrying a *D. melanogaster* chromosome and null alleles for *boi*, *trol*, or *tko* show similar levels of hybrid viability, embryonic lethality, and abdominal ablations at the same rate than *FM7::GFP/san*.

FIGURE S9. The *X*-chromosome balancer has no effect on the quantification of hybrid inviability in *mel/san* hybrid females.

FIGURE S10. Frequency of abdominal ablations in each deficiency cross shown in Figure 2.

FIGURE S11. gt^{mel} has no effect on the viability of *mel/tei*, *mel/mau*, and *mel/sim* hybrid females.

FIGURE S12. gt^{mel} has no effect on the viability of *D. melanogaster* F1 females.

FIGURE S13. *gt* transgene, removable piggyBac cassette design and crossing schemes involving *gt* transgenes.

FIGURE S14. Introgression of the *FM7::GFP* and gt^{X11} alleles into 200 lines of the DGRP lines.

FIGURE S15. *gt* alleles from six different species in the *melanogaster* species

690 **complex**.

691 **FIGURE S16. Maximum-likelihood ancestral sequence reconstruction of GT**

692 **protein, excluding polyQ.**

693 **FIGURE S17. The polyglutamine repeats (polyQ) show differences among the**

694 ***melanogaster* subspecies complex species.**

695 **FIGURE S18. *tll* alleles from six different species in the *melanogaster* species**

696 **complex**.

697 **FIGURE S19. Embryonic hybrid inviability does not occur in *mel/tei* hybrids.**

698 **FIGURE S20. Divergence in *giant* in the *melanogaster* species subgroup.**

699 **FIGURE S21. Experimental design to generated a GFP-mediated disruption of tll_{mel}.**

700

701

702

703

METHODS AND MATERIALS

1. STOCKS

1. 1. *Drosophila melanogaster* mutants

With two exceptions (see 1.1.2. *tll* alleles and 1.1.5. *gt* transgenics), all *D. melanogaster* mutant stocks used in this study were originally obtained from the Bloomington Stock Center (BSC) and are listed in Table S1.

1.1.1. gt *alleles*. We obtained multiple *gt* mutant alleles from BSC but we focused on a null allele: gt_{mel}^{X11} (y^1 sc^1 gt^{X11}/*FM6*; BDSC stock #1529). The gt_{mel}^{X11} has a frameshift mutation that abrogates the bZIP DNA-binding domain (Chang *et al.* 2021). First, we confirmed that this stock did not complement a deficiency of *giant* (*Df(1)Exel6231*; BDSC stock #7706) and verified gt^{X11} was indeed a loss-of function allele. To differentiate between embryos carrying the *gt* allele or the balancer, we rebalanced each stock with a *FM7 Actin::GFP* to allow for genotypic distinctions in all further crosses.

1.1.2. tll *alleles*. We used two tll_{mel} alleles. The first one was a loss-of-function allele of *tll*: tll^1 which was procured from the Bloomington Stock center (st^1 e^1 tll^1/*TM3,* Sb^1; BDSC stock #2729). We also obtained a CRISPR-mediated tll_{mel} *GFP* disruption: $tll_{mel}{}^{\Delta GFP}$. Construct design, construction were performed by Rainbow Transgenics (Camarillo, CA). The design for the disruption is shown in Figure S21. The construct was then injected into a *y* w^{1118} *D. melanogaster* stock. 105 larvae were injected and one showed a GFP integration. Heterozygote transformants were identified by the GFP marker. These heterozygote flies ($tll_{mel}{}^{\Delta GFP}$/tll^+) were then crossed to a *TM3, Sb*/*TM6B* stock to obtain $tll_{mel}{}^{\Delta GFP}$*/TM3, Sb* flies.

1.1.3. *Attached-X stocks*. We used two different attached-*X* stocks: *C(1)RM* and *C(1)DX*. These two stocks differ in the way that the two *X*-chromosomes are attached to each other. *C(1)RM*, or reverse metacentric, is a fusion of the *X*-chromosomes joint at their heterochromatic regions (Lindsley and Zimm 1992). *C(1)DX* is a fusion of *X*-chromosomes with a reverse acrocentric fusion (Lindsley and Zimm 1992). These chromosomes are a fusion of two *X*-chromosomes with

735 the centromere at one end and the two joint *X* chromosomes fused in opposite
736 directions.
737 1.1.4. X-Y *translocations.* (*Dp(1;Y)*) duplications and deficiencies are described below
738 in sections 2.2 and 2.3 respectively.
739 1.1.5. gt *transgenics*. We generated *gt* alleles that carried either the non-coding region
740 and coding region of gt_{mel} and gt_{san} using the phiC31 targeted transgene
741 integration system. Our goal was to generate four transgenes: one with the *mel*
742 non-coding and coding sequences, one with the *san* non-coding and coding
743 sequences, one with the *mel* non-coding sequences and the *san* coding sequence,
744 and one with the *san* non-coding sequences and the *mel* coding sequence. The
745 protocol to generate *gt* chimeric allels is described elsewhere (Chang *et al.* 2021).
746 Briefly, the gt_{mel} transgene contains a 1.422kb interval encoding the *gt* protein
747 (CDS), ~25kb of flanking non-coding DNA. The corresponding orthologous
748 whole-locus *gt* from *D. santomea*, $gt^{san:san}$ is approximately ~27kb in length,
749 containing 1.43kb coding region and ~26kb non-coding sequence. To generate the
750 transgenics, we used long-range PCR and amplified DNA fragments of
751 approximately 5kb. Besides the coding and non-coding elements described above,
752 we included two additional tags on each transgene. First, we included a piggyback
753 insertion on the 5' UTR of each chimeric allele. Second we included an eGFP tag
754 at the C-terminus. We used Sanger sequencing to verify the amplification had
755 introduced no extraneous mutations. Figure S13 shows a scheme with the
756 transgene design. These segments were then merged using Gibson assembly
757 (NEB E2611, (Gibson *et al.* 2009)) to generate all transgenics. Injections of the
758 transgenes were done by GenetiVision (Houston, TX). The piggyback insertion
759 was removed by crossing to a by crossing the transformed lines to a line
760 expressing a PiggyBac transposase ((Thibault *et al.* 2004), BDSC stock #8285).
761 While the transgenic flies with the piggyback insertion do not rescue viability a
762 gt_{mel}^{X11} mutant (Table S8), the lines with the excised insertion do rescue viability,
763 at least partially (Table 3). Please note that the san *gt* locus has a single short
764 intron, 75bp and 71bp for gt^{mel} and gt^{san}, respectively, with identical intron-exon
765 splice junction sequences. Although we cannot rule out the possibility that the

small ~70bp intron region of *gt* CDS may contribute to the functional divergence between gt^{mel} and gt^{san}, it is unlikely as this intron region does not harbor any known regulatory elements that might significantly affect *gt* expression. To compare the proportion of inviable embryos across genotypes we used 2-sample tests for equality of proportions with continuity correction as implemented in the R function *prop.test* (library *stats*, (R Core Team 2016).

1. 2. Other species stocks.

Initial surveys of HI alleles used outbred lines (i.e., lines derived from combined individuals from several isofemale lines) for interspecific crosses. In this report, we used isofemale lines collected in nature. This allowed us to survey whether HI was a line-specific or a species-wide phenomenon.

1.2.1 *Isofemale lines*. For interspecific crosses involving *D. melanogaster* gt_{mel}^{x11}*/FM7::GFP* and *D. melanogaster df(BSC)/FM7::GFP* we used 25 *D. santomea* isofemale lines collected in the island of São Tomé. We also quantified hybrid viability for hybrids from hybrids between females from these two *D. melanogaster* mutant crosses with 25 *D. mauritiana*, 25 *D. teissieri*, and 25 *D. simulans* lines. All lines, including their collection details, are listed in Table S6.

1.2.2. *Other mutant stocks*. Finally, we used five mutant stocks from three other species from *D. melanogaster*. Attached *X* stocks from *D. simulans* (*y w*, (Coyne 1985) reviewed in (Presgraves and Meiklejohn 2021)) were donated by D. Presgraves. Attached *X* from *D. yakuba* (*y*) were produced by J. Coyne (Coyne *et al.* 2004). Attached *X* from *D. santomea* (*gn*) were donated by A. Llopart (Coyne *et al.* 2004; Turissini *et al.* 2015; Llopart *et al.* 2018). *yellow* stocks from *D. simulans, and D. mauritiana* were obtained from the San Diego stock Center (now Cornell Stock Center).

2. INTERSPECIFIC GENETIC CROSSES

2. 1. Wild-type crosses

Pure species males and females of each species were collected as virgins within 8 hours of eclosion under CO_2 anesthesia and kept for three days in single-sex groups of 20 flies in 30mL, corn meal food-containing vials. Flies were kept at 24ºC under a 12 h light/dark cycle. On day four, we assessed whether there were larvae in the media. If the inspection revealed any progeny, the vial was discarded.

On the morning of day four after collection, we placed forty males and twenty females together at room temperature (21°–23°C) to mate *en masse* on corn meal media. To produce hybrid adults, vials were inspected every five days to assess the presence of larvae and/or dead embryos. In order to maximize the lifespan of the parental, we kept all the vials laying on their side. We transferred all the pure species adults to a new vial (without anesthesia) every five days. This procedure was repeated until the cross stopped producing progeny (i.e., females were dead). Once L_2 larvae were observed in a vial, we added a solution of 0.05% propionic acid and a KimWipe (Kimberly Clark, Kimwipes Delicate Task, Roswell, GA) to the vial. We counted the hybrids as they hatched by anesthetizing them with CO_2.

To quantify embryonic lethality, we mixed males and females as described above in a 30mL plastic vial with corn-meal or molasses food. After two days, we transferred the adults from the vials that showed larvae to an oviposition cage with apple juice media and yeast. The plates were inspected every 48 hours for the presence of viable eggs. To quantify embryonic lethality, we counted the number of egg cases (viable embryos) and the number of brown eggs (dead embryos) in each oviposition cage. Rates of embryonic lethality were calculated as the proportion of brown eggs over the total number of eggs. For all interspecific crosses within the *yakuba* species complex (*D. santomea*, *D. yakuba*, and *D. teissieri*), we only used lines that have been shown to be infected by *Wolbachia* (wB) to minimize any possible effect of endosymbionts on hybrid inviability (Cooper *et al.* 2017).

2. 2. Genome wide association studies (GWAS)

2.2.1. Hybrid inviability GWAS. We identified polymorphisms segregating in *D. melanogaster* associated with hybrid inviability and penetrance of abdominal ablations in

827 *mel/san* F1 hybrids. We leveraged the *Drosophila* Genetic Reference Panel (DGRP)
828 genotype information (MacKay *et al.* 2012; Huang *et al.* 2014) to identify variants within
829 *D. melanogaster* associated with the presence of abdominal ablations when crossed to *D.*
830 *santomea* males. In total, we used 200 *D. melanogaster* lines, all of which are listed in
831 Table S1. In order to identify SNPs associated with abdominal ablations in hybrids, we
832 mated females from each of the *D. melanogaster* lines with *D. santomea* males following
833 the procedure described in 2.1 (immediately above). The response phenotype was the
834 percentage of larvae that showed abdominal ablations (scored as described above).
835 We submitted the percentage of ablated embryos of the 200-line study, not sexed,
836 to the web portal dgrp2.gnets.ncsu.edu for analysis. Since we could not differentiate
837 between female and male embryos (DGRP lines do not carry a y^- marker), we collected a
838 single ablation score per line, combining the two sexes. Associations between the
839 phenotype (i.e. percentage of ablated embryos) and genome wide polymorphisms within
840 *D. melanogaster* were calculated by the DGRP algorithm, using a linear mixed model,
841 which accounts for any effects of *Wolbachia* infection, common polymorphic inversions,
842 and cryptic relatedness in the DGRP lines, as described in detail in (MacKay *et al.* 2012).
843 This GWAS incorporates information from 1.9 million SNP variants. The genome-wide
844 significant threshold at the 5% significance level was determined after a Bonferroni
845 correction for multiple testing (Johnson *et al.* 2010) and adjusting the critical P-value for
846 significance to as 2.60×10^{-8} (0.05/1,900,000).
847
848 *2.2.2. GWAS restricted to the autosomes.* Next, we assessed if any of the autosomal
849 segregating variants in the DGRP modified the effects of gt_{mel}^{X11}. To this end, we
850 introgressed an *FM7::GFP* balancer and the null allele of giant, gt_{mel}^{X11} into 200 lines
851 from the DGRP. The introgression protocol is shown in Figure S18 and involved
852 introgressing *FM7::GFP* (10 generations of backcrossing) by following the *Bar* and *GFP*
853 markers of the balancer (Figure S18A). On generation 11, and for each DGRP stock,
854 gt_{mel}^{X11}*/FM7* females, were crossed to a male from each of the DGRP stocks that carried a
855 *FM7:GFP* (from the first round of introgression). F1 females with yellow mouth parts
856 carried gt_{mel}^{X11} and *FM7::GFP* and were again crossed to DGRP males carrying
857 *FM7:GFP*. This procedure was repeated for 10 generations (Figure S18B). The result

from this crosses was having *FM7::GFP/*y_{mel}^{-} gt_{mel}^{X11} in 200 different genetic backgrounds.

Next, we assessed the effects of the different DGRP genetic backgrounds on the penetrance of gt_{mel}^{X11} in *mel/san* hybrids. We crossed females from each of these 200 stocks to *D. santomea* sanCAR1600.3 males. We separated the progeny into four different categories. Females have black mouthparts (i.e., *FM7::GFP/*X_{san} and y_{mel}^{-} gt_{mel}^{X11}/X_{san}; y_{san} rescue y_{mel}^{-}); males (either *FM7::GFP* /Y_{san} or y_{mel}^{-} gt_{mel}^{X11}/ Y_{san}) have brown mouthparts. Balancer carriers (i.e., *FM7::GFP/*X_{san} and *FM7::GFP*/ Y_{san}) have a *GFP* marker. The goal of this experiment was to find autosomal factors that would affect the frequency of abdominal ablations in a gt_{mel}^{X11} background in both females and males; we scored the percentage of ablated embryos in y_{mel}^{-} gt_{mel}^{X11}/ Y_{san} males and y_{mel}^{-} gt_{mel}^{X11}/ X_{san} hybrid females apart. Because of the experimental design (introgression of a full y_{mel}^{-} gt_{mel}^{X11}*X*-chromosome on multiple autosomal backgrounds), we did not study possible *X*-linked modifiers of the penetrance of gt_{mel}^{X11}. Association mapping was done as described immediately above but splitting the two sexes and excluding markers from the *X*-chromosome (section 2.2.1. Hybrid inviability GWAS).

2.3. Duplication mapping.

Duplication mapping identifies dominant (or semidominant) alleles in the *D. melanogaster X*-chromosome (X^{mel}) that cause inviability in hybrids resulting from interspecific crosses. The technique uses stocks provided by Bloomington Stock Center in which segments of the *X*-chromosome have been duplicated and attached to the *Y*-chromosome by BAC recombineering (Venken *et al.* 2010). We used two classical *Drosophila* techniques—attached-*X* females (described in section 1.1.2), and *X*-*Y* chromosome fusions—to finely characterize the identity of HI alleles in the X_{mel}. *Drosophila melanogaster* attached-*X* females carry two *X*-chromosome fused together which carry recessive alleles for easy identification. We used two genotypes of attached-*X* females: *C(1)DX* and *C(1)RM*. Unless otherwise noted, all crosses used *C(1)DX*. These females can carry a Y_{mel} chromosome and remain morphologically female. When these females carry both an attached-*X* and a *Y* chromosome, they produce attached-*X* gametes and Y_{mel} gametes.

889 Previous experiments have shown that when *C(1)DX* (or *C(1)RM*) females are
890 crossed with *D. santomea* males the only viable genotype are F_1 hybrid males with
891 genotype $X_{san}\ Y_{mel}$ (Figure S1, (Matute and Gavin-Smyth 2014)). *Drosophila*
892 *melanogaster C(1)DX* females can also be crossed to *D. simulans* (Orr 1993), *D.*
893 *mauritiana* (Cattani and Presgraves 2012), and *D. teissieri*. In the first two cases, the
894 cross produces viable hybrid males with an *X*-chromosome from the father, and a Y_{mel}. In
895 the cross with *D. teissieri* males, *C(1)DX* females produce viable larvae from both sexes
896 that die before molting into pupae.

897 We addressed whether the introduction of small pieces of X_{mel} in *mel/san* hybrid
898 males cause HI. We used a panel of small X_{mel}-chromosome fragments attached to the *Y*-
899 chromosome [*Dp(1;Y)*] that tilled the cytological bands 2, 3 and 4 in the *X*-chromosome
900 (12 duplications). These segments also carry two phenotypic markers: y_{mel}^{+}, and *Bar*.
901 Despite the multiple genetic modifications these stocks carry, the viability of these
902 crosses has been validated with several lines of wild-caught *D. melanogaster* (see below,
903 Section 3. Intraspecific crosses: dosage effects).

904 Since the procedure to produce interspecific hybrid males for the four species (*D.*
905 *santomea*, *D. teissieri*, *D. mauritiana*, and *D. simulans*) is identical, we only describe the
906 protocol for only one of them, *D. santomea*. We crossed attached-X^{mel} females [*C(1)DX*]
907 to *D. melanogaster Dp(1;Y)* males that carry small fragments of X_{mel} on their *Y*-
908 chromosome. The female progeny [*mel C(1)DX/Dp(1;Y)*] will carry both the attached-*X*
909 and the *Y*-chromosome with the small fragment of *X* to be tested. These virgin females
910 awee then crossed to *D. santomea* males to produce F_1 hybrid males harboring an X_{san}
911 and a (Y_{mel}, *Dp(1;Y)*) chromosomes. The crossing scheme to identify these dominant
912 alleles on the X_{mel} chromosome is shown in Figure S1. The effect of the X_{mel} fragment
913 was assessed by counting how many individuals survive the transition between three
914 developmental stages (embryo, larvae, pupae). This approach (shown in Figure S1) has
915 been used to identify alleles from X_{mel} that cause hybrid inviability (Sawamura and
916 Yamamoto 1993; Cattani and Presgraves 2012; Matute and Gavin-Smyth 2014).

917 A parallel set of *X*-duplications, was not attached to the *Y*-chromosome but the
918 third chromosome instead (*Dp(1;3)*; (Venken *et al.* 2010)). We introgressed these
919 duplications into a *C(1)DX, TM3*/+ background by repeated backcrossing (4 generations)

to produce *C(1)DX*; *Dp(1;3)/ Dp(1;3)* females. The effect of the *Dp(1;3)* was measured in the same manner as described above for *Dp(1;Y)* by measuring transition rates across developmental stages. Interspecific crosses using *C(1)DX, TM3* or *C(1)DX, TM6B* stocks yielded very low numbers of progeny which were not enough for embryo collection (Nagy *et al.* 2018).

2. 4. Deficiency mapping.

Traditionally, deficiency mapping has been used to find recessive alleles in the genome of the other species that are lethal when the *D. melanogaster* allele is deleted (Coyne *et al.* 1998; Presgraves 2003; Matute *et al.* 2010). We took a different approach and focused on dominant alleles: those that when removed increased hybrid viability. We used *mel* females from stocks containing known genomic deletions, or "deficiencies" (*df*, Bloomington *Drosophila* Fly Stock Center) maintained as heterozygotes against a balancer (*Bal*) chromosome carrying a dominant homozygous lethal mutation, to *D. santomea* (*san*) males. Seven deficiencies encompass gt_{mel} (listed in Table S1). Virgin *D. melanogaster* females were crossed to *D. santomea* males following previously described procedures (Matute *et al.* 2010; Miller and Matute 2017). (Behavioral isolation seems to be complete in the reciprocal direction (Gavin-Smyth and Matute 2013).) Crosses were kept until no more progeny was produced out of each vial, usually 45 days after they were set up. The effect of each hemizygous region on the viability of hybrid female offspring was measured by comparing the ratio of *df/san* to *Bal/san* hybrid females. The significance of the departure was assessed by a χ^2 test followed by a Sidak's multiple comparison correction. P-values were considered significant lower than 0.007 ($P < 0.05$ adjusted for 7 multiple comparisons). If the deletion has no effect on hybrid viability, the ratio of F_1 *df/san* to the total number of progeny (F_1 *Bal/san* + F_1 *df/san*) will not differ from 0.5. If the deletion reveals alleles in the *san* genome that cause complete inviability, the ratio will be equal to 0 (only progeny carrying the *Balancer* will survive). If the *D. melanogaster* deficiency uncovers a recessive region of the *D. santomea* genome that compromises hybrid fitness but does not cause complete lethality, the ratio (F_1 *df/san* /Total) will be greater than 0 and significantly lower than 0.5. Finally, and the target of this study, if the ratio (F_1 *df/san* /Total) is significantly higher than 0.5, then the *df* is

951 removing a dominant (or semidominant) contributor to HI. This last category must be
952 seen with caution as Balancer chromosomes carry deleterious alleles that might bias the
953 ratio upwards. To minimize the potentially deleterious effect of any given balancer, we
954 used seven different *X*-chromosome balancers to replicate crosses involving gt^{X11} and
955 *df(gt)*: *FM6::GFP*, *Binscy*, *Basc*, Bascy, *Binsn, Binsncy, FM4* and *FM7a*.

956 **3. INTRASPECIFIC CROSSES: DOSAGE EFFECTS.**

957

958 We tested whether any of the mutants caused phenotypic defects or inviability by
959 dosage effects. This is important because *Dp(1;Y)* carrying males have two copies of the
960 genes under study while wild-type males only have one copy. Similarly, *df*-carrying
961 females only have a single copy of a gene (i.e., they are hemizygous) while wild-type
962 females have two copies of that gene.

963 We studied whether any of the used duplications cause inviability in males for
964 being diploid (when they are normally hemizygous). All crosses were done as described
965 in section 2.3. (Duplication mapping) but instead of using heterospecific males, we used
966 males from 25 different *D. melanogaster* isofemale lines. The list of isofemale lines used
967 for these experiments is shown in Table S2. If there is a dosage effect (i.e., carrying
968 *Dp(1;Y)* and thus two copies of a gene while being male is deleterious), one would expect
969 inviability and/or developmental defects in these crosses.

970 We did a similar analysis to assess for potential haploinsufficiency in *df*-carrying
971 females. We tested whether any of the used deficiencies cause inviability in females for
972 being hemizygous (when they are normally diploid) in the same twenty-five *D.*
973 *melanogaster* backgrounds described immediately above. We measured the ratios of *df*-
974 and *Balancer*-carrying females using the methods described above.

975

976 **4. CUTICLE PREPARATION**

977

978 We generated cuticles for wild-type (i.e., progeny produced by crossing wild-type
979 stocks), *Dp(1;Y)*-carrying and gt^{x11}-carrying hybrids. The details for the production of the
980 three types of cuticles are described as follows.

4.1 Wild-type hybrids.

To collect sex-specific hybrid cuticles, we used *D. melanogaster* a y^1 *w* stock. *Drosophila melanogaster* y^1 *w* females were crossed to *D. santomea* males. Inseminated females were allowed to deposit on apple juice plates overnight and embryos were aged for 24 hours before scoring. To prepare cuticles, we used a slightly modified the protocol described in (Gavin-Smyth and Matute 2013; Matute and Gavin-Smyth 2014a) . Briefly, we dechorionated embryos using double-sided scotch tape. To devitellinize brown (dead) embryos. We made a cut on the vitelline membrane and removed the rest of the cuticle with a tungsten dissection needle and placed them in a 3:1 solution of acetic acid and glycerol for 48 hours. After this period, cuticles were mounted on a pre-clean glass slide (VMR VistaVision™, VWR; cat. no. 16004-422; Radnor, PA) on 20µl of a 1:1 solution of Hoyer's media (kindly donated by Dr. Daniel McKay) and acetic acid. Embryos without pigmentation of the mouth hooks were scored as male with the genotype y^1 *w* / Y_{san}. Embryos with black mouth parts were identified as females (y^1/ y_{san}) as the y^1 allele is complemented by the homologous y_{san}. Embryos were visualized and imaged with an Olympus BX61 dark-field microscope at the Microscopy facility of the Pathology department at UNC.

4.2. *Dp(1;Y)* carrying male hybrids.

To collect X_{san} Y_{mel} (*Dp1;Y*), we followed a similar procedure to that described immediately above (section 4.1). Individuals with brown mouth parts were concluded to be females carrying *C(1)DX* (y^-/y^- homozygotes). Individuals with black mouth parts had two possible genotypes: metafemales carrying three *X* chromosomes (*C(1)DX* y^- and X_{san}; y^-/y^-/y_{san}) or X_{san}/Y_{mel}, *Dp(1,Y)* males (y_{san}). Since metafemales (i.e., *C(1)DX* y^-/X_{san} females) are thought to show a low rate of embryonic defects (Matute and Gavin-Smyth 2014b), the pooling of these two categories underestimates the penetrance of the alleles responsible for the ablation. This bias is not a concern as it should occur at a similar rate in all crosses involving *C(1)DX*. All rates of penetrance using *C(1)DX, Dp1;Y* females should then be considered an underestimation.

4.3 gt_{mel}^{x11} carrying female hybrids.

We used a similar approach to collect cuticles for hybrids carrying a *gt*-null allele (gt_{mel}^{x11}). To score hybrid defects on gt^{-}-carriers, we used $y^1\ sc^1\ gt^{X11}$. This stock was purchased as $y^1\ sc^1\ gt^{X11}/FM6$ (Table S1, Row 1). We rebalanced the stock over a $y^1\ FM7$ chromosome carrying an *Gal4*-Actin::*UAS-GFP* reporter. To produce gt^{x11}/san cuticles, $gt^{x11}/FM7Actin::GFP$ *D. melanogaster* females were crossed to *D. santomea* males. *GFP* minus embryos that failed to hatch were separated and prepared for cuticle mounting using standard procedures (see (Gavin-Smyth and Matute 2013)). Both, *GFP* minus embryos (gt^{x11}-carriers) and *GFP* plus embryos (*FM7* carriers) were separated by the color of their mouth-hooks as described above to identify by sex. Cuticles of other interspecific crosses (e.g., *mel/tei, mel/mau, mau/sim*) were collected, prepared, and imaged using the same scheme.

5. GENOME SEQUENCING

We next studied the patterns of polymorphism in *gt* across the nine species of the *melanogaster* species subgroup. This involved (*i*) collecting flies in nature, (*ii*) sequencing their genomes, and (*iii*) aligning them. These three steps are described in detail as follows.

5.1. Stock collection

We collected lines from five species in the *melanogaster* group in their natural habitat. *Drosophila santomea* and *D. yakuba* were collected in the volcanic island of São Tomé. *Drosophila teissieri* was collected in the highlands of the island of Bioko, Equatorial Guinea. *Drosophila simulans* was collected in Bioko, São Tomé and Zambia. In all cases, single females were collected with banana traps, anesthetized with FlyNap (triethylamine, Carolina Biological Supply Co.) for 2-5 minutes. Individual females were then placed in plastic vials with instant potato fly media (Carolina Biological Supply Co.) and were allowed to oviposit until their death. Vials with progeny were hand carried to the USA (USDA permit: P526-150127-009) and progeny was transferred to a corn-meal diet in 100 mL vials. *Drosophila mauritiana* stocks were kindly donated by D. Presgraves.

5.2. Sequencing: Genomic data

All the genomes of the lines used in this study were previously published. We downloaded available raw reads (FASTQ files) for *D. yakuba* (Rogers *et al.* 2014, 2017; Turissini and Matute 2017; Turissini *et al.* 2018), *D. santomea* (Turissini and Matute 2017; Turissini *et al.* 2018), *D. teissieri* (Turissini and Matute 2017; Turissini *et al.* 2018), *D. mauritiana* (Garrigan *et al.* 2012; Brand *et al.* 2013), *D. sechellia* (Schrider *et al.* 2018; Turissini *et al.* 2018), *D. simulans* (Garrigan *et al.* 2012; Serrato-Capuchina *et al.* 2021), and *D. melanogaster* (Pool 2015; Lack *et al.* 2016) from NCBI and mapped them to the corresponding reference genome (see below). All the accession numbers are listed in Table S14.

5.3. Sequencing: Read mapping and variant calling

Reads were mapped to the closest reference genome using bwa version 0.7.12 (Li and Durbin 2009; Li 2013). Reads from *D. yakuba*, *D. teissieri*, and *D. santomea* were mapped to the *D. yakuba* genome version 1.04 (Drosophila 12 Genomes Consortium *et al.* 2007), and reads from *D. simulans, D. sechellia*, and *D. mauritiana* were mapped to the *D. simulans* w^{501} genome (Hu *et al.* 2013). We used Samtools version 0.1.19 (Li *et al.* 2009) to merge Bam files. We used GATK version 3.2-2 RealignerTargetCreator and IndelRealigner functions to identify indels and polymorphic sites (McKenna *et al.* 2010; DePristo *et al.* 2011). Read mapping and SNP genotyping were done independently for the *D. yakuba* and *D. simulans* clades using GATK UnifiedGenotyper but in both cases we used similar parameters and files. The parameter het was set to 0.01. We also used the following filters to all resulting vcf files: QD = 2.0, FS_filter = 60.0, MQ_filter = 30.0, MQ_Rank_Sum_filter = -12.5, and Read_Pos_Rank_Sum_filter = -8.0. If a site had a coverage below five reads or above than the 99th quantile of the genomic coverage distribution for the given line, that site was assigned an 'N'.

5.4. Sequencing: Indel identification

We studied the positions of indels in the giant locus across the *melanogaster* species subgroup. To genotype indels, we used GATK UnifiedGenotyper with the -glm INDEL

flag for just the sequence orthologous to the *D. melanogaster giant* gene. We then generated fasta files for the *giant* locus. No coverage thresholds were used for indel genotypes.

5.5. Genomic Alignments.

We next generated genome alignments that included *D. melanogaster*, *D. simulans* and *D. yakuba* . The *D. yakuba* and *D. simulans* reference genomes were separately aligned to the *D. melanogaster* genome using nucmer version 3.23 with parameters –r and –q. Next, we used the dmel6.01 annotation: ftp.flybase.net/genomes/Drosophila_melanogaster/dmel_r6.01_FB2014_04/gff/ dmel-all-r6.01.gff.gz (Dos Santos *et al.* 2015a) to identify the *giant* coding region (*D. melanogaster X* chromosome: 2,427,113 – 2,429,467). These alignments were the used to extract polymorphism data for this region for 8 species in the *melanogaster* species subgroup. In total, we included data for 903 sequences. The subsequent alignment was visually inspected using Mesquite version 3.04 (Maddison and Maddison 2010) to ensure indels were aligned and did not disrupt codons.

6. DETECTION OF NATURAL SELECTION

6.1. PAML

Next, we studied whether the *giant* locus had evolved though natural selection. The first approach to detect positive selection was to count the number of synonymous (dS) and non-synonymous (dN) substitutions in each branch and calculate the ratio between these two variables. First, we generated a consensus sequence for each of the species in the *melanogaster* species subgroup. Next, we ran PAML version 4.8 (Yang 1997, 2007) to calculate dN/dS ratios. We used four sets of parameters: basic model (model=0), free ratios (model=1), 3 ratios (model=2, tree = ((mel, (sim, sech, mau) $2)$1, ((yak, san), tei) $3);), and 2 ratios (model=2, tree = ((mel, (sim, sech, mau))$1, ((yak, san), tei) $2)). A dN/dS ratio significantly higher than 1 means positive selection, while a dN/dS ratio significantly lower than 1 means negative/purifying selection ((Yang 1997, 2007) but see

(Venkat *et al.* 2018)). dN/dS values not significantly different from zero represent neutral evolution.

SUPPLEMENTARY TABLES

TABLE S1. Rates of ablation in F1 hybrids between the species of the *yakuba* species complex. None of the six possible F1 hybrids show abdominal ablations.

Cross	Scored embryos	Dead embryos	Ablated embryos
♀ ***D. santomea*** × ♂ ***D. santomea***	120	2	0
♀ ***D. yakuba*** × ♂ ***D. yakuba***	162	4	0
♀ ***D. teissieri*** × ♂ ***D. teissieri***	149	7	0
♀ ***D. santomea*** × ♂ ***D. yakuba***	102	16	0
♀ ***D. santomea*** × ♂ ***D. teissieri***	110	21	0
♀ ***D. yakuba*** × ♂ ***D. santomea***	123	19	0
♀ ***D. yakuba*** × ♂ ***D. teissieri***	98	16	0
♀ ***D. teissieri*** × ♂ ***D. santomea***	101	15	0
♀ ***D. teissieri*** × ♂ ***D. yakuba***	98	10	0

TABLE S2. Hybrids between *D. melanogaster* females and *D. simulans* and *D. mauritiana* show no abdominal ablations or embryonic lethality. The reciprocal crosses (♀*D. simulans* × ♂ *D. melanogaster;* ♀*D. mauritiana* × ♂*D. melanogaster*) show high levels of female embryonic lethality but death occurs before embryogenesis stars.

Cross	Hatched embryos	Dead brown embryos	Ablated embryos
♀ ***D. melanogaster*** × ♂ ***D. melanogaster***	110	6	0
♀ ***D. simulans*** × ♂ ***D. simulans***	105	5	0
♀ ***D. sechellia*** × ♂ ***D. sechellia***	88	8	0
♀ ***D. mauritiana*** × ♂ ***D. mauritiana***	121	4	0
♀ ***D. melanogaster*** × ♂ ***D. simulans***	98	5	0
♀ ***D. melanogaster*** × ♂ ***D. mauritiana***	74	5	0
♀ ***D. melanogaster*** × ♂ ***D. sechellia***	99	41	0
♀ ***D. simulans*** × ♂ ***D. melanogaster***	101	6	0
♀ ***D. simulans*** × ♂ ***D. sechellia***	78	1	0
♀ ***D. simulans*** × ♂ ***D. mauritiana***	95	2	0
♀ ***D. sechellia*** × ♂ ***D. melanogaster***	73	2	0
♀ ***D. sechellia*** × ♂ ***D. simulans***	77	4	0
♀ ***D. sechellia*** × ♂ ***D. mauritiana***	71	6	0
♀ ***D. mauritiana*** × ♂ ***D.***	83	4	0

sechellia			
♀ ***D. mauritiana*** × ♂ ***D. simulans***	99	2	0
♀ ***D. mauritiana*** × ♂ ***D. melanogaster***	68	4	0

TABLE S3. Mutant stocks used in this study.

	Stock number	Genotype
1	53	gt1 wa
2	54	gt[13z]/Dp(1;2;Y)w[+]/C(1)DX, y[1] f[1]
3	1528	gt[Q292] rst[6]/FM7a
4	1529	y[1] sc[1] gt[X11]/FM6
5	1530	y[1] gt[E6] rst[6]
6	35	dor4/C(1)RM, y1 w1 f1
7	?	C(1)DX
8	17003	P{EP}boiEP1385 w1118
9	13245	y1 P{SUPor-P}boiKG03233
10	4283	tko3/FM7a/Dp(1;2;Y)w+
11	59642	y1 Mi{MIC}tkoMI15120 w*/FM7h
12	52400	y1 tkoA w* P{neoFRT}19A/FM7c, P{GAL4-Kr.C}DC1, P{UAS-GFP.S65T}DC5, sn+
13	52401	y1 tkoB w* P{neoFRT}19A/FM7c, P{GAL4-Kr.C}DC1, P{UAS-GFP.S65T}DC5, sn+
14	?	FM7::GFP
15	29799	Dp(1;Y)BSC75, y[+] P{w[+mW.Scer\FRT.hs3]=3'.RS5+3.3'}BSC3, B[S]/Df(1)ED6630, P{w[+mW.Scer\FRT.hs3]=3'.RS5+3.3'}ED6630 w[1118]/C(1)RA, In(1)sc[J1], In(1)sc[8], l(1)1Ac[1], sc[J1] sc[8]
16	29801	Dp(1;Y)BSC77, y[+] P{w[+mW.Scer\FRT.hs3]=3'.RS5+3.3'}BSC3, B[S]/Df(1)ED6630, P{w[+mW.Scer\FRT.hs3]=3'.RS5+3.3'}ED6630 w[1118]/C(1)RA, In(1)sc[J1], In(1)sc[8], l(1)1Ac[1], sc[J1] sc[8]
17	29803	Dp(1;Y)BSC79, y[+] P{w[+mW.Scer\FRT.hs3]=3'.RS5+3.3'}BSC3, B[S]/Df(1)ED6630, P{w[+mW.Scer\FRT.hs3]=3'.RS5+3.3'}ED6630 w[1118]/C(1)RA, In(1)sc[J1], In(1)sc[8], l(1)1Ac[1], sc[J1] sc[8]
18	29804	Dp(1;Y)BSC80, y[+] P{w[+mW.Scer\FRT.hs3]=3'.RS5+3.3'}BSC3, B[S]/Df(1)ED6630, P{w[+mW.Scer\FRT.hs3]=3'.RS5+3.3'}ED6630 w[1118]/C(1)RA, In(1)sc[J1], In(1)sc[8], l(1)1Ac[1], sc[J1] sc[8]

		Dp(1;Y)BSC81, y[+] P{w[+mW.Scer\FRT.hs3]=3'.RS5+3.3'}BSC3,
		B[S]/Df(1)ED6630, P{w[+mW.Scer\FRT.hs3]=3'.RS5+3.3'}ED6630
19	29805	w[1118]/C(1)RA, In(1)sc[J1], In(1)sc[8], l(1)1Ac[1], sc[J1] sc[8]
		Dp(1;Y)BSC82, y[+] P{w[+mW.Scer\FRT.hs3]=3'.RS5+3.3'}BSC3,
		B[S]/Df(1)Exel6233, w[1118] P{w[+mC]=XP-U}Exel6233/C(1)RA,
20	29806	In(1)sc[J1], In(1)sc[8], l(1)1Ac[1], sc[J1] sc[8]
		Dp(1;Y)BSC83, y[+] P{w[+mW.Scer\FRT.hs3]=3'.RS5+3.3'}BSC3,
		B[S]/Df(1)Exel6233, w[1118] P{w[+mC]=XP-U}Exel6233/C(1)RA,
21	29807	In(1)sc[J1], In(1)sc[8], l(1)1Ac[1], sc[J1] sc[8]
		Dp(1;Y)BSC84, y[+] P{w[+mW.Scer\FRT.hs3]=3'.RS5+3.3'}BSC3,
		B[S]/Df(1)Exel6233, w[1118] P{w[+mC]=XP-U}Exel6233/C(1)RA,
22	29808	In(1)sc[J1], In(1)sc[8], l(1)1Ac[1], sc[J1] sc[8]
		Dp(1;Y)BSC85, y[+] P{w[+mW.Scer\FRT.hs3]=3'.RS5+3.3'}BSC3,
		B[S]/Df(1)Exel6233, w[1118] P{w[+mC]=XP-U}Exel6233/C(1)RA,
23	29809	In(1)sc[J1], In(1)sc[8], l(1)1Ac[1], sc[J1] sc[8]
		Dp(1;Y)BSC87, y[+] P{w[+mW.Scer\FRT.hs3]=3'.RS5+3.3'}BSC3,
		B[S]/Df(1)Exel6233, w[1118] P{w[+mC]=XP-U}Exel6233/C(1)RA,
24	29811	In(1)sc[J1], In(1)sc[8], l(1)1Ac[1], sc[J1] sc[8]
		Dp(1;Y)BSC88, y[+] P{w[+mW.Scer\FRT.hs3]=3'.RS5+3.3'}BSC3,
		B[S]/Df(1)Exel6233, w[1118] P{w[+mC]=XP-U}Exel6233/C(1)RA,
25	29812	In(1)sc[J1], In(1)sc[8], l(1)1Ac[1], sc[J1] sc[8]
		Dp(1;Y)BSC90, y[+] P{w[+mW.Scer\FRT.hs3]=3'.RS5+3.3'}BSC3,
26	29814	B[S]/winscy/C(1)RA, In(1)sc[J1], In(1)sc[8], l(1)1Ac[1], sc[J1] sc[8]
		w[1118]; Dp(1;3)DC454, PBac{y[+mDint2]
27	32295	w[+mC]=DC454}VK00033/TM6C, Sb[1]
		w[1118]; Dp(1;3)DC045, PBac{y[+mDint2]
28	30233	w[+mC]=DC045}VK00033
		w[1118]; Dp(1;3)DC107, PBac{y[+mDint2]
29	30751	w[+mC]=DC107}VK00033
		w[1118]; Dp(1;3)RC013, PBac{y[+mDint2]
30	38476	w[+mC]=RC013}VK00033/TM6C, Sb[1]
		w[1118]; Dp(1;3)DC405, PBac{y[+mDint2]
31	31455	w[+mC]=DC405}VK00033
		w[1118]; Dp(1;3)DC453, PBac{y[+mDint2]
32	32294	w[+mC]=DC453}VK00033/TM6C, Sb[1]
		Df(1)ED409, P{w[+mW.Scer\FRT.hs3]=3'.RS5+3.3'}ED409
33	8950	w[1118]/FM7h
		Df(1)ED11354, P{w[+mW.Scer\FRT.hs3]=3'.RS5+3.3'}ED11354
34	9345	w[1118]/FM7h
		Df(1)ED11354, P{w[+mW.Scer\FRT.hs3]=3'.RS5+3.3'}ED11354
35	9054	w[1118]/FM7h
		Df(1)ED411, P{w[+mW.Scer\FRT.hs3]=3'.RS5+3.3'}ED411
36	8031	w[1118]/FM7j, B[1]
		Df(1)BSC717, P+PBac{w[+mC]=XP3.RB5}BSC717
37	26569	w[1118]/FM7h/Dp(2;Y)G, P{w[+mC]=hs-hid}Y
38	7705	Df(1)Exel6230, P{XP-U}Exel6230 w1118/FM7c

39 7706 Df(1)Exel6231, P{XP-U}Exel6231 w1118/FM7c
1112
1113

TABLE S4. *C(1)DX, Dp(1;3)/TM3* lay few eggs are thus not ideal to measure the magnitude of HI in crosses with *D. santomea*. The second and third column show the number of eggs produced by a singly-mated female when mated to a w^{1118} male over 4 days.

Duplication	**Stock**	***C(1)DX, Dp(1;3)/Dp(1;3)***	***C(1)DX, Dp(1;3)/TM3,Sb***	***C(1)DX, Dp(1;Y)***
Dp(1;3)DC405	31455	47	7	NA
Dp(1;3)DC301	31452	51	24	NA
Dp(1;3)DC112	31445	43	15	NA
Dp(1;3)DC272	30389	24	20	NA
Dp(1;Y)BSC87	29811	NA	NA	56
Dp(1;Y) BSC170	32117	NA	NA	68
Dp(1;Y)BSC58	29782	NA	NA	53
Dp(1;Y)BSC14	29782	NA	NA	64

TABLE S5. The cross involved a gt_{mel}^{X11}/*FM7* female and a male hemizygote for the duplication. In the case of *Dp(1;Y)* duplications, the male had a X_{mel}/Y_{mel}*Dp(1;Y)* genotype. In the case of *Dp(1;3*) duplication, the male had a X_{mel}/Y_{mel}, *Dp(1,3)/TM3,Sb* genotype.

Genotype	Stock	*Dp(1;Y)* or *Dp(1;3)*?	F1 male genotypes		Rescue Rate	X^2	P
			gt^{X11}/ Dp	*FM7*/Dp			
Dp(1;Y)BSC74	29798	*Dp(1;Y)*	81	73	0.526	0.117	0.732
Dp(1;Y)BSC78	29802	*Dp(1;Y)*	53	48	0.525	0.045	0.833
Dp(1;3)DC405	31455	*Dp(1;3)*	41	75	0.353	4.511	0.034
Dp(1;3)RC013	38476	*Dp(1;3)*	16	37	0.302	3.545	0.060

TABLE S6. Isofemale lines from four species used to assess whether HI in *mel/san* hybrids was a species-specific phenomenon or a line specific phenomenon. All lines were collected by D. R. Matute with the exception of the three *D. teissieri* lines marked with an asterisk. Those three lines were donated by J.R. David.

Species	**Line**	**Notation in Figures S4 and S19**	**Location**	**Year**
D. santomea	**Thena5**	**S1**	**São Tomé**	**2005**
D. santomea	sanCAR1490	S2	São Tomé	2005
D. santomea	sanCOST1250.5	S3	São Tomé	2009
D. santomea	sanCOST1270.1	S4	São Tomé	2009
D. santomea	sanOBAT1200	S5	São Tomé	2005
D. santomea	sanOBAT1200.2	S6	São Tomé	2009
D. santomea	sanRain39	S7	São Tomé	2009
D. santomea	sanCAR1600.3	S8	São Tomé	2009
D. santomea	Carv2015.1	S9	São Tomé	2015
D. santomea	Carv2015.5	S10	São Tomé	2015
D. santomea	Carv2015.11	S11	São Tomé	2015
D. santomea	Carv2015.16	S12	São Tomé	2015
D. santomea	Pico1680.1	S13	São Tomé	2015
D. santomea	Pico1659.2	S14	São Tomé	2015
D. santomea	Pico1659.3	S15	São Tomé	2015
D. santomea	Amelia2015.1	S16	São Tomé	2015
D. santomea	Amelia2015.6	S17	São Tomé	2015
D. santomea	Amelia2015.12	S18	São Tomé	2015
D. santomea	A1200.7	S19	São Tomé	2009
D. santomea	Rain42	S20	São Tomé	2009
D. teissieri	Balancha_1	T1	Bioko, Equatorial	2013

			Guinea	
D. teissieri	Balancha_2	T2	Bioko, Equatorial Guinea	2013
D. teissieri	Balancha_3	T3	Bioko, Equatorial Guinea	2013
D. teissieri	House_Bioko_0	T4	Bioko, Equatorial Guinea	2013
D. teissieri	House_Bioko_1	T5	Bioko, Equatorial Guinea	2013
D. teissieri	House_Bioko_2	T6	Bioko, Equatorial Guinea	2013
D. teissieri	La_Lope_Gabon*	T7	Gabón	~1975
D. teissieri	Selinda*	T8	Gabón	~1975
D. teissieri	Zimbabwe*	T9	Gabón	~1975
D. teissieri	cascade_2_1	T10	Bioko, Equatorial Guinea	2013
D. teissieri	cascade_2_2	T11	Bioko, Equatorial Guinea	2013
D. teissieri	cascade_2_4	T12	Bioko, Equatorial Guinea	2013
D. teissieri	cascade_4_1	T13	Bioko, Equatorial Guinea	2013
D. teissieri	cascade_4_2	T14	Bioko, Equatorial Guinea	2013
D. teissieri	cascade_4_3	T15	Bioko, Equatorial Guinea	2013
D. teissieri	cascade_4_4	T16	Bioko, Equatorial Guinea	2013
D. teissieri	cascade_4_5	T17	Bioko, Equatorial Guinea	2013

D. teissieri	cascade_4_6	T18	Bioko, Equatorial Guinea	2013
D. teissieri	Bata_2	T19	Bata, Equatorial Guinea	2009
D. teissieri	Bata_8	T20	Bata, Equatorial Guinea	2009

1133

1134

TABLE S7. **Complementation mapping using loss-of function and hypomoprhic alleles show that *gt* mutants are the only alleles in cytological region 3A3 that lead to an increase of female viability in *mel/san* hybrid.** *mutant/san* refers to the number of F1 hybrids carrying the mutant allele. gt^{X11} is a loss of function (amorphic) allele (Eldon and Pirrotta 1991; Chang *et al.* 2021). Both boi^{d04197} and boi^{e01708} shows significantly lower RNA production than wild-type flies (Hartman *et al.* 2010). $trol^{G0271}$is a hypomorph (Skeath *et al.* 2017). tko^{3} is null allele. Carriers of the allele die as larvae but are able to complete embryogenesis (Toivonen *et al.* 2001).

Gene	**Allele**	***FM7::GFP/san***	***mutant/san***	***Ratio (F1 mutant/san)/Total***
giant	gt^{X11}	256	610	0.704
boi	P{XP}boi^{d04197}	440	478	0.521
boi	PBac{RB}boi^{e01708}	561	610	0.521
troll	$trol^{G0271}$	510	464	0.476
tko	tko^{3}	501	457	0.477

TABLE S8. The *gt*-vector does not carry extraneous elements that rescue the viability of *D. melanogaster* gt_{mel}^{X11}-carriers. When the *gt* alleles are disrupted by a piggyBac stop cassette , none of the transgenics causes rescue of a gt_{mel}^{X11} null allele.

Allele	Non-coding	Coding	F1 male genotypes		Rescue Rate
			gt^{X11}/Y; transgene/+	FM6/Y; transgene/+	
$gt_{mel:mel\text{-}STOP}$	*mel*	*mel-STOP*	0	150	0
$gt_{san:mel\text{-}STOP}$	*san*	*mel-STOP*	0	221	0
$gt_{mel:san\text{-}STOP}$	*mel*	*san-STOP*	0	180	0
$gt_{san:san\text{-}STOP}$	*san*	*San-STOP*	0	300	0

TABLE S9. Confirmation that *tll*^{mel} exacerbates the defects caused by *gt*^{mel} in *mel/san* hybrids using a different *tll* mutant. The analysis is similar to that shown in Table 1 with the difference that the χ^2 test has 4 degrees of freedom and not two as the tests in Table 1. **A.** Female viability **B.** Frequency of abdominal ablations in hybrid males. **C.** Frequency of abdominal ablations in hybrid females.

A. Female hybrid viability				
	FM7; sqh::mCherry/X^{san}*; TM3, Act::GFP, Ser/3*^{san}	*FM7; sqh::mCherry/X*^{san}*; tll*^{1}*/3*^{san}	*gt*^{X11}*; /X*^{san}*; TM3, Act::GFP, Ser/3*^{san}	*gt*^{X11}*; /X*^{san}*; tll*^{1}*/3*^{san}
	18	22	34	54
	χ^2_1=0.40, P=0.527		χ^2_1=4.55, P=0.033	
B. Proportion of male embryos showing abdominal ablations (100 embryos each)				
	FM7; sqh::mCherry/Y^{san}*; TM3, Act::GFP, Ser/3*^{san}	*FM7; sqh::mCherry/Y*^{san}*; tll*^{1}*/3*^{san}	*gt*^{X11}*; /Y*^{san}*; TM3, Act::GFP, Ser/3*^{san}	*gt*^{X11}*; /Y*^{san}*; tll*^{1}*/3*^{san}
	94	88	23	9
	χ^2_1= 1.526, P= 0.217		χ^2_1= 6.287, P = 0.012	
C. **Proportion of female embryos showing abdominal ablations (100 embryos each)**				
	FM7; sqh::mCherry/X^{san}*; TM3, Act::GFP, Ser/3*^{san}	*FM7; sqh::mCherry/X*^{san}*; tll*^{1}*/3*^{san}	*gt*^{X11}*; /X*^{san}*; TM3, Act::GFP, Ser/3*^{san}	*gt*^{X11}*; /X*^{san}*; tll*^{1}*/3*^{san}
	48	35	16	6
	χ^2_1= 2.966, P= 0.08505		χ^2_1= 4.137, P= 0.0420	

TABLE S10. **Double mutant analysis of survival in hybrids between *D. melanogaster* females and three males from four different species (*D. melanogaster*, *D. simulans*, *D. mauritiana*, and *D. teissieri*).** Individuals that are hemizygote for both alleles do not show different viability from individuals that are hemizygote for one allele and heterozygote for the other one, or heterozygote for both alleles.

	tll^{1}						
	FM7; sqh::mCherry/X^{san}; TM3, Act::GFP, Ser/3^{san}	*FM7; sqh::mCherry/X^{san}; $tll^{1}/3^{san}$*	χ^2	*gt^{X11}; /X^{san}; TM3, Act::GFP, Ser/3^{san}*	*gt^{X11}; /X^{san}; $tll^{1}/3^{san}$*	χ^2, df =3	P-value
D. melanogaster	95	104		121	98	1.8695	0.5999
D. simulans	34	31		28	29	0.33864	0.9526
D. mauritiana	52	41		39	41	1.1436	0.7666
D. teissieri	19	22		15	20	0.71574	0.8695
	$tll^{\Delta GFP}$						
	FM7; sqh::mCherry/X^{san}; TM3, Act::GFP, Ser/3^{san}	*FM7; sqh::mCherry/X^{san}; $tll^{1}/3^{san}$*	χ^2	*gt^{X11}; /X^{san}; TM3, Act::GFP, Ser/3^{san}*	*gt^{X11}; /X^{san}; $tll^{1}/3^{san}$*	χ^2	
D. melanogaster	104	87		99	78	2.1428	0.5433

D. simulans	42	36		39	44	0.46075	0.9274
D. mauritiana	51	38		49	43	1.1815	0.7575
D. teissieri	20	25		21	26	0.56722	0.9039

TABLE S11. **A *tll*$_{san}^{\Delta dsRed}$ has no effect on HI in crosses between *mel* females from four different backgrounds.**

	tll$^{\Delta dsRed}$/*3*$_{mel}$	*3*$_{san}$/*3*$_{mel}$	χ^2	P-value
mel AkLa	31	36	0.067	0.795
mel Zs2	62	74	1.600	0.206
mel Senegal	49	41	0.200	0.654
mel NC103	62	71	0.184	0.668

TABLE S12. Abrogating the *tll*$_{san}$ allele has no viability effect in *gt*$_{mel}^{X11}$ *mel*/san hybrids.

A. Female hybrid viability				
	FM7; Act::GFP/X$_{san}$*; 3*$_{mel}$*, tll*$_{san}^{dsRed}$	*FM7; Act::GFP/X*$_{san}$*; 3*$_{mel}$*, 3*$_{san}$	*gt*$_{mel}^{X11}$*/X*$_{san}$*; 3*$_{mel}$*, tll*$_{san}^{dsRed}$	*gt*$_{mel}^{X11}$*/X*$_{san}$*; 3*$_{mel}$*, 3*$_{san}$
	12	20	41	44
	χ^2_1=0.571, P=0.450		χ^2_1=0.006, P=0.939	

TABLE S13. *gt* and *tll* are slowly evolving genes as measured by the rate of aminoacid substitutions. We show K_A/K_S values for two species comparisons (*D. melanogaster* vs. *D. santomea*, and *D. melanogaster* vs. *D. yakuba*) and the quantiles of the K_A/K_S values compared to the rest of the genome. We used four different parametrizations in PAML (listed in the first column). *D. melanogaster*: *mel*, *D. santomea*: *san*; *D. yakuba*: *yak*.

Giant									
Parameter model	CG	K_A *mel* vs.*san*	K_S *mel* vs. *san*	K_A/K_s *mel* vs. *san*	Quantile K_A *mel* vs. *san*	K_A *mel* vs. *yak_*	K_S *mel* vs. *yak*	K_A/K_s *mel* vs. *yak*	Quantile K_A *mel* vs. *yak*
2_ratios	CG7952	0.0062	0.2192	0.0283	0.2227	0.0060	0.2074	0.0289	0.2281
3_ratios	CG7952	0.0062	0.2189	0.0283	0.2427	0.0060	0.2071	0.0290	0.2499
basic_model	CG7952	0.0055	0.2218	0.0248	0.1869	0.0052	0.2102	0.0247	0.1862
free_ratios	CG7952	0.0055	0.2222	0.0248	0.2278	0.0044	0.2139	0.0206	0.1960
Tailless									
Parameter model	CG	K_A *mel* vs.*san*	K_S *mel* vs. *san*	K_A/K_s *mel* vs. *san*	Quantile K_A *mel* vs. *san*	K_A *mel* vs. *yak_*	K_S *mel* vs. *yak*	K_A/K_s *mel* vs. *yak*	Quantile K_A *mel* vs. *yak*
2_ratios	CG1378	0.0045	0.384	0.012	0.095	0.0045	0.376	0.012	0.0977
3_ratios	CG1378	0.0034	0.395	0.009	0.086	0.0034	0.383	0.009	0.0872
basic_model	CG1378	0.0037	0.389	0.010	0.075	0.0037	0.380	0.010	0.076
free_ratios	CG1378	0.0028	0.389	0.007	0.087	0.0028	0.381	0.007	0.091

TABLE S14. **Sequencing details and coverage for all the lines included in this study.**

Species	Line	Read type	Average coverage	Source	SRA
D. mauritiana	mau12w	pe	153.67		SRR1555246,SRR1560430, SRR1560444, SRR483621
D. mauritiana	MauKiti	se	13.86		
D. mauritiana	mauST	se	3.11		
D. mauritiana	MS17	se,pe	60.56		SRR556195, SRR556206, SRR556199, SRR556196
D. mauritiana	R23	pe	115.98		SRR1560090, SRR1560089, SRR1560087
D. mauritiana	R31	pe	99.96		SRR1560098, SRR1560097, SRR1560095
D. mauritiana	R32	pe	120.55		SRR1560102, SRR1560100, SRR1560103
D. mauritiana	R39	pe	116.33		SRR1560110, SRR1560109, SRR1560108
D. mauritiana	R41	pe	145.38		SRR1560130, SRR1560132, SRR1560131
D. mauritiana	R44	pe	122.59		SRR1560147, SRR1560146, SRR1560133
D. mauritiana	R56	pe	121.66		SRR1560150, SRR1560149, SRR1560148
D. mauritiana	R61	pe	140.32		SRR1560268, SRR1560267, SRR1560269
D. mauritiana	R8	pe	90.27		SRR1560276, SRR1560275
D. santomea	Qiuja630.39	se	24.16	(Turissini and Matute 2017; Turissini *et al.* 2018)	SRX3029341

D. santomea	Quija37	se	11.74	(Turissini and Matute 2017; Turissini *et al.* 2018)	SRX3029336
D. santomea	sanC1350.14	se	18.62	(Turissini and Matute 2017; Turissini *et al.* 2018)	SRX3029340
D. santomea	sanCAR1490.5	se	15.77	(Turissini and Matute 2017; Turissini *et al.* 2018)	SRX3029339
D. santomea	sanCOST1250.5	se	13.27	(Turissini and Matute 2017; Turissini *et al.* 2018)	SRX3029322
D. santomea	sanCOST1270.6	se	14.76	(Turissini and Matute 2017; Turissini *et al.* 2018)	SRX3029337
D. santomea	sanOBAT1200.13	se	14.47	(Turissini and Matute 2017; Turissini *et al.* 2018)	SRX3029334
D. santomea	sanOBAT1200.5	se	16.82	(Turissini and Matute 2017; Turissini *et al.* 2018)	SRX3029332
D. santomea	sanRain39	se	15.81	(Turissini and Matute 2017; Turissini *et al.* 2018)	SRX3029333:
D. santomea	sanSTO7	se	15.29	(Turissini and Matute 2017; Turissini *et al.* 2018)	SRX3029335
D. santomea	sanThena5	se	12.98	(Turissini and Matute 2017; Turissini *et al.* 2018)	SRX3029338
D. sechellia	Anro_B1	pe	36.85	(Schrider *et al.* 2018; Turissini *et al.* 2018)	SRX3029286
D. sechellia	Anro_B2	pe	34.56	(Schrider *et al.* 2018; Turissini *et al.* 2018)	SRX3029285
D. sechellia	Anro_B3	pe	38.75	(Schrider *et al.* 2018; Turissini *et al.* 2018)	SRX3029281
D. sechellia	Anro_B5	pe	38.36	(Schrider *et al.* 2018; Turissini *et al.* 2018)	SRX3029270
D. sechellia	Anro_B6	pe	33.48	(Schrider *et al.* 2018; Turissini *et al.* 2018)	SRX3029283

D. sechellia	Anro_B7	pe	39.25	(Schrider *et al.* 2018; Turissini *et al.* 2018)	SRX3029301
D. sechellia	Anro_B8	pe	34.84	(Schrider *et al.* 2018; Turissini *et al.* 2018)	SRX3029373
D. sechellia	Denis124	se	24.73	(Schrider *et al.* 2018; Turissini *et al.* 2018)	SRX3029315
D. sechellia	Denis135	se	32.4	(Schrider *et al.* 2018; Turissini *et al.* 2018)	SRX3029275
D. sechellia	Denis7_2	se	28	(Schrider *et al.* 2018; Turissini *et al.* 2018)	SRX3029314
D. sechellia	Denis7_8	se	28	(Schrider *et al.* 2018; Turissini *et al.* 2018)	SRX3029277
D. sechellia	DenisAMT	se	14.44	(Schrider *et al.* 2018; Turissini *et al.* 2018)	SRX3029303
D. sechellia	DenisAT3	se	28.03	(Schrider *et al.* 2018; Turissini *et al.* 2018)	SRX3029317
D. sechellia	DenisDNJ6	se	22.63	(Schrider *et al.* 2018; Turissini *et al.* 2018)	SRX3029319
D. sechellia	DenisJT1	se	23.99	(Schrider *et al.* 2018; Turissini *et al.* 2018)	SRX3029316
D. sechellia	DenisMCL	se	46.04	(Schrider *et al.* 2018; Turissini *et al.* 2018)	SRX3029276
D. sechellia	DenisNF100	se	10.12	(Schrider *et al.* 2018; Turissini *et al.* 2018)	SRX3029307
D. sechellia	DenisNF123	se	13.07	(Schrider *et al.* 2018; Turissini *et al.* 2018)	SRX3029306
D. sechellia	DenisNF13	se	24.12	(Schrider *et al.* 2018; Turissini *et al.* 2018)	SRX3029313
D. sechellia	DenisNF134	se	14.45	(Schrider *et al.* 2018; Turissini *et al.* 2018)	SRX3029302

D. sechellia	DenisNF155	se	15.84	(Schrider *et al.* 2018; Turissini *et al.* 2018)	SRX3029321
D. sechellia	DenisNF66	se	27.16	(Schrider *et al.* 2018; Turissini *et al.* 2018)	SRX3029312
D. sechellia	DenisNoni10	se	14.63	(Schrider *et al.* 2018; Turissini *et al.* 2018)	SRX3029320
D. sechellia	DenisNoni101	se	25.07	(Schrider *et al.* 2018; Turissini *et al.* 2018)	SRX3029278
D. sechellia	DenisNoni60	se	19.35	(Schrider *et al.* 2018; Turissini *et al.* 2018)	SRX3029318
D. sechellia	LD11_sech	pe	44.37	(Schrider *et al.* 2018; Turissini *et al.* 2018)	SRX3029282
D. sechellia	LD12	pe	37.29	(Schrider *et al.* 2018; Turissini *et al.* 2018)	SRX3029284
D. sechellia	LD13	pe	45.52	(Schrider *et al.* 2018; Turissini *et al.* 2018)	SRX3029289
D. sechellia	LD14	pe	34.93	(Schrider *et al.* 2018; Turissini *et al.* 2018)	SRX3029288
D. sechellia	LD15	pe	49.06	(Schrider *et al.* 2018; Turissini *et al.* 2018)	SRX3029362
D. sechellia	LD16	pe	40.63	(Schrider *et al.* 2018; Turissini *et al.* 2018)	SRX3029290
D. sechellia	LD8	pe	41.54	(Schrider *et al.* 2018; Turissini *et al.* 2018)	SRX3029364
D. sechellia	mariane_1	pe	49.51	(Schrider *et al.* 2018; Turissini *et al.* 2018)	SRX3029287
D. sechellia	maria_3	pe	39.82	(Schrider *et al.* 2018; Turissini *et al.* 2018)	SRX3029376
D. sechellia	PNF10	pe	34.48	(Schrider *et al.* 2018; Turissini *et al.* 2018)	SRX3029280

D. sechellia	PNF11	pe	39.12	(Schrider *et al.* 2018; Turissini *et al.* 2018)	SRX3029279
D. sechellia	PNF3	pe	46.24	(Schrider *et al.* 2018; Turissini *et al.* 2018)	SRX3029272
D. sechellia	PNF4	pe	32.94	(Schrider *et al.* 2018; Turissini *et al.* 2018)	SRX3029363
D. sechellia	PNF5	pe	41.99	(Schrider *et al.* 2018; Turissini *et al.* 2018)	SRX3029273
D. sechellia	PNF7	pe	28.88	(Schrider *et al.* 2018; Turissini *et al.* 2018)	SRX3029271
D. sechellia	PNF8	pe	55.93	(Schrider *et al.* 2018; Turissini *et al.* 2018)	SRX3029274
D. simulans	Bioko_cascade_1	pe	38.1	(Serrato-Capuchina *et al.* 2020, 2021)	SRX7116491
D. simulans	Bioko_H1	pe	38.4	(Serrato-Capuchina *et al.* 2020, 2021)	SRX7116492
D. simulans	Bioko_LB1	pe	38.26	(Serrato-Capuchina *et al.* 2020, 2021)	SRX7116493
D. simulans	Bioko_Riaba_9	pe	32.7	(Serrato-Capuchina *et al.* 2020, 2021)	SRX7116489
D. simulans	Bioko_Riaba_mixed	pe	32.53	(Serrato-Capuchina *et al.* 2020, 2021)	SRX7116490
D. simulans	Kib32	se,pe	52.05	(Rogers *et al.* 2014, 2017)	SRR580348, SRR580347, SRR580350, SRR580349
D. simulans	MD06	pe	128.34	(Rogers *et al.* 2014, 2017)	SRX6458044
D. simulans	MD105	pe	101.25	(Rogers *et al.* 2014, 2017)	SRX6458047
D. simulans	MD106	pe	104.11	(Rogers *et al.* 2014, 2017)	SRX6458049
D. simulans	MD15	pe	115.94	(Rogers *et al.* 2014, 2017)	SRX6458052
D. simulans	MD199	pe	128.89	(Rogers *et al.* 2014, 2017)	SRX8034374
D. simulans	MD221	pe	115.61	(Rogers *et al.* 2014, 2017)	SRX6458058

D. simulans	MD233	pe	139.25	(Rogers *et al.* 2014, 2017)	SRX6458061
D. simulans	MD251	pe	133.51	(Rogers *et al.* 2014, 2017)	SRX6458064
D. simulans	MD63	pe	64.75	(Rogers *et al.* 2014, 2017)	SRX6458067
D. simulans	MD73	pe	130.06	(Rogers *et al.* 2014, 2017)	SRX6458070
D. simulans	NS05	pe	135.43	(Rogers *et al.* 2014, 2017)	SRX6458073
D. simulans	NS113	pe	125.58	(Rogers *et al.* 2014, 2017)	SRX6458076
D. simulans	NS137	pe	111.69	(Rogers *et al.* 2014, 2017)	SRX6458078
D. simulans	NS33	pe	125	(Rogers *et al.* 2014, 2017)	SRX6458081
D. simulans	NS39	pe	136.06	(Rogers *et al.* 2014, 2017)	SRX6458084
D. simulans	NS40	pe	136.32	(Rogers *et al.* 2014, 2017)	SRX6458087
D. simulans	NS50	pe	131.23	(Rogers *et al.* 2014, 2017)	SRX6458090
D. simulans	NS67	pe	139.1	(Rogers *et al.* 2014, 2017)	SRX6458093
D. simulans	NS78	pe	136.03	(Rogers *et al.* 2014, 2017)	SRX6458096
D. simulans	NS79	pe	135.12	(Rogers *et al.* 2014, 2017)	SRX6458099
D. simulans	tsimbazazaa	pe	38.11		SRR869580, SRR869579
D. simulans	w501	pe	26.35	(Hu *et al.* 2013)	SRR520350
D. teissieri	Balancha_1	pe	30.37	(Turissini and Matute 2017)	SRX3029331
D. teissieri	Bata2	se	20.7	(Turissini and Matute 2017)	SRX3029370
D. teissieri	Bata8	se	18.56	(Turissini and Matute 2017)	SRX3029369
D. teissieri	cascade_2_1	pe	29.2	(Turissini and Matute 2017)	SRX3029323
D. teissieri	cascade_2_2	pe	33.88	(Turissini and Matute 2017)	SRX3029330
D. teissieri	cascade_2_4	pe	26.91	(Turissini and Matute 2017)	SRX3029324
D. teissieri	cascade_4_1	pe	27.07	(Turissini and Matute 2017)	SRX3029328
D. teissieri	cascade_4_2	pe	39.54	(Turissini and Matute 2017)	SRX3029374
D. teissieri	cascade_4_3	pe	23.26	(Turissini and Matute 2017)	SRX3029329
D. teissieri	House_Bioko	pe	35.7	(Turissini and Matute 2017)	SRX3029325
D. teissieri	La_Lope_Gabon	pe	36.6	(Turissini and Matute 2017)	SRX3029375
D. teissieri	Selinda	pe	27.74	(Turissini and Matute 2017)	SRX3029326

D. yakuba	1_19	se	18.51	(Turissini and Matute 2017)	SRX3029345
D. yakuba	1_5	se	19.27	(Turissini and Matute 2017)	SRX3518253
D. yakuba	1_6	se	20.16	(Turissini and Matute 2017)	SRX3029348
D. yakuba	1_7	se	22.01	(Turissini and Matute 2017)	SRX3029297
D. yakuba	2_11	se	19.51	(Turissini and Matute 2017)	SRX3029350
D. yakuba	2_14	se	19.15	(Turissini and Matute 2017)	SRX3029347
D. yakuba	2_6	se	23.43	(Turissini and Matute 2017)	SRX3029353
D. yakuba	2_8	se	20.38	(Turissini and Matute 2017)	SRX3029343
D. yakuba	3_16	se	19.82	(Turissini and Matute 2017)	SRX3029344
D. yakuba	3_2	se	21.89	(Turissini and Matute 2017)	SRX3029356
D. yakuba	3_23	se	22.11	(Turissini and Matute 2017)	SRX3029291
D. yakuba	4_21	se	22.44	(Turissini and Matute 2017)	SRX3029299
D. yakuba	Abidjan_12	se	23.79	(Turissini and Matute 2017)	SRX3029360
D. yakuba	Airport_16_5	se	20.11	(Turissini and Matute 2017)	SRX3029355
D. yakuba	Anton_1_Principe	se	19.54	(Turissini and Matute 2017)	SRX3029295
D. yakuba	Anton_2_Principe	se	21.38	(Turissini and Matute 2017)	SRX3029361
D. yakuba	BAR_1000_2	se	21.23	(Turissini and Matute 2017)	SRX3029367
D. yakuba	BIOKO_NE_4_6	se	17.17	(Turissini and Matute 2017)	SRX3029351
D. yakuba	Bosu_1235_14	se	17.22	(Turissini and Matute 2017)	SRX3029300
D. yakuba	Cascade_18	se	23.96	(Turissini and Matute 2017)	SRX3029354
D. yakuba	Cascade_19_16	se	16.5	(Turissini and Matute 2017)	SRX3029342
D. yakuba	Cascade_21	se	20.59	(Turissini and Matute 2017)	SRX3029368
D. yakuba	Cascade_SN6_1	se	18.85	(Turissini and Matute 2017)	SRX3029358
D. yakuba	COST_1235_2	se	17.69	(Turissini and Matute 2017)	SRX3029296
D. yakuba	COST_1235_3	se	15.42	(Turissini and Matute 2017)	SRX3029349
D. yakuba	CY01A	pe	196.72	(Rogers *et al.* 2014, 2017)	SRX6457979, SRX6457980 , SRX6457981, SRX6457982

D. yakuba	CY02B5	pe	69.98	(Rogers *et al.* 2014, 2017)	SRX6457983, SRX6457984, SRX6457985
D. yakuba	CY04B	pe	157.94	(Rogers *et al.* 2014, 2017)	SRX6457986, SRX6457987, SRX6457988, SRX6457989
D. yakuba	CY08A	pe	75.04	(Rogers *et al.* 2014, 2017)	SRX6457990, SRX6457991, SRX6457992
D. yakuba	CY13A	pe	72.72	(Rogers *et al.* 2014, 2017)	SRX6457990, SRX6457991, SRX6457992
D. yakuba	CY17C	pe	193.88	(Rogers *et al.* 2014, 2017)	SRX6457996, SRX6457997, SRX6457998, SRX6457999
D. yakuba	CY20A	pe	183.65	(Rogers *et al.* 2014, 2017)	SRX6458000, SRX6458001, SRX6458002
D. yakuba	CY21B3	pe	173.17	(Rogers *et al.* 2014, 2017)	SRX6458003, SRX6458004, SRX6458005
D. yakuba	CY22B	pe	69.84	(Rogers *et al.* 2014, 2017)	SRX6458006, SRX6458007, SRX6458008
D. yakuba	CY28	pe	110.16	(Rogers *et al.* 2014, 2017)	SRX6458009, SRX6458010, SRX6458011
D. yakuba	Montecafe_17_17	se	19.97	(Turissini and Matute 2017)	SRX3029359

D. yakuba	NY141	pe	143.54	(Turissini and Matute 2017)	SRX6458037, SRX6458038, SRX6458039
D. yakuba	NY42	pe	118.02	(Turissini and Matute 2017)	SRX6458040, SRX6458041
D. yakuba	NY48	pe	84.99	(Rogers *et al.* 2014, 2017)	SRX6458013, SRX6458014, SRX6458015
D. yakuba	NY56	pe	88.65	(Rogers *et al.* 2014, 2017)	SRX6458016, SRX6458017, SRX6458018
D. yakuba	NY62	pe	94.51	(Rogers *et al.* 2014, 2017)	SRX6458019, SRX6458020, SRX6458021
D. yakuba	NY65	pe	91.46	(Rogers *et al.* 2014, 2017)	SRX6458022, SRX6458023, SRX6458024
D. yakuba	NY66	pe	148.65	(Rogers *et al.* 2014, 2017)	SRX6458025, SRX6458026, SRX6458027
D. yakuba	NY73	pe	92.08	(Rogers *et al.* 2014, 2017)	SRX6458028, SRX6458029, SRX6458030
D. yakuba	NY81	pe	148.42	(Rogers *et al.* 2014, 2017)	SRX6458031, SRX6458032, SRX6458033
D. yakuba	NY85	pe	99.03	(Rogers *et al.* 2014, 2017)	SRX6458034, SRX6458035, SRX6458036
D. yakuba	OBAT_1200_5	se	22.7	(Turissini and Matute 2017)	SRX3029357
D. yakuba	SanTome_city_14_26	se	22.75	(Turissini and Matute 2017)	SRX3029372

D. yakuba	SA_3	se	18.64	(Turissini and Matute 2017)	SRX3029294
D. yakuba	SJ14	se	15.77	(Turissini and Matute 2017)	SRX3029293
D. yakuba	SJ4	se	25.82	(Turissini and Matute 2017)	SRX3029292
D. yakuba	SJ7	se	19.51	(Turissini and Matute 2017)	SRX3029352
D. yakuba	SJ_1	se	21.35	(Turissini and Matute 2017)	SRX3029371
D. yakuba	SN7	se	23.66	(Turissini and Matute 2017)	SRX3029366
D. yakuba	SN_Cascade_22	se	21.78	(Turissini and Matute 2017)	SRX3029365
D. yakuba	Tai_18	se	22.17	(Turissini and Matute 2017)	SRX3029298

SUPPLEMENTARY FIGURES

FIGURE S1. X_{mel}, X_{sim} and X_{mau} cause abdominal ablations in hybrid males with *D. santomea*. Hybrid males from the ♀*sim* × ♂*san* and ♀*mau* × ♂ *san* crosses show high frequency of abdominal ablations similar to those observed in than in ♀*mel* × ♂ *san* hybrids. Hybrid females from the same crosses show a lower frequency of ablations. The nature of the defect in these hybrid males is identical to that seen in *mel/san* hybrid males, a characteristic ablation of abdominal segments (as shown in Figure 1).

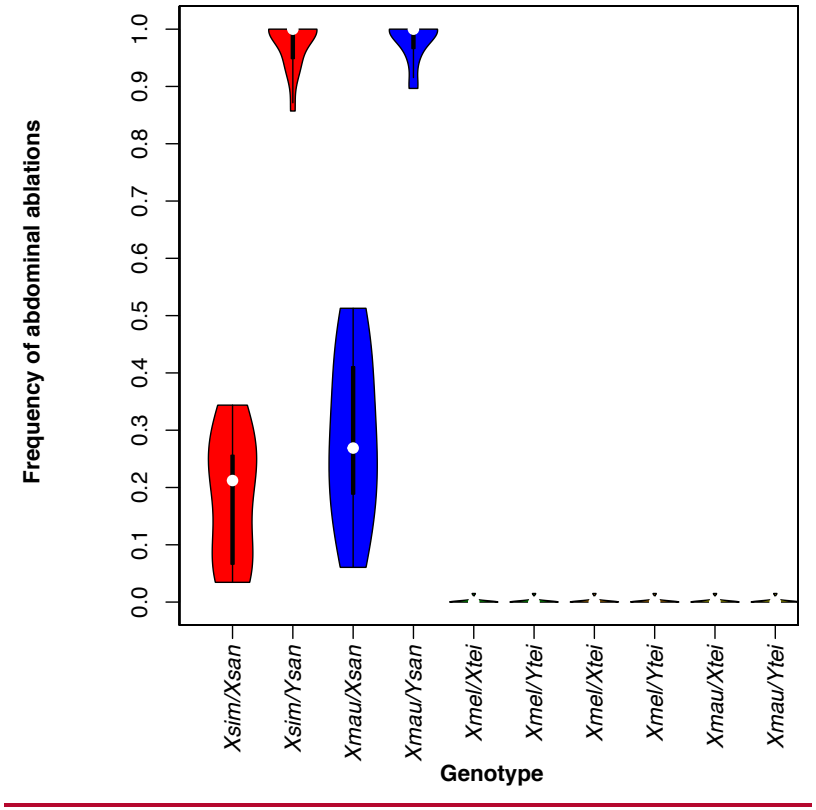

FIGURE S2. Crossing design to assess whether small piece of the X_{mel} cause hybrid inviability and abdominal ablations. Blue bars represent *D. santomea* chromosomes; yellow bars represent *D. melanogaster* chromosomes. Solid colors: sex chromosomes, stripped bars: autosomes. This approach is a modified version of (Sawamura and Yamamoto 1993; Cattani and Presgraves 2012; Matute and Gavin-Smyth 2014).

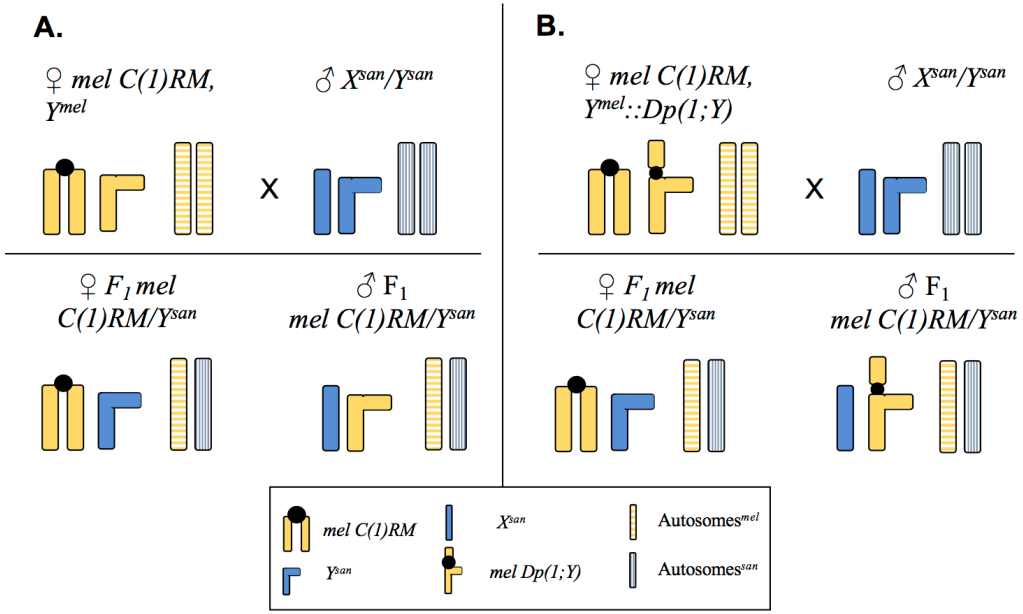

FIGURE S3. Frequency of abdominal ablations caused by the X_{mel} translocations shown in Figure 2 in X_{san}/Y_{mel} hybrid males.

Each Bloomington stock number is shown within the bar. The precise genotype of each stock is shown in Table S1.

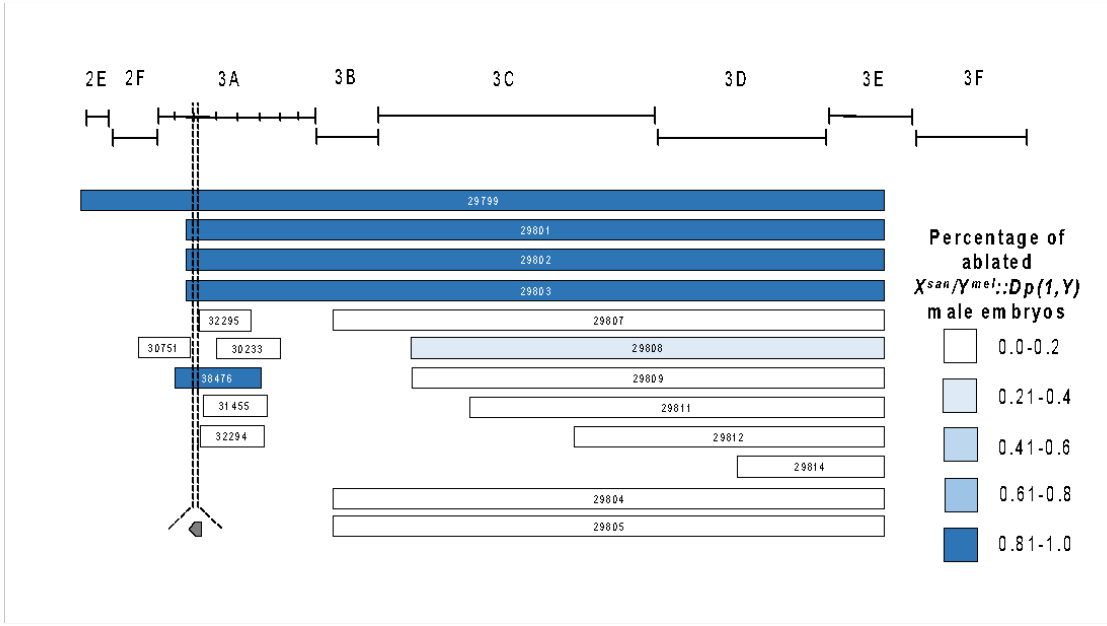

FIGURE S4. The presence of gt_{mel} causes HI in *mel/san* hybrids produced with all *D. santomea* lines but the magnitude of the inviability varies. We measured frequency of abdominal ablations in hybrid X_{mel}/Y_{san} males (**A**). The magnitude of the frequency of abdominal ablations and of hybrid female inviability are correlated among lines (panel **B**; $\rho = 0.1734$, $P = 0.0141$). Boxes in the boxplot are ordinated from the lower median (left) to the highest (right). S1: Thena5; S2: sanCAR1490; S3: sanCOST1250.5; S4: sanCOST1270.1; S5: sanOBAT1200; S6: sanOBAT1200.2; S7: sanRain39; S8: sanCAR1600.3; S9: Carv2015.1; S10: Carv2015.5; S11: Carv2015.11; S12: Carv2015.16; S13: Pico1680.1; S14: Pico1659.2; S15: Pico1659.3; S16: Amelia2015.1; S17: Amelia2015.6; S18: Amelia2015.12; S19: A1200.7; S20: Rain42.

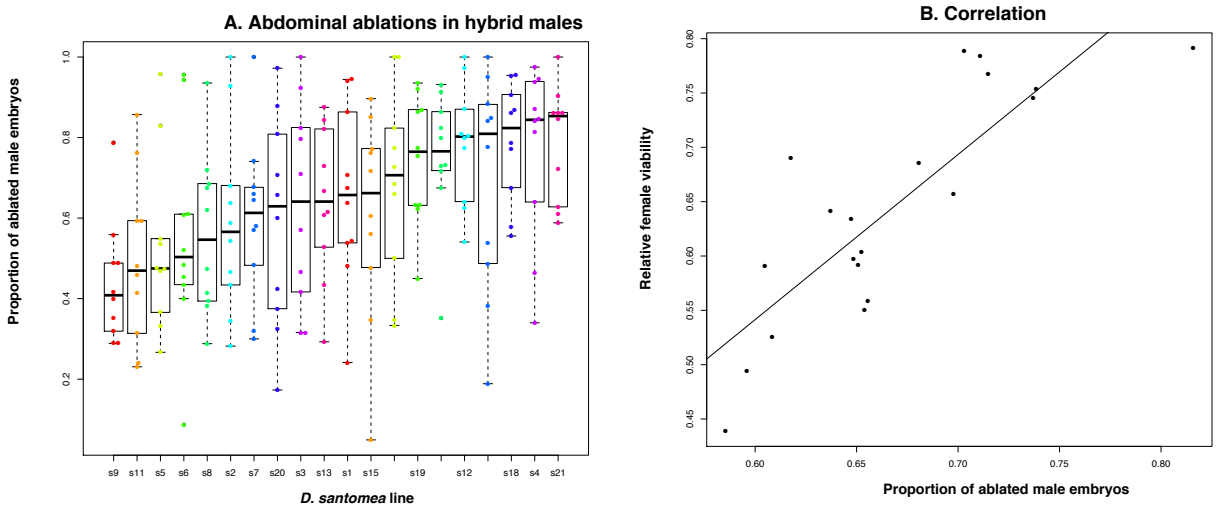

FIGURE S5. Crosses between *D. melanogaster* females harboring *Dp(1;Y)* duplications and males from the *simulans* species group (*D. mauritiana*, and *D. simulans*) show no evidence of male embryo lethality or abdominal ablations. *Dp(1;Y)* duplications containing gt_{mel} cause no embryonic defects and do not cause heightened hybrid inviability. The color code is the same as used in Figure 2C. The lack of gray bars indicates that none of the duplications caused hybrid inviability in any of the crosses. Please note that embryonic lethality is low in all these crosses and consequently the number of dissected embryos (Panels D-F) is also low.

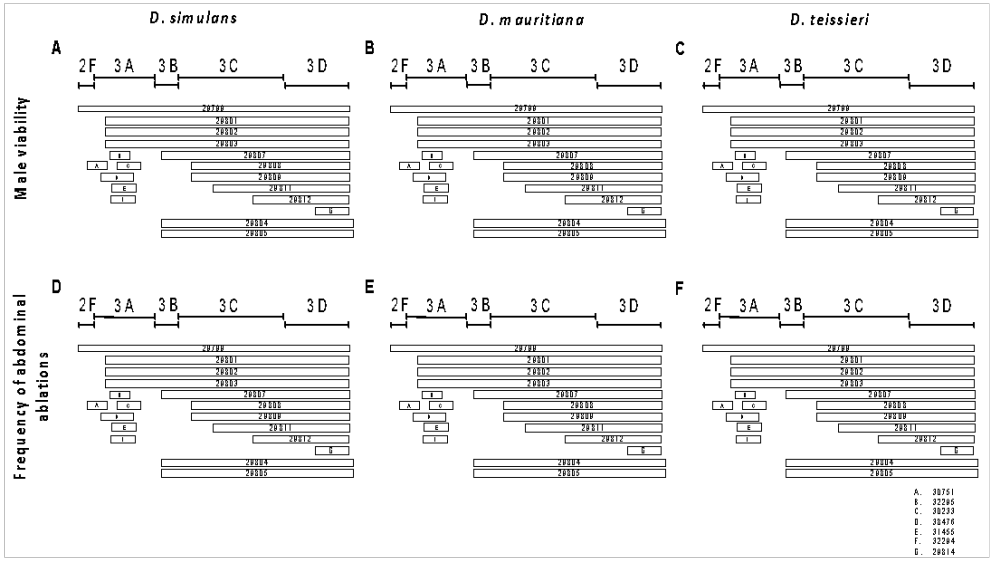

FIGURE S6. Crosses between *D. melanogaster* females harboring *Dp(1;Y)* duplications and males from different lines of *D. melanogaster* show no evidence of male embryo lethality or abdominal ablations. *Dp(1:Y)* duplications containing gt^{mel} cause no embryonic defects and do not cause heightened hybrid inviability. The color code is the same as used in Figure 2C. The lack of gray bars indicates that none of the duplications caused hybrid inviability in any of the crosses. Please note that embryonic lethality is exceptionally low in all these crosses and consequently the number of dissected embryos (Panels D-F) is also low.

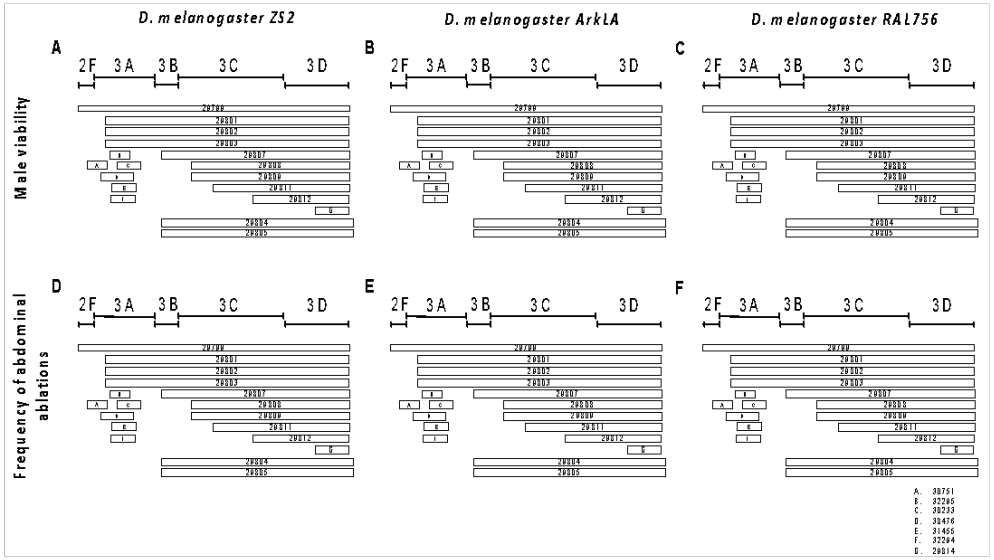

FIGURE S7. Hybrid male embryos carrying a *gt$_{mel}^{X11}$ D. melanogaster* allele show a variety of developmental defects.

gt$_{mel}^{X11}$/Y$_{san}$ males are inviable and show a variety of developmental defects (A-C). Some individuals also show abdominal ablations (D).

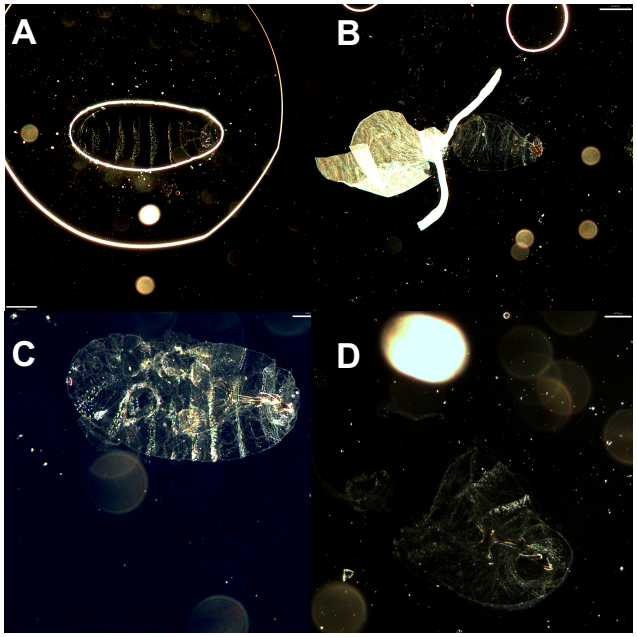

FIGURE S8. *mel/san* hybrids carrying a *D. melanogaster* chromosome and null alleles for *boi*, *trol*, or *tko* show similar levels of hybrid viability. This is in contrast to males also carrying a *D. melanogaster* chromosome but a *gt* null allele (gt_{mel}^{X11}) which show a significant reduction in abdominal ablations (shown in Figure 2). These three genes have no effect in hybrids between *D. melanogaster* and three more species (*D. teissieri* [B], *D. simulans* [C], and *D. mauritiana* [D]).

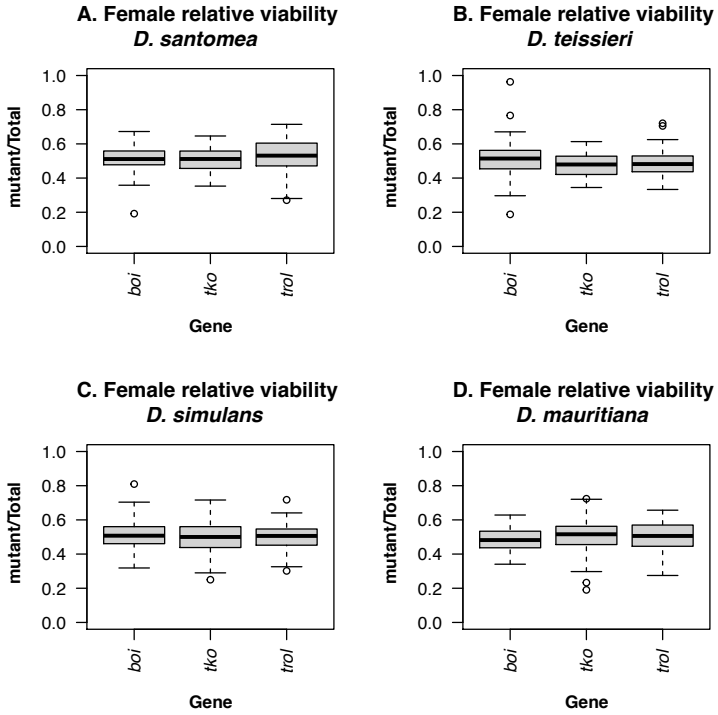

FIGURE S9. The *X*-chromosome balancer has no effect on the quantification of hybrid inviability in *mel/san* hybrid females. We found no heterogeneity in the relative viability of gt_{mel}^{X11} when different balancer chromosomes are used (One-way ANOVA, $F_{6,109}$= 0.694, P= 0.655). We used seven different *X*-chromosomes balancers and none of them had a major effect on the quantification of the relative frequency of gt_{mel}^{X11} viability in any of the hybrid crosses.

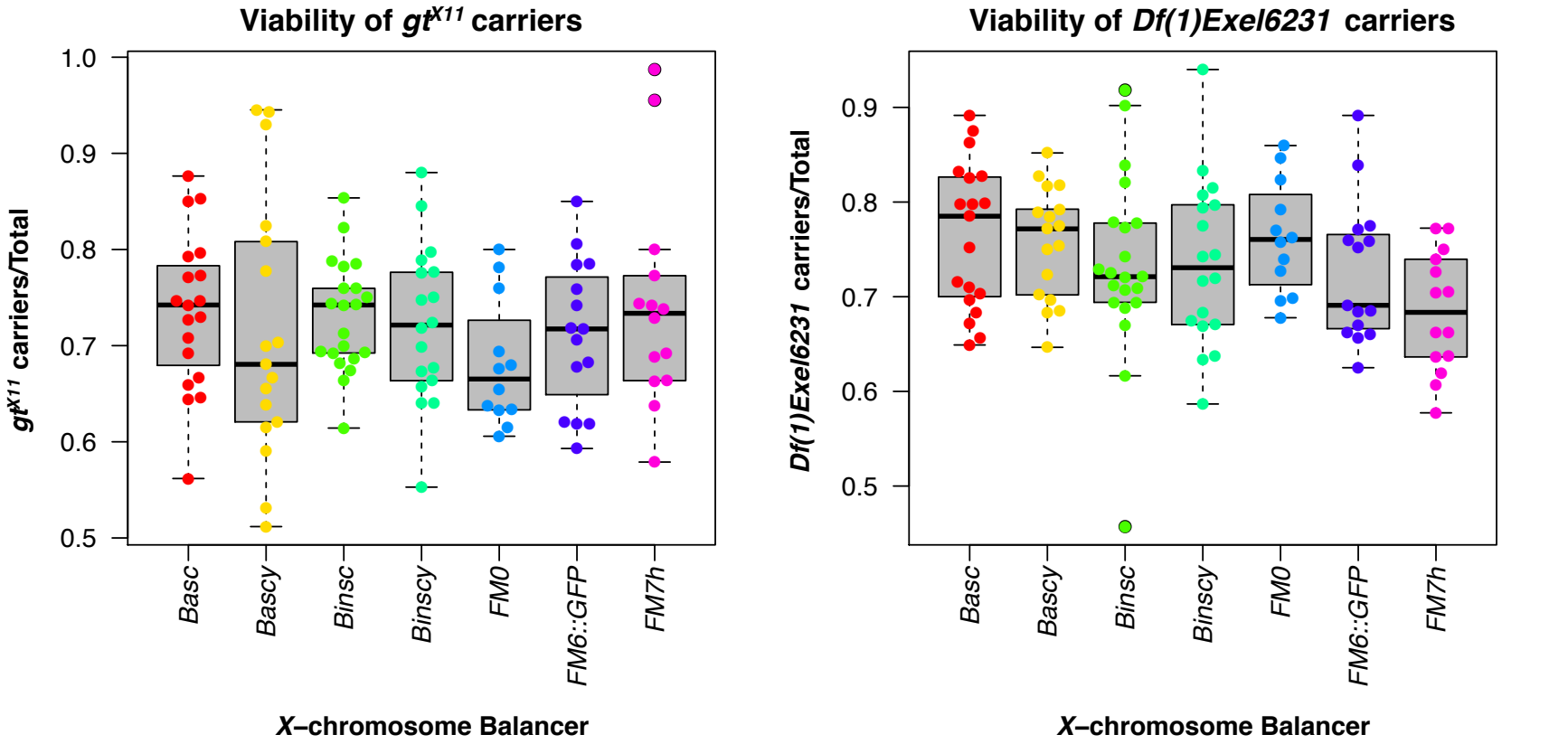

FIGURE S10. Frequency of abdominal ablations in each deficiency cross shown in Figure 2. Deficiency chromosomes that contain a functional gt_{mel} (e.g., 8031, 9054, and 8950) were prone to show abdominal ablations than deficiencies that harbored other genes. On the other hand, deficiency chromosomes with no functional copy of gt_{mel} show reduced rates of abdominal ablations. The mean proportion of abdominal ablation in X_{mel}/X_{san} hybrid females is 0.420.

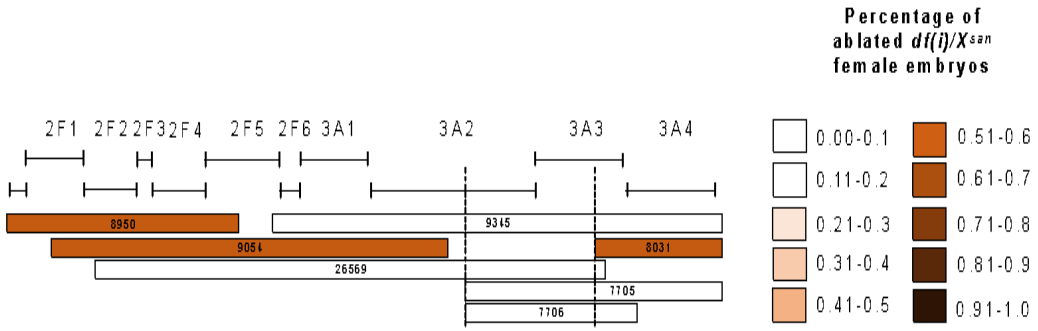

FIGURE S11. gt^{mel} has no effect on the viability of *mel/tei*, *mel/mau*, and *mel/sim* hybrid females. We used the same deficiency chromosomes reported to detect the effect of gt_{mel} in *mel/san* hybrid females (Figure 3A). In all three cases, *df/FM7::GFP* crossed to males of each of the species led to 1:1 ratios in female progeny. The color code is the same as in Figure 3A but since no deficiency departed from the 1:1 expected (i.e., no gt_{mel} effect on hybrid viability), there are no gray bars.

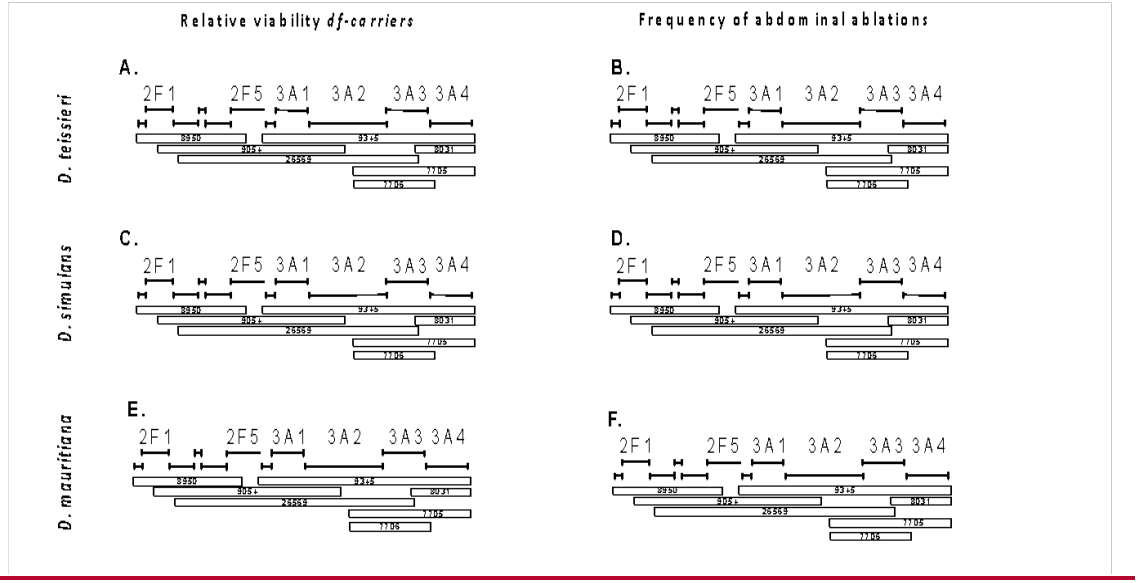

FIGURE S12. gt_{mel} has no effect on the viability of pure-species *D. melanogaster* F1 females. We used the same deficiency chromosomes reported to detect the effect of gt_{mel} in *mel/san* hybrid females (Figure 3A). In all three types of crosses (three isofemale lines), *df/FM7::GFP* crossed to males of each of the species led to 1:1 ratios in female progeny. The color code is the same as in Figure 3A but since no deficiency departed from the 1:1 expected (i.e., no gt_{mel} effect on hybrid viability), there are no gray bars. No cross showed any abdominal ablation.

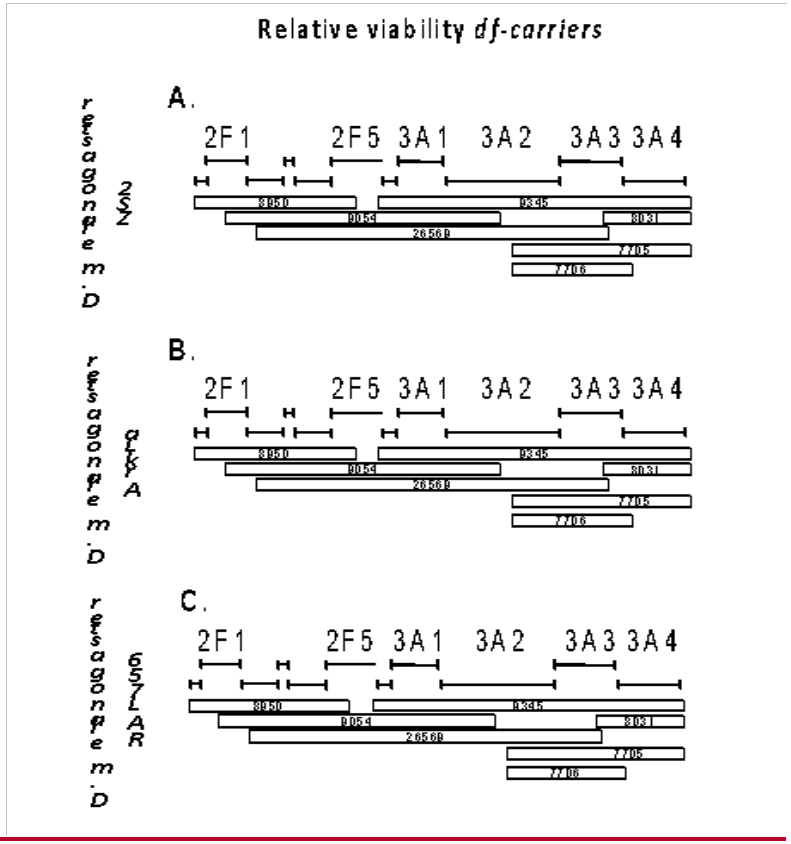

FIGURE S13. *gt* transgene, removable piggyBac cassette design and crossing schemes involving *gt* transgenes. Panel **A** shows the general experimental design to generate the four chimeric alleles included in this study and the insertion site for their integration (attP2 site in the 3rd chromosome). Panel **B** shows a detail of the 5' UTR common to all the four alleles with piggyBac cassette. Panel **C** shows the crosses used in Table 1 when measuring giant's effects on hybrid embryonic lethality. Panel **D** shows the crosses used in Table 2 when measuring the effects of different alleles of *giant* on adult hybrid female lethality.

A.

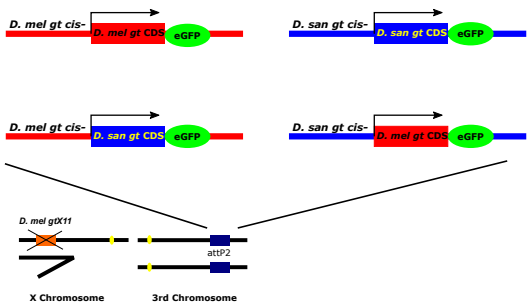

B.

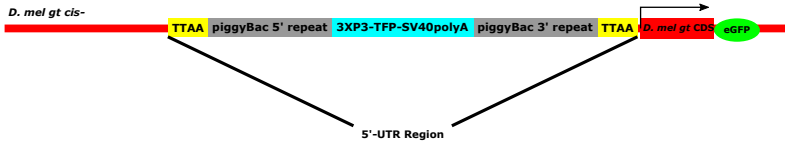

C.

$$\text{♀♀}\ \frac{gt^{X11}_{D.mel}}{gt^{X11}_{D.mel}};\frac{\text{P}\{D.mel\ gt\}\text{attP2}}{\text{P}\{D.mel\ gt\}\text{attP2}} \quad \times \quad \text{♂♂}\ \frac{X_{D.san}}{Y_{D.san}};\frac{+_{D.san}}{+_{D.san}}$$

↓

Count the number of dead embryos in F1s

Sex	Genotype	Embryonic Lethality
Both Sex Pooled	$\frac{X_{D.san}\text{ or }Y_{D.san}}{gt^{X11}_{D.mel}};\frac{+_{D.san}}{\text{P}\{D.mel\ gt\}\text{attP2}}$	$\frac{\#\text{Dead Embryos}}{\#\text{Total Embryos}}$

D.

$$\text{♀♀}\ \frac{gt^{X11}_{D.mel}}{gt^{X11}_{D.mel}};\frac{\text{P}\{D.mel\ gt\}\text{attP2}}{+} \quad \times \quad \text{♂♂}\ \frac{X_{D.san}}{Y_{D.san}};\frac{+_{D.san}}{+_{D.san}}$$

↓

Count number of different genotypes by fluorescent markers in hybrid F1 females

Genotype	Expectation
$\frac{X_{D.san}}{gt^{X11}_{D.mel}};\frac{+_{D.san}}{+_{D.mel}}$	1
$\frac{X_{D.san}}{gt^{X11}_{D.mel}};\frac{+_{D.san}}{\text{P}\{D.mel\ gt\}\text{attP2}}$	Relative Viability

FIGURE S14. Introgression of the *FM7::GFP* and gt^{X11} alleles into 200 lines of the DGRP lines. Each bar represents a chromosome. Short bars are the *X*-chromosome while longer bars represent the autosomes (only one set of autosomes shown). The bar with dashed lines represents the *FM7::GFP* balancer. Solid yellow represent the *FM7::GFP* background. Red bars represent each of the DGRP genetic backgrounds. Dashed blue lines represent the t the gt^{X11} chromosome, while solid blue lines represent the autosomal background of the gt^{X11} stock. **A.** The first step of the experimental design involves introgressing the *FM7::GFP* balancer into each of the 200 DGRP backgrounds. After ten generations of repeating backcrossing, we obtained both females and males that carried the balancer and the DGRP background. **B.** Males from the cross shown in **A** (carriers of the *FM7::GFP* balancer) were crossed the gt^{X11}*/FM7::GFP* females. This cross produces females that carry the gt^{X11} chromosome, the *FM7::GFP* balancer and a mixed genetic background. These females were crossed to males that had the DGRP autosomal background and a *FM7::GFP* balancer (**C**). We repeated this backcrossing approach for ten generations. After, 11 generations we obtained gt^{X11}*/FM7::GFP* females with DGRP autosomal backgrounds. These females were then crossed to *D. santomea* and the percentage of ablated progeny were scored.

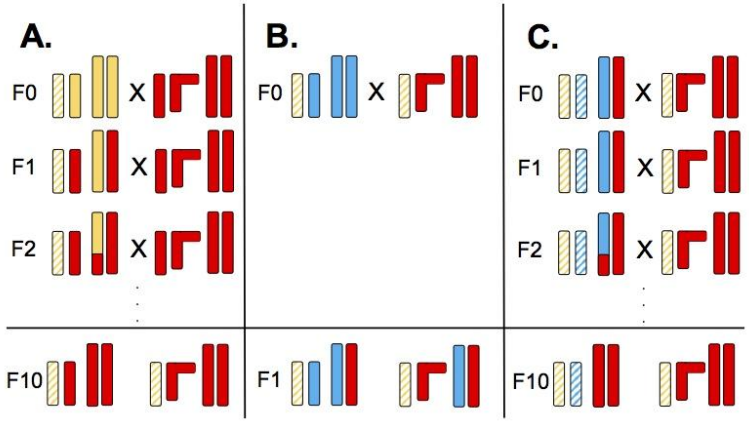
A.
F0
X
F1
X
F2
X
F10
B.
F0
X
F1
C.
F0
X
F1
X
F2
X
F10

FIGURE S15. ***gt*** **alleles from six different species in the** ***melanogaster*** **species complex**. We found no major differences at the coding portion of the gene between the *melanogaster* species supercomplex (*D. melanogaster*, *D. simulans*, and *D. sechellia*) and that the *D. santomea/D. yakuba* species pair is the structure of poly-glutamine repeats. melgt: *D. melanogaster*, simgt: *D. simulans*, sechgt: *D. sechellia*, sangt: *D. santomea*, eregt: *D. erecta*. Asterisks show residues that are conserved across the whole group.

```
melgt      1   MLMHEKLMAG QFFDLKTDRK PLMHHHQYQH HQQQPLHHLP HSQLPVQGSL
simgt      1   MLMHEKLMAG QFFDLKTDRK PLMHHHQYQH HQQQPLHHLP HSQLPVQGSL
secgt      1   MLMHEKLMAG QFFDLKTDRK PLMHHHQYQH HQQQPLHHLP HSQLPVQGSL
yakgt      1   MLMHEKLMAG QFFDLKTDRK PLMHHHQYQH HQQQPLHHLP HSQLPVQGSL
sangt      1   MLMHEKLMAG QFFDLKTDRK PLMHHHQYQH HQQQPLHHLP HSQLPVQGSL
ecegt      1   MLMHEKLMAG QFFDLKTDRK PLMHHHQYQH HQQQPLHHLP HSQLPVQGSL
               ********** ********** ********** ********** **********

melgt     51   GLPKMDLYTA YAYQQQLLGA ALSQQQQQQQ QQ-------Q QH---QQLQQ
simgt     51   GLPKMDLYTA YAYQQQLLGA ALSQQQQQQQ Q--------Q QH---QQLQQ
secgt     51   GLPKMDLYTA YAYQQQLLGA ALSQQQQQHQ QQ-------Q QH---QQLQQ
yakgt     51   GLPKMDLYTA YAYQQQLLGA ALSQQQQQQQ Q--------Q QHQQMQQQQQ
sangt     51   GLPKMDLYTA YAYQQQLLGA ALSQQQQQQ- ----QQQQHQ QM---QQQQQ
ecegt     51   GLPKMDLYTA YAYQQQLLGA ALSQQQQQQQ -Q-------Q HQ---QLQQQ
               ********** ********** *******

melgt     91   QHTSSAEVLD LSRRCDSVET PRKTPSPYQT SYSYGSGSPS ASPTSNLLYA
simgt     90   QHTSSAEVLD LSRRCDSVET PRKTPSPYQT SYSYGSGSPS ASPTSNLLYA
secgt     91   QQTSSAEVLD LSRRCDSVET PRKTPSPYQT SYSYGSGSPS ASPTSSLLYA
yakgt     93   QQTSSAEVLD LSRRCDSVET PRKTPSPYQT SYSYGSGSPS ASPTSNLLYA
sangt     93   QQTSSAEVLD LSRRCDSVET PRKTPSPYQT SYSYGSGSPS ASPTSNLLYA
ecegt     90   QQSSSAEVLD LSRRCDSVET PRKTPSPYQT SYSYGSGSPS ASPTSNLLYA
               *  ******* ********** ********** ********** **********

melgt    141   AQMQQQQHQ- QQQQQQQQQQ QLASLYPAFY YSNIKQEQAT PTAAPPKVTP
simgt    140   AQMQQQQHQ- QQQQQQQQ-- -LASLYPAFY YSNIKQEQAT PTAAPPKVTP
secgt    141   AQMQQQQNQ- QQQQQQQQ-- -LASLYPAFY YSNIKQEQAT PTAAPPKVTP
yakgt    143   AQMQQQQQQH QQQQQQQQ-- -LASLYPAFY YSNIKQEQAT PTAAPPKVTP
sangt    143   AQMQQQQQQH QQQQQQQQ-- -LASLYPAFY YSNIKQEQAT PTAAPPKVTP
ecegt    140   AQMQQQQQQH QQQQh-QQ-- -LASLYPAFY YSNIKQEQAT PTAAPPKVTP
               *********  ****        ********** ********** **********

melgt    190   TANLLQTFAA ASAAAAAAAA ASSTNSPRPA SNASTMQIDV LENPLSPAVE
simgt    186   TANLLQTFAA ASAAA--AAA ASSTNSPRPA SNASTMQIDV LENPQSPAVE
secgt    187   TANLLQTFAA ASAAAAAAAA ASSTNSPRPA SNASTMQIDV LENPQSPAVE
yakgt    190   TANLLQTFAA ASAAAAAAAA ASATNSPRPA SNASTMQIDV LENPQSPAVE
sangt    190   TANLLQTFAA ASAAAAAAAA ASATNSPRPA SNASTMQIDV LENPQSPAVE
ecegt    186   TANLLQTFAA ASAAAAAAAA ASSTNSPRPA SNASTMQIDV LDNPQSPAVE
               ********** *****  *** ********** ********** **********

melgt    240   ATTPTTSSSG EAGKNTRPFK AFPRDPLVIA ANFAATDVLL DNPRVERYTE
simgt    234   ATTPTTSSSG EAGKNTRPFK AFPRDPLVIA ANFAATDVLL DNPRVERYTE
secgt    237   ATTPTTSSSG EAGKSTRPFK AFPRDPLVIA ANFAATDVLL DNPRVERYTE
yakgt    240   ATTPTTSSSG EAGKNTRPFK AFPRDPLVIA ANFAATDVLL DNPRVERYTE
sangt    240   ATTPTTSSSG EAGKNTRPFK AFPRDPLVIA ANFAATDVLL DNPRVERYTE
ecegt    236   ATTPTTSSSG EAGKNTRPFK AFPRDPLVIA ANFAATDVLL DNPRVERYTE
               ********** ********** ********** ********** **********

melgt    290   YRKRVLEQIR SSNGGSRTVT NPKMRRTNSR SGSVNEGSSS NNNSESEDRA
simgt    284   YRKRVLEQIR SSNGGSRTVT NPKMRRTNSR SGSVNEGSSS NNNSESEDRA
secgt    287   YRKRVLEQIR SSNGGSRTVT NPKMRRTNSR SGSVNEGSSS NNNSESEDRA
yakgt    290   YRKRVLEQIR SSNGGSRTVT NPKMRRTNSR SGSVNEGSSS NNNSESEDRA
sangt    290   YRKRVLEQIR SSNGGSRTVT NPKMRRTNSR SGSVNEGSSS NNNSESEDRA
ecegt    286   YRKRVLEQIR SSNGGSRTVT NPKMRRTNSR SGSVNEGSSS NNNSESEDRA
               ********** ********** ********** ********** **********

melgt    340   AAEESSDCDS QAGNFESKSA TSSSSNLANA TAANSGISSG SQVKDAAYYE
simgt    334   AAEESSDCDS QAGNFEGKSA TSSSSNLANA TAANSGISSG SQVKDAAYYE
secgt    337   AAEESSDCDS QAGNFEGKSA TSSSSNLANA TAANSGISSG SQVKDAAYYE
yakgt    340   AAEESSDCDS QAGNFEGKSA TSSSSNLANA TAANSGISSG SQVKDAAYYE
sangt    340   AAEESSDCDS QVGNFEGKSA TSSSSNLANA TAANSGISSG SQVKDAAYYE
ecegt    336   AAEESSDCDS QAGNFEGKSA TSSSSNLANA TAANAGISSG SQVKDAAYYE
               ********** ********** ********** ********** **********

melgt    390   RRRKNNAAAK KSRDRRRIKE DEIAIRAAYL ERQNIELLCQ IDALKVQLAA
simgt    384   RRRKNNAAAK KSRDRRRIKE DEIAIRAAYL ERQNIELLCQ IDALKAQLAA
secgt    387   RRRKNNAAAK KSRDRRRIKE DEIAIRAAYL ERQNIELLCQ IDALKAQLAA
yakgt    390   RRRKNNAAAK KSRDRRRIKE DEIAIRAAYL ERQNIELLCQ IDALKAQLAA
sangt    390   RRRKNNAAAK KSRDRRRIKE DEIAIRAAYL ERQNIELLCQ IDALKAQLAA
ecegt    386   RRRKNNAAAK KSRDRRRIKE DEIAIRAAYL ERQNIELLCQ IDALKAQLAA
               ********** ********** ********** ********** **********

melgt    440   FTSAKVTTA
simgt    434   FTSAKVTTA
secgt    437   FTSAKVTTA
yakgt    440   FTSAKVTTA
sangt    440   FTSAKVTTA
ecegt    436   FTSAKVTTA
               *********
```

FIGURE S16. Maximum-likelihood ancestral sequence reconstruction of GT protein, excluding polyQ. All ancestral sites could be reconstructed with high confidence (posterior probability > 0.98), except for polyQ tracks. Ancestral substitutions beyond D. ere were not displayed. AA positions based on *D. melanogaster GT* protein.

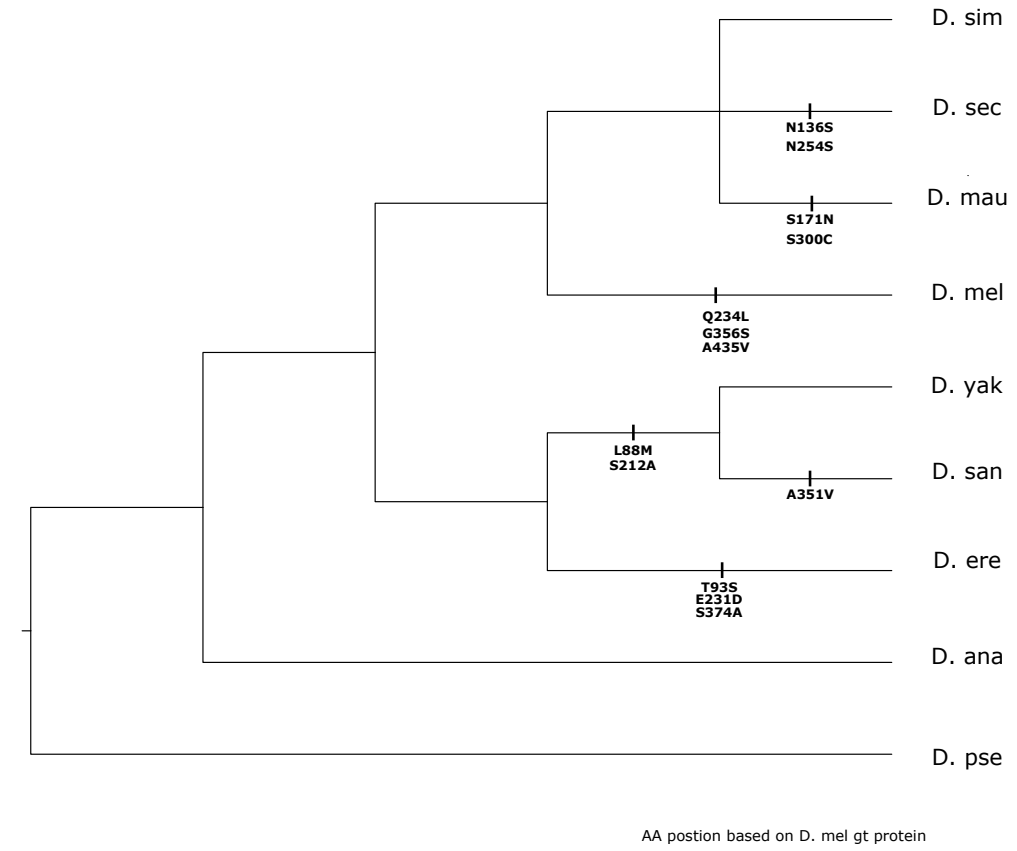

FIGURE S17. The polyglutamine repeats (polyQ) show differences among the *melanogaster* subspecies complex species.

Maximum-parsimony ancestral sequence reconstruction of 2 polyQ tracks of gt protein. The conserved H within polyQ tracks helps to delineate both polyQ tracks to two parts. Due to the lack of proper substitution models, this maximum-parsimony based ancestral reconstruction for polyQ tracks may subject to bias due to alignment error, arbitrary choice of polyQ unit etc.

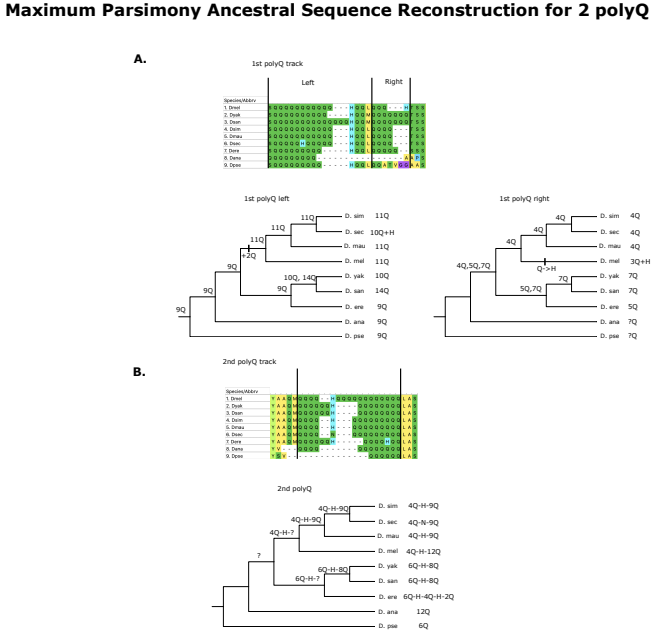

FIGURE S18. *tll* alleles from six different species in the *melanogaster* species complex. We found no major differences at the coding portion of the gene between the *melanogaster* species supercomplex (*D. melanogaster*, *D. simulans*, and *D. sechellia*) and that the *D. santomea/D. yakuba* species pair is the structure of poly-glutamine repeats. melgt: *D. melanogaster*, simgt: *D. simulans*, sechgt: *D. sechellia*, sangt: *D. santomea*, eregt: *D. erecta*. Asterisks show residues that are conserved across the whole group.

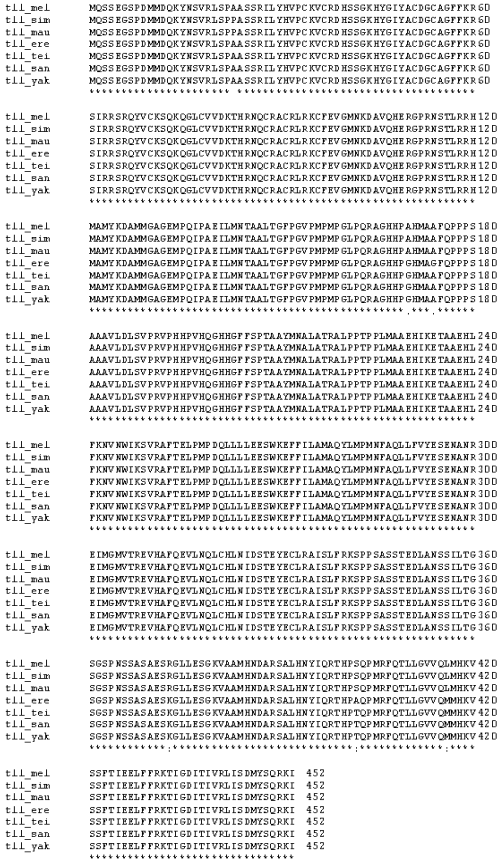

FIGURE S19. Embryonic hybrid inviability does not occur in *mel/tei* hybrids. No line of *D. teissieri* showed either embryonic inviability or abdominal ablations when crossed with *D. melanogaster*, *D. simulans*, or *D. mauritiana* females. The vast majority of assays revealed no dead embryos. **A.** *mel/tei* male hybrids. **B.** *sim/tei* male hybrids. **C.** *mau/tei* male hybrids. **D.** *mel/tei* female hybrids. **E.** *sim/tei* female hybrids. **F.** *mau/tei* female hybrids. tei1: Balancha_1; tei2: Balancha_2, tei3: Balancha_3, tei4: House_Bioko_0, tei5: House_Bioko_1, tei6: House_Bioko_2, tei7: La_Lope_Gabon, tei8: Selinda, tei9: Zimbabwe, tei10: cascade_2_1, tei11: cascade_2_2; tei12: cascade_2_4, tei13: cascade_4_1, tei14: cascade_4_2, tei15: cascade_4_3, tei16: cascade_4_4, tei17: cascade_4_5, tei18: cascade_4_6, tei19: Bata_2, tei20: Bata_8.

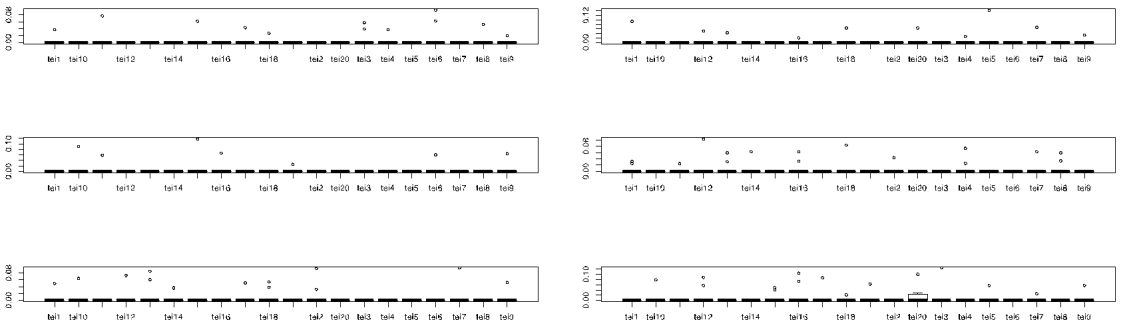

FIGURE S20. **Divergence in *giant* in the *melanogaster* species subgroup. A**. The evolutionary timing of gt^{mel} and its interactor leading to HI. The *gt* allele responsible for HI in hybrids with *D. santomea* evolved before *mel, sim, and mau* had a common ancestor (Blue branch). At least one of the interactors of gt^{mel} is not shared with *D. teissieri* which indicates that such element must have evolved after the last common ancestor of *D. santomea* and *D. teissieri* speciated (Red branch).

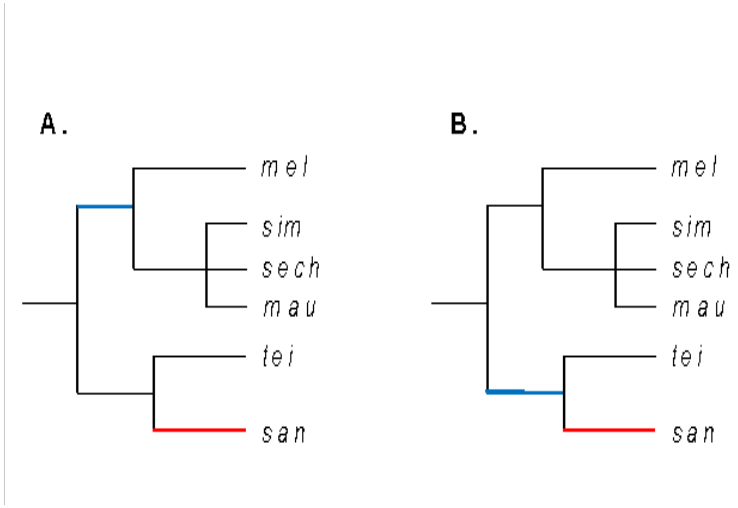

FIGURE S21. Experimental design to generated a GFP-mediated disruption of *tll_{mel}*.

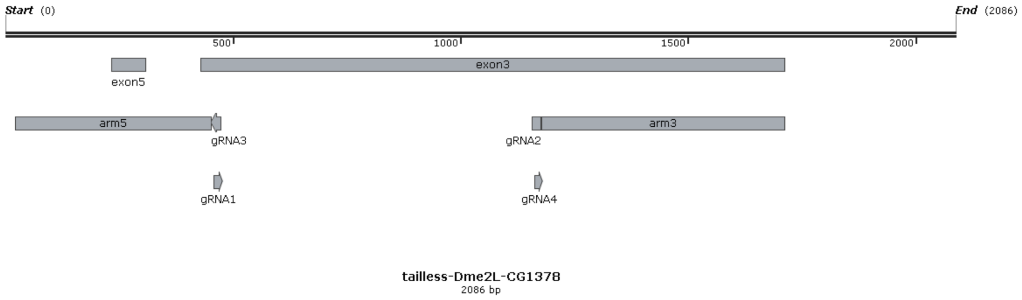

REFERENCES

Bachtrog D., K. Thornton, A. Clark, and P. Andolfatto, 2006 Extensive introgression of mitochondrial DNA relative to nuclear genes in the *Drosophila yakuba* species group. Evolution 60: 292–302.

Bischof J., R. K. Maeda, M. Hediger, F. Karch, and K. Basler, 2007 An optimized transgenesis system for *Drosophila* using germ-line-specific φC31 integrases. PNAS 104: 3312–3317.

Bomblies K., J. Lempe, P. Epple, N. Warthmann, C. Lanz, *et al.*, 2007 Autoimmune response as a mechanism for a Dobzhansky-Muller-type incompatibility syndrome in plants. PLoS Biology. https://doi.org/10.1371/journal.pbio.0050236

Brand C. L., S. B. Kingan, L. Wu, and D. Garrigan, 2013 A selective sweep across species boundaries in *Drosophila*. Molecular Biology and Evolution. https://doi.org/10.1093/molbev/mst123

Brideau N. J., H. A. Flores, J. Wang, S. Maheshwari, X. Wang, *et al.*, 2006 Two Dobzhansky-Muller Genes interact to cause hybrid lethality in *Drosophila*. Science 314: 1292–1295. https://doi.org/10.1126/science.1133953

Brönner G., Q. Chu-LaGraff, C. Q. Doe, B. Cohen, D. Weigel, *et al.*, 1994 Sp1/egr-like zinc-finger protein required for endoderm specification and germ-layer formation in *Drosophila*. Nature 369: 664–668. https://doi.org/10.1038/369664a0

Brown J. B., N. Boley, R. Eisman, G. E. May, M. H. Stoiber, *et al.*, 2014 Diversity and dynamics of the *Drosophila* transcriptome. Nature 512: 393–399. https://doi.org/10.1038/nature12962

Bucher G., 2004 Divergent segmentation mechanism in the short germ insect *Tribolium* revealed by giant expression and function. Development 131: 1729–1740. https://doi.org/10.1242/dev.01073

Capovilla M., E. D. Eldon, and V. Pirrotta, 1992 The giant gene of *Drosophila* encodes a b-ZIP DNA-binding protein that regulates the expression of other segmentation gap genes. Development (Cambridge, England) 114: 99–112.

Cattani M. V., and D. C. Presgraves, 2012 Incompatibility between *X* chromosome factor and pericentric heterochromatic region causes lethality in hybrids between *Drosophila* melanogaster and its sibling species. Genetics 191: 549–559.

Cauret C. M. S., M.-T. Gansauge, A. S. Tupper, B. L. S. Furman, M. Knytl, *et al.*, 2020 Developmental systems drift and the drivers of sex chromosome evolution. Molecular Biology and Evolution 37: 799–810. https://doi.org/10.1093/molbev/msz268

Cerny A. C., D. Grossmann, G. Bucher, and M. Klingler, 2008 The *Tribolium* ortholog of *knirps* and *knirps*-related is crucial for head segmentation but plays a minor role during abdominal patterning. Developmental Biology 321: 284–294. https://doi.org/10.1016/j.ydbio.2008.05.527

Chang W., D. R. Matute, and M. Kreitman, 2021 Rapid evolution of the functionally conserved gap gene *giant* in *Drosophila*. bioRxiv 2021.07.08.451553. https://doi.org/10.1101/2021.07.08.451553

Clark A. G., M. B. Eisen, D. R. Smith, C. M. Bergman, and the *Drosophila* 12 Genomes Consortium, 2007 Evolution of genes and genomes on the *Drosophila* phylogeny. Nature 450: 203–218. https://doi.org/10.1038/nature06341

Cook R. K., M. E. Deal, J. A. Deal, R. D. Garton, C. A. Brown, *et al.*, 2010 A new resource for characterizing *X*-linked genes in *Drosophila melanogaster*: Systematic coverage and subdivision of the *X* chromosome with nested, *Y*-linked duplications. Genetics 186: 1095–1109. https://doi.org/10.1534/genetics.110.123265

Cooper B. S., P. S. Ginsberg, M. Turelli, and D. R. Matute, 2017 *Wolbachia* in the *Drosophila yakuba* complex: Pervasive frequency variation and weak cytoplasmic incompatibility, but no apparent effect on reproductive isolation. Genetics 205: 333–351. https://doi.org/10.1534/genetics.116.196238

Coughlan J. M., and D. R. Matute, 2020 The importance of intrinsic postzygotic barriers throughout the speciation process. Philosophical Transactions of the Royal Society B: Biological Sciences 375: 20190533. https://doi.org/10.1098/rstb.2019.0533

Coyne J. A., 1985 Genetic studies of three sibling species of *Drosophila* with relationship to theories of speciation. Genetical Research. https://doi.org/10.1017/S0016672300022643

Coyne J. A., S. Simeonidis, and P. Rooney, 1998 Relative paucity of genes causing inviability in hybrids between *Drosophila melanogaster* and *D. simulans*. Genetics 150: 1091–1103.

Coyne J. A., S. Elwyn, S. Y. Kim, and A. Llopart, 2004 Genetic studies of two sister species in the *Drosophila melanogaster* subgroup, *D. yakuba* and *D. santomea*. Genetics Research 84: 11–26.

Coyne J. A., and H. A. Orr, 2004 *Speciation*. Sinauer Associates.

Crombach A., M. A. García-Solache, and J. Jaeger, 2014 Evolution of early development in dipterans: Reverse-engineering the gap gene network in the moth midge *Clogmia albipunctata* (Psychodidae). BioSystems 123: 74–85. https://doi.org/10.1016/j.biosystems.2014.06.003

Crombach A., K. R. Wotton, E. Jiménez-Guri, and J. Jaeger, 2016 Gap gene regulatory dynamics evolve along a genotype network. Molecular Biology and Evolution 33: 1293–1307. https://doi.org/10.1093/molbev/msw013

Cutter A. D., and J. D. Bundus, 2020 Speciation and the developmental alarm clock. eLife 9: e56276. https://doi.org/10.7554/eLife.56276

Darwin C., 1859 *The origin of species by means of natural selection*.

DePristo M. A., E. Banks, R. Poplin, K. V. Garimella, J. R. Maguire, *et al.*, 2011 A framework for variation discovery and genotyping using next-generation DNA sequencing data. Nature genetics 43: 491–498.

Dobzhansky T., 1937 Genetic nature of species differences. The American Naturalist 71: 404–420. https://doi.org/10.2307/2457293

Dos Santos G., A. J. Schroeder, J. L. Goodman, V. B. Strelets, M. A. Crosby, *et al.*, 2015a FlyBase: Introduction of the *Drosophila melanogaster* Release 6 reference genome assembly and large-scale migration of genome annotations. Nucleic Acids Research 43: D690–D697. https://doi.org/10.1093/nar/gku1099

Eldon E. D., and V. Pirrotta, 1991 Interactions of the *Drosophila* gap gene *giant* with maternal and zygotic pattern-forming genes. Development (Cambridge, England) 111: 367–378.

Ferree P. M., and D. A. Barbash, 2009 Species-specific heterochromatin prevents mitotic chromosome segregation to cause hybrid lethality in *Drosophila*. PLOS Biology 7: e1000234. https://doi.org/10.1371/journal.pbio.1000234

García-Solache M., J. Jaeger, and M. Akam, 2010 A systematic analysis of the gap gene system in the moth midge Clogmia albipunctata. Developmental Biology 344: 306–318. https://doi.org/10.1016/j.ydbio.2010.04.019

Garrigan D., S. B. Kingan, A. J. Geneva, P. Andolfatto, A. G. Clark, *et al.*, 2012 Genome sequencing reveals complex speciation in the *Drosophila simulans* clade. Genome Research 22: 1499–1511. https://doi.org/10.1101/gr.130922.111

Gaunt S. J., 2002 Conservation in the *Hox* code during morphological evolution. International Journal of Developmental Biology 38: 549–552.

Gavin-Smyth J., and D. R. Matute, 2013 Embryonic lethality leads to hybrid male inviability in hybrids between *Drosophila melanogaster* and *D. santomea*. Ecology and Evolution 3: 1580–1589. https://doi.org/10.1002/ece3.573

Gibson D. G., L. Young, R.-Y. Chuang, J. C. Venter, C. A. Hutchison, *et al.*, 2009 Enzymatic assembly of DNA molecules up to several hundred kilobases. Nature methods 6: 343–345.

Goltsev Y., W. Hsiong, G. Lanzaro, and M. Levine, 2004 Different combinations of gap repressors for common stripes in Anopheles and Drosophila embryos. Developmental Biology 275: 435–446. https://doi.org/10.1016/j.ydbio.2004.08.021

Gordon K. L., and I. Ruvinsky, 2012 Tempo and mode in evolution of transcriptional regulation. PLOS Genetics 8: e1002432. https://doi.org/10.1371/journal.pgen.1002432

Groth A. C., M. Fish, R. Nusse, and M. P. Calos, 2004 Construction of transgenic *Drosophila* by using the site-specific integrase from phage φC31. Genetics 166: 1775–1782.

Hare E. E., B. K. Peterson, and M. B. Eisen, 2008a A careful look at binding site reorganization in the even-skipped enhancers of *Drosophila* and sepsids. PLoS genetics, 4(11), p.e1000268.

Hare E. E., B. K. Peterson, V. N. Iyer, R. Meier, and M. B. Eisen, 2008b Sepsid *even-skipped* enhancers are functionally conserved in *Drosophila* despite lack of sequence conservation. PLoS Genetics 4. https://doi.org/10.1371/journal.pgen.1000106

Hartman T. R., D. Zinshteyn, H. K. Schofield, E. Nicolas, A. Okada, *et al.*, 2010 *Drosophila Boi* limits hedgehog levels to suppress follicle stem cell proliferation. Journal of Cell Biology 191: 943–952. https://doi.org/10.1083/jcb.201007142

He B. Z., A. K. Holloway, S. J. Maerkl, and M. Kreitman, 2011 Does positive selection drive transcription factor binding site turnover? a test with *Drosophila cis*-regulatory modules. PLoS Genetics 7. https://doi.org/10.1371/journal.pgen.1002053

Hu T. T., M. B. Eisen, K. R. Thornton, and P. Andolfatto, 2013 A second-generation assembly of the *Drosophila simulans* genome provides new insights into patterns of lineage-specific divergence. Genome Research 23: 89–98. https://doi.org/10.1101/gr.141689.112

Huang W., A. Massouras, Y. Inoue, J. Peiffer, M. Ràmia, *et al.*, 2014 Natural variation in genome architecture among 205 *Drosophila melanogaster* Genetic Reference Panel lines. Genome Research 24: 1193–1208. https://doi.org/10.1101/gr.171546.113

Jaeger J., 2011 *The gap gene network*.

Janssens H., K. Siggens, D. Cicin-Sain, E. Jiménez-Guri, M. Musy, *et al.*, 2014 A quantitative atlas of *even-skipped* and *Hunchback* expression in *Clogmia albipunctata* (Diptera: Psychodidae) blastoderm embryos. EvoDevo 5. https://doi.org/10.1186/2041-9139-5-1

Johnson N. A., and A. H. Porter, 2007 Evolution of branched regulatory genetic pathways: Directional selection on pleiotropic loci accelerates developmental system drift. Genetica 129: 57–70. https://doi.org/10.1007/s10709-006-0033-2

Johnson N. A., 2010 Hybrid incompatibility genes: Remnants of a genomic battlefield? Trends in Genetics, 26: 317-325.

Johnson R. C., G. W. Nelson, J. L. Troyer, J. A. Lautenberger, B. D. Kessing, *et al.*, 2010 Accounting for multiple comparisons in a genome-wide association study (GWAS). BMC genomics 11: 1–6.

Kaminker J., C. Bergman, B. Kronmiller, J. Carlson, R. Svirskas, *et al.*, 2002 The transposable elements of the *Drosophila melanogaster* euchromatin: a genomics perspective. Genome Biology 3: 1–20. https://doi.org/10.1186/gb-2002-3-12-research0084

Kinsey J. D., 1967 Studies on an embryonic lethal hybrid in *Drosophila.* Development 17: 405–423.

Kondrashov A. S., S. Sunyaev, and F. A. Kondrashov, 2002 Dobzhansky–Muller incompatibilities in protein evolution. PNAS 99: 14878–14883. https://doi.org/10.1073/pnas.232565499

Kraut R., and M. Levine, 1991 Mutually repressive interactions between the gap genes *giant* and *Krüppel* define middle body regions of the Drosophila embryo. Development 111: 611–621.

Lack J. B., J. D. Lange, A. D. Tang, R. B. Corbett-Detig, and J. E. Pool, 2016 A thousand fly genomes: An expanded *Drosophila* genome Nexus. Molecular Biology and Evolution 33: 3308–3313. https://doi.org/10.1093/molbev/msw195

Lee A. P., E. G. Koh, A. Tay, S. Brenner, and B. Venkatesh, 2006 Highly conserved syntenic blocks at the vertebrate Hox loci and conserved regulatory elements within and outside Hox gene clusters. Proceedings of the National Academy of Sciences 103: 6994–6999.

Lee H. Y., J. Y. Chou, L. Cheong, N. H. Chang, S. Y. Yang, *et al.*, 2008 Incompatibility of nuclear and mitochondrial genomes causes hybrid sterility between two yeast species. Cell 135: 1065–1073. https://doi.org/10.1016/j.cell.2008.10.047

Li H., B. Handsaker, A. Wysoker, T. Fennell, J. Ruan, *et al.*, 2009 The sequence alignment/map format and SAMtools. Bioinformatics 25: 2078–2079.

Li H., and R. Durbin, 2009 Fast and accurate short read alignment with Burrows-Wheeler transform. Bioinformatics 25: 1754–1760. https://doi.org/10.1093/bioinformatics/btp324

Li H., 2013 Aligning sequence reads, clone sequences and assembly contigs with BWA-MEM. arXiv preprint arXiv 00: 3. https://doi.org/arXiv:1303.3997 [q-bio.GN]

Lindsley D. L., and G. G. Zimm, 1992 The genome of *Drosophila melanogaster*.

Llopart A., E. Brud, N. Pettie, and J. M. Comeron, 2018 Support for the dominance theory in *Drosophila* transcriptomes. Genetics 210: 703–718. https://doi.org/10.1534/genetics.118.301229

Ludwig M. Z., A. Palsson, E. Alekseeva, C. M. Bergman, J. Nathan, *et al.*, 2005 Functional evolution of a *cis*-regulatory module. PLoS Biology 3: 0588–0598. https://doi.org/10.1371/journal.pbio.0030093

Lynch V. J., 2009 Use with caution: Developmental systems divergence and potential pitfalls of animal models. Yale J Biol Med 82: 53–66.

Mack K. L., and M. W. Nachman, 2017 Gene regulation and speciation. Trends in Genetics 33: 68–80.

MacKay T. F. C., S. Richards, E. A. Stone, A. Barbadilla, J. F. Ayroles, *et al.*, 2012 The *Drosophila melanogaster* Genetic Reference Panel. Nature 482: 173–178. https://doi.org/10.1038/nature10811

Maddison W., and D. Maddison, 2010 Mesquite 2. Manual 1–258.

Maheshwari S., and D. A. Barbash, 2011 The genetics of hybrid incompatibilities. Annual Review of Genetics 45: 331–355. https://doi.org/10.1146/annurev-genet-110410-132514

Manu, M. Z. Ludwig, and M. Kreitman, 2013 Sex-specific pattern formation during early *Drosophila* development. Genetics 194: 163–173. https://doi.org/10.1534/genetics.112.148205

Manzanares M., H. Wada, N. Itasaki, P. A. Trainor, R. Krumlauf, *et al.*, 2000 Conservation and elaboration of Hox gene regulation during evolution of the vertebrate head. Nature 408: 854–857.

Matute D. R., I. A. Butler, D. A. Turissini, and J. A. Coyne, 2010 A test of the snowball theory for the rate of evolution of hybrid incompatibilities. Science 329: 1518–1521. https://doi.org/10.1126/science.1193440

Matute D. R., and J. Gavin-Smyth, 2014 fine mapping of dominant *X*-linked incompatibility alleles in *Drosophila* hybrids. PLoS Genetics 10. https://doi.org/10.1371/journal.pgen.1004270

Matute D. R., J. Gavin-Smyth, and G. Liu, 2014 Variable post-zygotic isolation in *Drosophila melanogaster/D. simulans* hybrids. Journal of Evolutionary Biology. https://doi.org/10.1111/jeb.12422

McKenna A., M. Hanna, E. Banks, A. Sivachenko, K. Cibulskis, *et al.*, 2010 The Genome Analysis Toolkit: A MapReduce framework for analyzing next-generation DNA sequencing data. Genome Res. 20: 1297–1303. https://doi.org/10.1101/gr.107524.110

Miller C. J. J., and D. R. Matute, 2017 The effect of temperature on *Drosophila* hybrid fitness. G3 Genes|Genomes|Genetics 7: 377–385. https://doi.org/10.1534/g3.116.034926

Mohler J., E. D. Eldon, and V. Pirrotta, 1989 A novel spatial transcription pattern associated with the segmentation gene, *giant*, of *Drosophila*. The EMBO journal 8: 1539–1548.

Moran B. M., C. Y. Payne, D. L. Powell, E. N. K. Iverson, S. M. Banerjee, *et al.*, 2021 A lethal genetic incompatibility between naturally hybridizing species in Mitochondrial Complex I. BioRxiv. doi: https://doi.org/10.1101/2021.07.13.452279

Moyle L. C., and T. Nakazato, 2010 Hybrid incompatibility "snowballs" between *Solanum* species. Science 329: 1521–1523. https://doi.org/10.1126/science.1193063

Muller H. J., 1942 Isolating mechanisms, evolution and temperature. Biology Symposium, 6, 71-125.

Nagy O., I. Nuez, R. Savisaar, A. E. Peluffo, A. Yassin, *et al.*, 2018 Correlated evolution of two copulatory organs via a single *cis*-regulatory nucleotide change. Current Biology 28: 3450–3457.

Ni X., Y. E. Zhang, N. Nègre, S. Chen, M. Long, *et al.*, 2012 Adaptive evolution and the birth of ctcf binding sites in the *Drosophila* genome. PLoS Biology 10. https://doi.org/10.1371/journal.pbio.1001420

Nitta K. R., A. Jolma, Y. Yin, E. Morgunova, T. Kivioja, *et al.*, 2015 Conservation of transcription factor binding specificities across 600 million years of bilateria evolution, (B. Ren, Ed.). eLife 4: e04837. https://doi.org/10.7554/eLife.04837

Nosil P., and D. Schluter, 2011 The genes underlying the process of speciation. Trends in ecology & evolution, 26(4), pp.160-167.

Orr H. a, 1993 Haldane's rule has multiple genetic causes. Nature 361: 532–533. https://doi.org/10.1038/361532a0

Palmer M. E., and M. W. Feldman, 2009 Dynamics of hybrid incompatibility in gene networks in a constant environment. Evolution 63: 418–431. https://doi.org/10.1111/j.1558-5646.2008.00577.x

Pavlicev M., and G. P. Wagner, 2012 A model of developmental evolution: Selection, pleiotropy and compensation. Trends in Ecology & Evolution, 27(6), pp.316-322.

Perrimon N., L. Engstrom, and A. P. Mahowald, 1984 Developmental genetics of the 2e-F region of the *Drosophila X* chromosome: A region rich in "developmentally important" genes. Genetics 108: 559–572.

Petschek J. P., N. Perrimon, and A. P. Mahowald, 1987 Region-specific defects in *l(1)giant* embryos of *Drosophila melanogaster*. Developmental Biology 119: 175–189. https://doi.org/10.1016/0012-1606(87)90219-3

Phadnis N., and H. A. Orr, 2009 A single gene causes both male sterility and segregation distortion in *Drosophila* hybrids. Science. https://doi.org/10.1126/science.1163934

Phadnis N., E. P. Baker, J. C. Cooper, K. A. Frizzell, E. Hsieh, *et al.*, 2015 An essential cell cycle regulation gene causes hybrid inviability in *Drosophila*. Science (New York, N.Y.) 350: 1552–5. https://doi.org/10.1126/science.aac7504

Pool J. E., 2015 The mosaic ancestry of the *Drosophila* genetic reference panel and the *D. melanogaster* reference genome reveals a network of epistatic fitness interactions. Molecular biology and evolution 32: 3236–3251.

Powell D. L., M. García-Olazábal, M. Keegan, P. Reilly, K. Du, *et al.*, 2020 Natural hybridization reveals incompatible alleles that cause melanoma in swordtail fish. Science 368: 731–736.

Presgraves D. C., 2003 A fine-scale genetic analysis of hybrid incompatibilities in Drosophila. Genetics 163: 955–972.

Presgraves D. C., and C. D. Meiklejohn, 2021 Hybrid sterility, genetic conflict and complex speciation: lessons from the *Drosophila simulans* clade species. Front. Genet. 0. https://doi.org/10.3389/fgene.2021.669045

R Core Team, 2016 R Development Core Team.

Rebeiz M., M. Ramos-Womack, S. Jeong, P. Andolfatto, T. Werner, *et al.*, 2009 Evolution of the *tan* Locus contributed to pigment loss in *Drosophila santomea*: A Response to Matute et al. Cell 139: 1189–1196. https://doi.org/10.1016/j.cell.2009.11.004

Reinitz J., and M. Levine, 1990 Control of the initiation of homeotic gene expression by the gap genes *giant* and *tailless* in *Drosophila*. Developmental Biology 140: 57–72. https://doi.org/10.1016/0012-1606(90)90053-L

Rivera-Pomar R., X. Lu, N. Perrimon, H. Taubert, and H. Jäckle, 1995 Activation of posterior gap gene expression in the *Drosophila* blastoderm. Nature, 376: 253-256

Rogers R. L., J. M. Cridland, L. Shao, T. T. Hu, P. Andolfatto, *et al.*, 2014 Landscape of standing variation for tandem duplications in *Drosophila yakuba* and *Drosophila simulans*. Molecular Biology and Evolution 31: 1750–1766. https://doi.org/10.1093/molbev/msu124

Rogers R. L., L. Shao, and K. R. Thornton, 2017 Tandem duplications lead to novel expression patterns through exon shuffling in *Drosophila yakuba.* PLoS Genetics 13. https://doi.org/10.1371/journal.pgen.1006795

Santini S., J. L. Boore, and A. Meyer, 2003 Evolutionary conservation of regulatory elements in vertebrate Hox gene clusters. Genome research 13: 1111–1122.

Santos G. Dos, A. J. Schroeder, J. L. Goodman, V. B. Strelets, M. A. Crosby, *et al.*, 2015b FlyBase: Introduction of the *Drosophila melanogaster* Release 6 reference genome assembly and large-scale migration of genome annotations. Nucleic Acids Research 43: D690–D697. https://doi.org/10.1093/nar/gku1099

Sawamura K., T. Taira, and T. K. Watanabe, 1993a Hybrid lethal systems in the *Drosophila melanogaster* species complex. I. The maternal hybrid rescue (*mhr*) gene of *Drosophila simulans*. Genetics 133: 299–305.

Sawamura K., and M. T. Yamamoto, 1993 Cytogenetical localization of Zygotic hybrid rescue (*Zhr*), a *Drosophila melanogaster* gene that rescues interspecific hybrids from embryonic lethality. MGG Molecular & General Genetics. https://doi.org/10.1007/BF00276943

Sawamura K., M. T. Yamamoto, and T. K. Watanabe, 1993b Hybrid lethal systems in the *Drosophila melanogaster* species complex. II. The Zygotic hybrid rescue (*Zhr*) gene of *D. melanogaster*. Genetics 133: 307–313.

Schiffman J. S., and P. L. Ralph, 2021 System drift and speciation. Evolution. https://doi.org/10.1111/evo.14356

Schrider D. R., J. Ayroles, D. R. Matute, and A. D. Kern, 2018 Supervised machine learning reveals introgressed loci in the genomes of *Drosophila simulans* and *D. sechellia*. PLoS genetics. https://doi.org/10.1371/journal.pgen.1007341

Schulz C., and D. Tautz, 1995 Zygotic caudal regulation by *hunchback* and its role in abdominal segment formation of the *Drosophila* embryo. Development (Cambridge, England) 121: 1023–1028.

Serrato-Capuchina A., J. Wang, E. Earley, D. Peede, K. Isbell, *et al.*, 2020a Paternally inherited p-element copy number affects the magnitude of hybrid dysgenesis in *Drosophila simulans* and *D. melanogaster*. Genome Biol Evol 12: 808–826. https://doi.org/10.1093/gbe/evaa084

Serrato-Capuchina A., E. R. R. D'Agostino, D. Peede, B. Roy, K. Isbell, *et al.*, 2021 P-elements strengthen reproductive isolation within the *Drosophila simulans* species complex. Evolution 75: 2425-2440

Shull G. H., 1923 The species concept from the point of view of a geneticist. American Journal of Botany 10: 221–228. https://doi.org/10.2307/2435375

Skeath J. B., B. A. Wilson, S. E. Romero, M. J. Snee, Y. Zhu, *et al.*, 2017 The extracellular metalloprotease AdamTS-A anchors neural lineages in place within and preserves the architecture of the central nervous system. Development, 144: 3102-3113. https://doi.org/10.1242/dev.145854

Sommer R. J., 2012 Evolution of regulatory networks: Nematode vulva induction as an example of developmental systems drift, pp. 79–91 in *Evolutionary Systems Biology*, Advances in Experimental Medicine and Biology. edited by Soyer O. S. Springer, New York, NY.

Struhl G., P. Johnston, and P. A. Lawrence, 1992 Control of *Drosophila* body pattern by the hunchback morphogen gradient. Cell 69: 237–249. https://doi.org/10.1016/0092-8674(92)90405-2

Sturtevant A. H., 1920 Genetic Studies on *Drosophila Simulans*. I. Introduction. Hybrids with *Drosophila melanogaster.* Genetics 5: 488–500. https://doi.org/10.1002/jez.b.21128

Suvorov A., B. Y. Kim, J. Wang, E. E. Armstrong, D. Peede, *et al.*, 2021 Widespread introgression across a phylogeny of 155 *Drosophila* genomes. Current Biology. https://doi.org/10.1016/j.cub.2021.10.052

Tamura K., S. Subramanian, and S. Kumar, 2004 Temporal patterns of fruit fly (*Drosophila*) evolution revealed by mutation clocks. Molecular Biology and Evolution 21: 36–44. https://doi.org/10.1093/molbev/msg236

Tang S., and D. C. Presgraves, 2009 Evolution of the *Drosophila* nuclear pore complex results in multiple hybrid incompatibilities. Science 323: 779–782. https://doi.org/10.1126/science.1169123

Thibault S. T., M. A. Singer, W. Y. Miyazaki, B. Milash, N. A. Dompe, *et al.*, 2004 A complementary transposon tool kit for *Drosophila melanogaster* using *P* and *piggyBac*. Nature genetics 36: 283–287.

Toivonen J. M., K. M. C. O'Dell, N. Petit, S. C. Irvine, G. K. Knight, *et al.*, 2001 *Technical knockout*, a *Drosophila* model of mitochondrial deafness. Genetics. Genetics, 159: 241-254.

True J. R., and E. S. Haag, 2001 Developmental system drift and flexibility in evolutionary trajectories. Evolution & development, 3: 109-119.

Tulchinsky A. Y., N. A. Johnson, and A. H. Porter, 2014 Hybrid incompatibility despite pleiotropic constraint in a sequence-based bioenergetic model of transcription factor binding. Genetics 198: 1645–1654. https://doi.org/10.1534/genetics.114.171397

Turissini D. A., G. Liu, J. R. David, and D. R. Matute, 2015 The evolution of reproductive isolation in the *Drosophila yakuba* complex of species. J. Evol. Biol. 28: 557–575. https://doi.org/10.1111/jeb.12588

Turissini D. A., and D. R. Matute, 2017 Fine scale mapping of genomic introgressions within the *Drosophila yakuba* clade. PLOS Genetics 13: e1006971. https://doi.org/10.1371/journal.pgen.1006971

Turissini D. A., J. A. McGirr, S. S. Patel, J. R. David, and D. R. Matute, 2018 The rate of evolution of postmating-prezygotic reproductive isolation in *Drosophila*. Molecular Biology and Evolution 35: 312–334. https://doi.org/10.1093/molbev/msx271

Venkat A., M. W. Hahn, and J. W. Thornton, 2018 Multinucleotide mutations cause false inferences of lineage-specific positive selection. Nature Ecology and Evolution. 2: 1280-1288. https://doi.org/10.1038/s41559-018-0584-5

Venken K. J. T., E. Popodi, S. L. Holtzman, K. L. Schulze, S. Park, *et al.*, 2010 A molecularly defined duplication set for the *X* chromosome of *Drosophila melanogaster.* Genetics 186: 1111–1125. https://doi.org/10.1534/genetics.110.121285

Wang X., and R. J. Sommer, 2011 Antagonism of LIN-17/Frizzled and LIN-18/Ryk in Nematode vulva induction reveals evolutionary alterations in core developmental pathways. PLOS Biology 9: e1001110. https://doi.org/10.1371/journal.pbio.1001110

Wang R. J., M. A. White, and B. A. Payseur, 2015 The pace of hybrid incompatibility evolution in house mice. Genetics 201: 229–242. https://doi.org/10.1534/genetics.115.179499

Weir J. J., 1885 An unnoticed factor in evolution. Nature 31: 194–194. https://doi.org/10.1038/031194b0

Weiss K. M., and S. M. Fullerton, 2000 Phenogenetic drift and the evolution of genotype-phenotype relationships. Theoretical population biology, 57: 187-195.

Wellbrock C., E. Geissinger, A. Gómez, P. Fischer, K. Friedrich, *et al.*, 1998 Signalling by the oncogenic receptor tyrosine kinase Xmrk leads to activation of STAT5 in *Xiphophorus* melanoma. Oncogene 16: 3047–3056. https://doi.org/10.1038/sj.onc.1201844

Wilson M. J., M. Havler, and P. K. Dearden, 2010 Giant, Krüppel, and caudal act as gap genes with extensive roles in patterning the honeybee embryo. Developmental Biology 339: 200–211. https://doi.org/10.1016/j.ydbio.2009.12.015

Wotton K. R., E. Jimenez-Guri, A. Crombach, H. Janssens, A. Alcaine-Colet, *et al.*, 2015a Quantitative system drift compensates for altered maternal inputs to the gap gene network of the scuttle fly *Megaselia abdita*. eLife 2015. https://doi.org/10.7554/eLife.04785

Wu X., R. Vakani, and S. Small, 1998 Two distinct mechanisms for differential positioning of gene expression borders involving the *Drosophila* gap protein *giant*. Development 125: 3765–3774.

Yang Z., 1997 PAML: a program package for phylogenetic analysis by maximum likelihood. Computer applications in the biosciences, 13: 555-556.

Yang Z., 2007 PAML 4: Phylogenetic analysis by maximum likelihood. Molecular Biology and Evolution. 24: 1586-1591.https://doi.org/10.1093/molbev/msm088

Zuellig M. P., and A. L. Sweigart, 2018 Gene duplicates cause hybrid lethality between sympatric species of *Mimulus*. PLOS Genetics 14: e1007130. https://doi.org/10.1371/journal.pgen.1007130